

Solving Maxwell's Equations

William D. Henshaw,
Department of Mathematical Sciences,
Rensselaer Polytechnic Institute,
Troy, NY, USA, 12180. July 12, 2015

Abstract:

We describe some approximations for Maxwell's equations.

Contents

1	Introduction	1
2	Background	1
3	Three Dimensions	4
4	Boundary Conditions	4
4.1	Symmetry Boundary Conditions	4
5	Two Dimensions	5
6	Yee Scheme	5
7	The DSI scheme	6
7.1	Stability of the DSI scheme	8
7.2	Artificial diffusion	9
8	Stability	9
8.1	Time step limit with artificial dissipation	11
9	Analysis of Gedney et. al	12
10	Energy Estimates	13
11	The Non-orthogonal FDTD method of Lee, Palandech and Mittra	14
12	Symmetric Difference Approximations on Curvilinear Grids	15
13	Discrete Boundary Conditions	18
13.1	Boundary conditions for the magnetic field	18
13.2	Second-order accurate boundary conditions	19
13.3	Fourth-order accurate boundary conditions	19
13.3.1	Two dimensions	20
13.3.2	Three dimensions	21
13.4	Sixth- and higher-order accurate boundary conditions	23
13.5	Boundary conditions for the magnetic field	24
13.6	Extended boundaries in two-dimensions	25
13.7	Corners in two-dimensions	26
13.8	Extended boundaries in three-dimensions	27
13.9	Ghost points outside edges in three-dimensions	28

13.10	Corners in three-dimensions	30
14	Boundary conditions at material interfaces in 2D	31
15	Boundary conditions at material interfaces in 3D	33
15.1	Discrete boundary conditions for material interfaces	34
15.2	Reflection and Transmission for a planar material interface	35
16	Absorbing Boundary Conditions	36
16.1	Engquist-Majda one-way wave equations	36
16.2	Second-order accurate discretization	37
16.3	Fourth-order accuracy	38
16.4	Absorbing boundary conditions on a curvilinear grid	38
16.5	Non-reflecting Boundary Conditions and Incident Fields	38
17	Radiation Boundary Conditions	40
17.0.1	Non-local exact boundary conditions for a periodic strip	40
17.0.2	Non-local exact boundary conditions for an annular boundary	40
18	Higher-order accurate self-adjoint approximations on curvilinear grids	42
19	Higher-order accurate time stepping for the second-order wave equation	44
20	Higher-order time stepping with the Modified Equation approach	46
20.1	Modified Equation Time Stepping and Complex Index of Refraction	47
20.2	Modified Equation Time Stepping and Divergence Cleaning	48
21	Symmetric approximations on triangular grids	51
22	Exact Solutions	53
22.1	Eigenfunctions of a 2D disk	53
22.2	Eigenfunctions of a 3D cylinder	54
22.3	Scattering of a plane wave by a dielectric cylinder	56
22.4	Scattering by a dielectric sphere	57
23	Scattering by a dielectric sphere	57
23.1	Numerical results for scattering from a dielectric sphere	60
23.1.1	Scattering from a dielectric sphere - results for the FDTD (Yee) scheme	62
23.2	Timings	62
23.3	Scattering by a PEC sphere	63
24	Numerical results	65
25	Convergence results	69
25.1	The method of analytic solutions	69
25.2	Eigenfunctions on a disk	70
25.3	Eigenfunctions of a cylinder	71
25.4	Scattering by a cylinder	71
25.5	Scattering by a sphere	72
25.6	Computing eigenvalues of an L-shaped domain with time series	76
25.7	Computing eigenvalues of a cylinder with time series	78
25.8	Computing eigenvalues of a pill-box with time series	79
25.9	Computing eigenvalues of a sphere with time series	80
25.10	Scattering of a plane wave by a dielectric cylinder	81
25.11	Serial performance and memory usage	82
25.12	Parallel performance	83

1 Introduction

Some issues to be addressed:

Stability of the DSI scheme : What is the best way to stabilize the scheme?

- Add a high-order spatial or temporal dissipation.
- Add a high-order spatial dissipation only locally where needed
- Devise a symmetric version of the DSI scheme which will be stable and non-dissipative.

Higher-order accurate schemes : Approaches

- devise a higher-order accurate DSI scheme
- Embedded boundary grid (work of Kreiss, Petersson and Yström).
- Higher-order Hermite scheme (Hagstrom and Henshaw)
- Overlapping grids (Henshaw)
- Higher-order FEM approach (requires a mass matrix) (Dan White LLNL).

Improved efficiency for cartesian dominated grids

2 Background

Reference Taflove and Hagness [?], Jackson [?], Andersson[?] Peterson, Ray and Mittra[?].

Maxwell's equations are

$$\nabla \cdot \mathbf{D} = \rho \quad (\text{Gauss's law}) \quad (1)$$

$$\nabla \cdot \mathbf{B} = 0 \quad (\text{Gauss's law}) \quad (2)$$

$$\partial_t \mathbf{B} = -\nabla \times \mathbf{E} \quad (\text{Faraday's law}) \quad (3)$$

$$\partial_t \mathbf{D} = \nabla \times \mathbf{H} - \mathbf{J} \quad (\text{Ampere's law}) \quad (4)$$

For linear, isotropic and non-dispersive materials

$$\mathbf{B} = \mu \mathbf{H}, \quad \mathbf{D} = \epsilon \mathbf{E}$$

and thus

$$\nabla \cdot (\epsilon \mathbf{E}) = \rho \quad (5)$$

$$\nabla \cdot (\mu \mathbf{H}) = 0 \quad (6)$$

$$\partial_t \mathbf{H} = -\frac{1}{\mu} \nabla \times \mathbf{E} \quad (7)$$

$$\partial_t \mathbf{E} = \frac{1}{\epsilon} \nabla \times \mathbf{H} - \frac{1}{\epsilon} \mathbf{J} \quad (8)$$

The last two equations can be written as a system,

$$\mathbf{u}_t + A\mathbf{u}_x + B\mathbf{u}_y + C\mathbf{u}_z = 0$$

where $\mathbf{u} = (\mathbf{E}^T, \mathbf{H}^T)$ and

$$A = \begin{bmatrix} 0 & 0 & 0 & 0 & 0 & 0 \\ 0 & 0 & 0 & 0 & 0 & -1/\epsilon \\ 0 & 0 & 0 & 0 & 1/\epsilon & 0 \\ 0 & 0 & 0 & 0 & 0 & 0 \\ 0 & 0 & 1/\mu & 0 & 0 & 0 \\ 0 & -1/\mu & 0 & 0 & 0 & 0 \end{bmatrix} \quad B = \begin{bmatrix} 0 & 0 & 0 & 0 & 0 & 1/\epsilon \\ 0 & 0 & 0 & 0 & 0 & 0 \\ 0 & 0 & 0 & -1/\epsilon & 0 & 0 \\ 0 & 0 & -1/\mu & 0 & 0 & 0 \\ 0 & 0 & 0 & 0 & 0 & 0 \\ 1/\mu & 0 & 0 & 0 & 0 & 0 \end{bmatrix}$$

$$C = \begin{bmatrix} 0 & 0 & 0 & 0 & -1/\epsilon & 0 \\ 0 & 0 & 0 & 1/\epsilon & 0 & 0 \\ 0 & 0 & 0 & 0 & 0 & 0 \\ 0 & 1/\mu & 0 & 0 & 0 & 0 \\ -1/\mu & 0 & 0 & 0 & 0 & 0 \\ 0 & 0 & 0 & 0 & 0 & 0 \end{bmatrix}$$

If we substitute the plane wave $\mathbf{u} = \mathbf{a} \exp i(\mathbf{k} \cdot \mathbf{x} - \omega t)$, we get

$$-\omega \mathbf{a} + \begin{bmatrix} 0 & 0 & 0 & 0 & -k_3/\epsilon & k_2/\epsilon \\ 0 & 0 & 0 & k_3/\epsilon & 0 & -k_1/\epsilon \\ 0 & 0 & 0 & -k_2/\epsilon & k_1/\epsilon & 0 \\ 0 & k_3/\mu & -k_2/\mu & 0 & 0 & 0 \\ -k_3/\mu & 0 & k_1/\mu & 0 & 0 & 0 \\ k_2/\mu & -k_1/\mu & 0 & 0 & 0 & 0 \end{bmatrix} \mathbf{a} = 0$$

The eigenvalues are $-c, -c, 0, 0, c, c$ where $c = 1/\sqrt{\epsilon\mu}$ is the speed of light. Thus in the direction \mathbf{k} there will be two characteristics propagating to the right and two to the left. This implies we need two boundary conditions (for the two incoming characteristics) at any boundary.

If we nondimensionalize with

$$\tilde{x} = x/L, \quad \tilde{t} = t/T, \quad \tilde{\mathbf{E}} = \mathbf{E}/E_0, \quad \tilde{\mathbf{H}} = \mathbf{H}/H_0$$

then

$$\partial_{\tilde{t}} \tilde{\mathbf{H}} = -\frac{E_0}{H_0} \frac{T}{\mu L} \nabla_{\tilde{x}} \times \tilde{\mathbf{E}}$$

$$\partial_{\tilde{t}} \tilde{\mathbf{E}} = \frac{H_0}{E_0} \frac{T}{\epsilon L} \nabla_{\tilde{x}} \times \tilde{\mathbf{H}}$$

Taking $L/T = c = 1/\sqrt{\epsilon\mu}$ and $E_0/H_0 = \sqrt{\mu/\epsilon} = \mu c = 1/(\epsilon c)$, and $(\mathbf{u}, \mathbf{v}) = (\tilde{\mathbf{E}}, \tilde{\mathbf{H}})$ gives

$$\begin{aligned} \partial_t \mathbf{v} &= -\nabla \times \mathbf{u} \\ \partial_t \mathbf{u} &= \nabla \times \mathbf{v} \end{aligned}$$

We can get an energy estimate on a periodic domain. Taking the inner product of \mathbf{u} times the second equation and using integration by parts

$$\begin{aligned} (\mathbf{u}, \partial_t \mathbf{u}) &= (\mathbf{u}, \nabla \times \mathbf{v}) \\ &= (u_1(\partial_y v_3 - \partial_z v_2) + u_2(\partial_z v_1 - \partial_x v_3) + u_3(\partial_x v_2 - \partial_y v_1)) \\ &= (v_1(\partial_y u_3 - \partial_z u_2) + v_2(\partial_z u_1 - \partial_x u_3) + v_3(\partial_x u_2 - \partial_y u_1)) \\ &= (\mathbf{v}, \nabla \times \mathbf{u}) \end{aligned}$$

and thus

$$\frac{1}{2} \partial_t \{ \|\mathbf{u}\|^2 + \|\mathbf{v}\|^2 \} = 0$$

Therefore the energy

$$\mathcal{E} = \frac{1}{2} \{ \|\mathbf{u}\|^2 + \|\mathbf{v}\|^2 \}$$

remains constant in the periodic case.

3 Three Dimensions

Maxwell's equations written out in components in three dimensions are

$$\epsilon \partial_t E_x = \partial_y H_z - \partial_z H_y \quad (9)$$

$$\epsilon \partial_t E_y = \partial_z H_x - \partial_x H_z \quad (10)$$

$$\epsilon \partial_t E_z = \partial_x H_y - \partial_y H_x \quad (11)$$

$$\mu \partial_t H_x = - [\partial_y E_z - \partial_z E_y] \quad (12)$$

$$\mu \partial_t H_y = - [\partial_z E_x - \partial_x E_z] \quad (13)$$

$$\mu \partial_t H_z = - [\partial_x E_y - \partial_y E_x] \quad (14)$$

4 Boundary Conditions

For perfect electrical conductors (PEC) the boundary conditions are

$$\mathbf{n} \times \mathbf{E} = 0, \quad (15)$$

$$\mathbf{n} \cdot \mathbf{H} = 0. \quad (16)$$

It will also be true that

$$\mathbf{n} \cdot \epsilon \mathbf{E} = \rho_s$$

$$\mathbf{n} \times \mathbf{H} = \mathbf{J}_s$$

For a perfect magnetic conductor (PMC) the boundary conditions will be

$$\mathbf{n} \times \mathbf{H} = 0, \quad (17)$$

$$\mathbf{n} \cdot \mathbf{E} = 0. \quad (18)$$

See Balanis [?] for further details.

4.1 Symmetry Boundary Conditions

Sometimes it is convenient to define a *symmetry* boundary condition on a flat boundary of the computational domain.

Consider, for example, a symmetry boundary at $x = 0$. From Maxwell's equations (9)-(14) we see that the equations are preserved under the transformation $x \rightarrow -x$ provided the solution satisfies

$$\begin{aligned} E_x &\rightarrow E_x, \quad E_y \rightarrow -E_y, \quad E_z \rightarrow -E_z, \\ H_x &\rightarrow -H_x, \quad H_y \rightarrow H_y, \quad H_z \rightarrow H_z. \end{aligned}$$

In the general case this condition will be

$$\mathbf{n} \cdot \mathbf{E} = \text{has even symmetry}, \quad \mathbf{n} \cdot \mathbf{E}(-x, y, z, t) = \mathbf{n} \cdot \mathbf{E}(+x, y, z, t) \quad (19)$$

$$\tau \cdot \mathbf{E} = \text{has odd symmetry}, \quad \tau \cdot \mathbf{E}(-x, y, z, t) = 2\tau \cdot \mathbf{E}(0, y, z, t) - \tau \cdot \mathbf{E}(+x, y, z, t) \quad (20)$$

$$\mathbf{n} \cdot \mathbf{H} = \text{has odd symmetry}, \quad \mathbf{n} \cdot \mathbf{H}(-x, y, z, t) = 2\mathbf{n} \cdot \mathbf{H}(0, y, z, t) - \mathbf{n} \cdot \mathbf{H}(+x, y, z, t) \quad (21)$$

$$\tau \cdot \mathbf{H} = \text{has even symmetry}, \quad \tau \cdot \mathbf{H}(-x, y, z, t) = \tau \cdot \mathbf{H}(+x, y, z, t) \quad (22)$$

Here $\tau \cdot \mathbf{E}$ denotes a tangential component of the field (we could also have written $\mathbf{n} \times \mathbf{E}$). Note that for the *odd* symmetry condition we do not need to require the odd component to be zero at $x = 0$. This symmetry condition is closely related to the PEC boundary condition (15).

There is another symmetry condition that corresponds to the PMC boundary condition where we change even to odd in the above symmetry conditions.

We thus have a choice in symmetry conditions to use at a *symmetry* boundary.

5 Two Dimensions

There are a variety of two-dimensional variations of Maxwell's equation. The so-called TE_Z mode satisfies the equations

$$\begin{aligned}\partial_t E_x - \frac{1}{\epsilon} \partial_y H_z &= 0 \\ \partial_t E_y + \frac{1}{\epsilon} \partial_x H_z &= 0 \\ \partial_t H_z + \frac{1}{\mu} [\partial_x E_y - \partial_y E_x] &= 0\end{aligned}$$

This solution represents an **E**-field propagating in the z -direction with non-zero components only in the transverse x and y directions.

6 Yee Scheme

The Yee scheme in two dimensions on a rectangular grid is defined by

$$D_{+t}(E_x)_{i+\frac{1}{2},j}^{n-\frac{1}{2}} = \frac{1}{\epsilon} D_{-y} H_{i+\frac{1}{2},j+\frac{1}{2}}^n \quad (23)$$

$$D_{+t}(E_y)_{ij+\frac{1}{2}}^{n-\frac{1}{2}} = -\frac{1}{\epsilon} D_{-x} H_{i+\frac{1}{2},j+\frac{1}{2}}^n \quad (24)$$

$$D_{+t} H_{i+\frac{1}{2},j+\frac{1}{2}}^n = \frac{1}{\mu} \left[-D_{+x}(E_y)_{i,j+\frac{1}{2}}^{n+\frac{1}{2}} + D_{+y}(E_x)_{i+\frac{1}{2},j}^{n+\frac{1}{2}} \right] \quad (25)$$

$$(26)$$

or

$$\begin{aligned}D_{+t} u_{i+\frac{1}{2},j}^{n-\frac{1}{2}} &= D_{-y} w_{i+\frac{1}{2},j+\frac{1}{2}}^n \\ D_{+t} v_{ij+\frac{1}{2}}^{n-\frac{1}{2}} &= -D_{-x} w_{i+\frac{1}{2},j+\frac{1}{2}}^n \\ D_{+t} w_{i+\frac{1}{2},j+\frac{1}{2}}^n &= \left[-D_{+x} v_{i,j+\frac{1}{2}}^{n+\frac{1}{2}} + D_{+y} u_{i+\frac{1}{2},j}^{n+\frac{1}{2}} \right]\end{aligned}$$

To get a discrete energy estimate on a periodic domain we multiply the last equation by $(w_{i+\frac{1}{2},j+\frac{1}{2}}^n + w_{i+\frac{1}{2},j+\frac{1}{2}}^{n-1})$ and use summation by parts

$$\begin{aligned}\sum_{ij} |w_{i+\frac{1}{2},j+\frac{1}{2}}^n|^2 - |w_{i+\frac{1}{2},j+\frac{1}{2}}^{n-1}|^2 &= \sum_{ij} \left\{ -(w_{i+\frac{1}{2},j+\frac{1}{2}}^n + w_{i+\frac{1}{2},j+\frac{1}{2}}^{n-1}) D_{+x} v_{i,j+\frac{1}{2}}^{n+\frac{1}{2}} \right. \\ &\quad \left. + (w_{i+\frac{1}{2},j+\frac{1}{2}}^n + w_{i+\frac{1}{2},j+\frac{1}{2}}^{n-1}) D_{+y} u_{i+\frac{1}{2},j}^{n+\frac{1}{2}} \right\} \\ &= \sum_{ij} \left\{ + D_{-x} (w_{i+\frac{1}{2},j+\frac{1}{2}}^n + w_{i+\frac{1}{2},j+\frac{1}{2}}^{n-1}) v_{i,j+\frac{1}{2}}^{n+\frac{1}{2}} \right. \\ &\quad \left. - D_{-y} (w_{i+\frac{1}{2},j+\frac{1}{2}}^n + w_{i+\frac{1}{2},j+\frac{1}{2}}^{n-1}) u_{i+\frac{1}{2},j}^{n+\frac{1}{2}} \right\}\end{aligned}$$

From the equation for u we can derive the expression

$$\begin{aligned}u_{i+\frac{1}{2},j}^{n+\frac{1}{2}} D_{+t} u_{i+\frac{1}{2},j}^{n+\frac{1}{2}} + u_{i+\frac{1}{2},j}^{n+\frac{1}{2}} D_{+t} u_{i+\frac{1}{2},j}^{n-\frac{1}{2}} &= u_{i+\frac{3}{2},j}^{n+\frac{1}{2}} u_{i+\frac{1}{2},j}^{n+\frac{1}{2}} - u_{i+\frac{1}{2},j}^{n+\frac{1}{2}} u_{i+\frac{1}{2},j}^{n-\frac{1}{2}} \\ &= D_{+t} u_{i+\frac{1}{2},j}^{n+\frac{1}{2}} u_{i+\frac{1}{2},j}^{n-\frac{1}{2}} \\ &= u_{i+\frac{1}{2},j}^{n+\frac{1}{2}} D_{-y} (w_{i+\frac{1}{2},j+\frac{1}{2}}^n + w_{i+\frac{1}{2},j+\frac{1}{2}}^{n-1})\end{aligned}$$

Thus

$$D_{+t} \sum_{ij} |w_{i+\frac{1}{2},j+\frac{1}{2}}^n|^2 + u_{i+\frac{1}{2},j}^{n+\frac{1}{2}} u_{i+\frac{1}{2},j}^{n-\frac{1}{2}} + v_{ij+\frac{1}{2}}^{n+\frac{1}{2}} v_{ij+\frac{1}{2}}^{n-\frac{1}{2}} = 0$$

and the discrete “energy”

$$\mathcal{E} = \sum_{ij} |w_{i+\frac{1}{2},j+\frac{1}{2}}^n|^2 + u_{i+\frac{1}{2},j}^{n+\frac{1}{2}} u_{i+\frac{1}{2},j}^{n-\frac{1}{2}} + v_{ij+\frac{1}{2}}^{n+\frac{1}{2}} v_{ij+\frac{1}{2}}^{n-\frac{1}{2}} \Delta x \Delta y$$

is constant. Note that this “energy” can apparently be negative. However provided Δt satisfies a stability condition one can show (?) that \mathcal{E} is positive.

One can also see that the discrete divergence $\delta_{i,j} = D_{-x}(E_x)_{i+\frac{1}{2},j}^{n-\frac{1}{2}} + D_{-y}(E_y)_{ij+\frac{1}{2}}^{n-\frac{1}{2}}$ is constant since by taking D_{-x} of equation (23) and D_{-y} of equation (24) it follows that

$$D_{+t}\delta_{i,j} = 0$$

7 The DSI scheme

The discrete-surface integral method was first introduced by Madsen [?]. See also the version by Gedney, Lansing and Rascoe [?].

In two dimensions the scheme is defined as follows. See figure (1).

Given the grid points \mathbf{x}_{ij} of the primary mesh define the mesh points of the secondary mesh as the cell centers,

$$\mathbf{x}_{i+\frac{1}{2},j+\frac{1}{2}} = \frac{1}{4} \sum_{\alpha,\beta=0}^1 \mathbf{x}_{i+\alpha,j+\beta} .$$

Then define the vectors

$$\begin{aligned} \Delta \mathbf{x}_{i,j+\frac{1}{2}} &= \mathbf{x}_{i+\frac{1}{2},j+\frac{1}{2}} - \mathbf{x}_{i-\frac{1}{2},j+\frac{1}{2}} \\ \Delta \mathbf{x}_{i+\frac{1}{2},j} &= \mathbf{x}_{i+\frac{1}{2},j+\frac{1}{2}} - \mathbf{x}_{i+\frac{1}{2},j-\frac{1}{2}} \\ \mathbf{n}_{i,j+\frac{1}{2}} &= (-\Delta y_{i,j+\frac{1}{2}}, \Delta x_{i,j+\frac{1}{2}}) \\ \mathbf{n}_{i+\frac{1}{2},j} &= (-\Delta y_{i+\frac{1}{2},j}, \Delta x_{i+\frac{1}{2},j}) \\ \mathbf{p}_{i,j+\frac{1}{2}} &= D_{+y} \mathbf{x}_{ij} \\ \mathbf{p}_{i+\frac{1}{2},j} &= D_{+x} \mathbf{x}_{ij} \end{aligned}$$

We first advance

$$D_{+t}(\mathbf{E} \cdot \mathbf{n})_{i+\frac{1}{2},j}^{n-\frac{1}{2}} = \frac{1}{\epsilon} [D_{-y} H_{i+\frac{1}{2},j+\frac{1}{2}}^n] \quad (27)$$

$$D_{+t}(\mathbf{E} \cdot \mathbf{n})_{ij+\frac{1}{2}}^{n-\frac{1}{2}} = -\frac{1}{\epsilon} [D_{-x} H_{i+\frac{1}{2},j+\frac{1}{2}}^n] \quad (28)$$

The first equation gives one component of the $\mathbf{E}_{i+\frac{1}{2},j}^{n+\frac{1}{2}}$ field on each “vertical” face of the secondary cell.

To get the full $\mathbf{E}_{i+\frac{1}{2},j}^{n+\frac{1}{2}}$ -vector we make use of 4 nearby values on the horizontal faces, $(\mathbf{E} \cdot \mathbf{n})_{i+\alpha,j-\frac{1}{2}+\beta}^{n+\frac{1}{2}}$, $\alpha = 0, 1$, $\beta = 0, 1$. We solve the system

$$\begin{aligned} \mathbf{E}_{\alpha\beta} \cdot \mathbf{n}_{i+\frac{1}{2},j} &= g_0 \equiv (\mathbf{E} \cdot \mathbf{n})_{i+\frac{1}{2},j}^{n+\frac{1}{2}} \\ \mathbf{E}_{\alpha\beta} \cdot \mathbf{n}_{i+\alpha,j-\frac{1}{2}+\beta} &= g_{\alpha\beta} \equiv (\mathbf{E} \cdot \mathbf{n})_{i+\alpha,j-\frac{1}{2}+\beta}^{n+\frac{1}{2}} \end{aligned}$$

To give 4 possible values, $\mathbf{E}_{\alpha\beta}$ for $\mathbf{E}_{i+\frac{1}{2},j}^{n+\frac{1}{2}}$. We average these values

$$\mathbf{E}_{i+\frac{1}{2},j}^{n+\frac{1}{2}} = \sum w_{\alpha\beta} \mathbf{E}_{\alpha\beta}$$

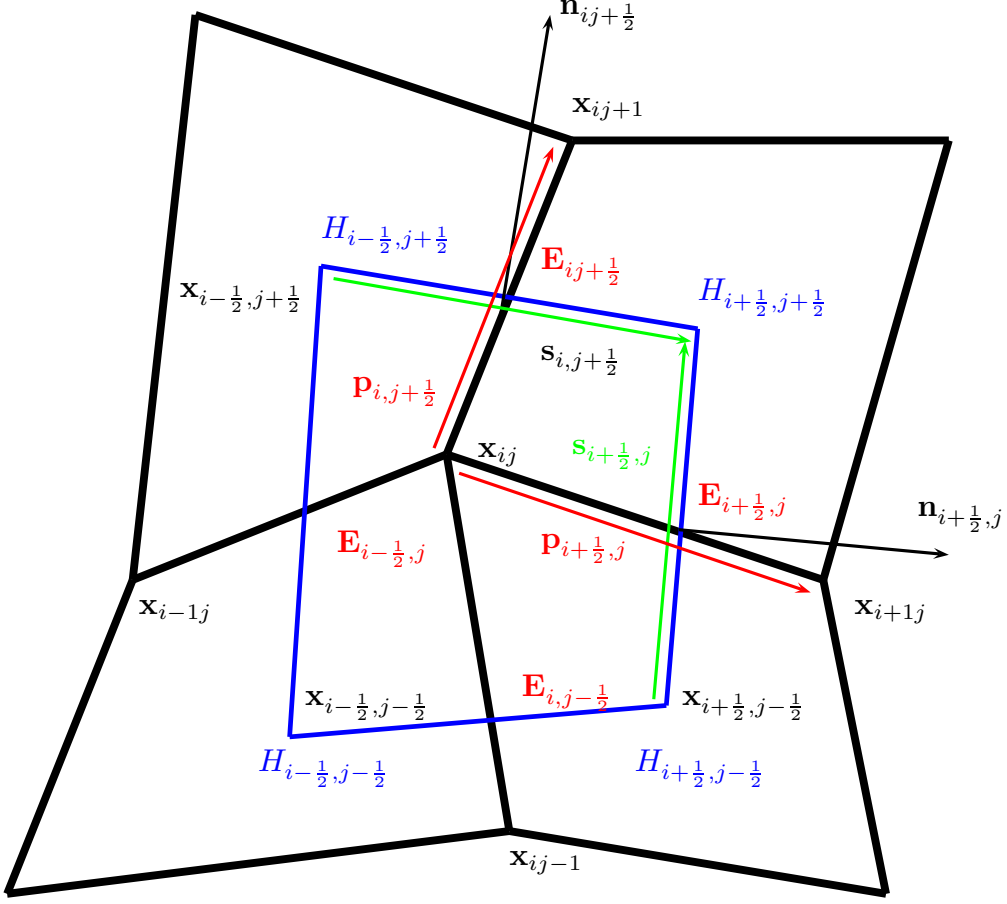


Figure 1: The two dimensional DSI scheme. H is centered in the middle of the primary cell and the \mathbf{E} values are located on the faces of the primary cell. The secondary cell joins the cell centres.

Similarly we compute $\mathbf{E}_{i,j+\frac{1}{2}}^{n+\frac{1}{2}}$ on all “horizontal” faces.

NOTE: In the Madsen paper the time derivative of \mathbf{E} is obtained by the above averaging procedure rather than \mathbf{E} itself. Gedney et.al. use the above approach.

Given the \mathbf{E} field on all faces the \mathbf{H} field is obtained from

$$D_{+t} H_{i+\frac{1}{2},j+\frac{1}{2}}^n = \frac{1}{\mu} \left[-D_{+x}(\mathbf{E} \cdot \mathbf{p})_{i,j+\frac{1}{2}}^{n+\frac{1}{2}} + D_{+y}(\mathbf{E} \cdot \mathbf{p})_{i+\frac{1}{2},j}^{n+\frac{1}{2}} \right] / \Delta A_{i+\frac{1}{2},j+\frac{1}{2}}$$

where $\Delta A_{i+\frac{1}{2},j+\frac{1}{2}}$ is the area of the primary cell centred at $\mathbf{x}_{i+\frac{1}{2},j+\frac{1}{2}}$.

Discrete divergence What about the discrete divergence of \mathbf{E} ? Taking D_{-x} of equation (27) and D_{-y} of equation (28) shows that

$$D_{+t} \left(D_{-x}(\mathbf{E} \cdot \mathbf{n})_{i+\frac{1}{2},j}^{n-\frac{1}{2}} + D_{-y}(\mathbf{E} \cdot \mathbf{n})_{ij+\frac{1}{2}}^{n-\frac{1}{2}} \right) = 0$$

and thus $\delta_{ij} = D_{-x}(\mathbf{E} \cdot \mathbf{n})_{i+\frac{1}{2},j}^{n-\frac{1}{2}} + D_{-y}(\mathbf{E} \cdot \mathbf{n})_{ij+\frac{1}{2}}^{n-\frac{1}{2}}$ remains constant.

7.1 Stability of the DSI scheme

The report by Brandon and Rambo [?] points out that the DSI scheme may become unstable for long time integrations. They present a stability analysis in 2D for the so-called “chevron” grid and show that the scheme is unconditionally unstable for this grid.

Gedney et.al.[?] also report the instability.

Consider the so-called Chevron grid which is a perturbed Cartesian grid,

$$\begin{aligned}x_{ij} &= i\Delta x \\y_{i,j} &= j\Delta y + (-1)^i \delta/2 \\\tan(\theta) &= \delta/\Delta x\end{aligned}$$

Consider a discretization of the TEz equations

$$\begin{aligned}u_t &= w_y \\v_t &= -w_x \\w_t &= u_y - v_x\end{aligned}$$

using the DSI approach:

$$\begin{aligned}\Delta x \Delta y \partial_t w_{ij} &= -\Delta y \Delta_{+r} v_{i-\frac{1}{2}} + \Delta x \Delta_{+s} (\mathbf{p}_{j-\frac{1}{2}} \cdot \mathbf{u}_{j-\frac{1}{2}}) \\\Delta y \partial_t u_{i,j-\frac{1}{2}} &= \Delta_{+s} w_{j-1} \\\Delta x \partial_t v_{i,j-\frac{1}{2}} &= -\Delta_{+r} w_{i-1} \\\mathbf{p}_{j-\frac{1}{2}} \cdot \mathbf{u}_{j-\frac{1}{2}} &= u_{j-\frac{1}{2}} - (-1)^i \tan(\theta) \bar{v}_{j-\frac{1}{2}} \\\bar{v}_{j-\frac{1}{2}} &= \frac{1}{4} [v_{i-\frac{1}{2},j-1} + v_{i-\frac{1}{2},j+1} + v_{i+\frac{1}{2},j+1}]\end{aligned}$$

It follows that

$$D_{+t} D_{-t} w_{ij} = D_{+x} D_{-x} w_{ij} + D_{+y} D_{-y} w_{ij} + (-1)^i \tan(\theta) D_{0x} D_{0y} w_{ij}$$

Note that the equation for w_{ij} changes for i even or odd. It is evident that this method will probably not be stable since this last difference operator is not self-adjoint. To proceed with the analysis introduce

$$\begin{aligned}U_{ij}^n &= w_{ij}^n && \text{for } i \text{ even} \\V_{ij}^n &= w_{ij}^n && \text{for } i \text{ odd}\end{aligned}$$

and make the anstaz

$$\begin{aligned}U_{ij}^n &= \kappa^n \hat{U}_{\mathbf{k}} e^{i(k_x x_{ij} + k_y y_{ij})} \\V_{ij}^n &= \kappa^n \hat{V}_{\mathbf{k}} e^{i(k_x x_{ij} + k_y y_{ij})}\end{aligned}$$

Then

$$\begin{aligned}[A(\kappa) - B(\mathbf{k})] \hat{U}_{\mathbf{k}} &= (C(\mathbf{k}) - D(\mathbf{k})) \hat{V}_{\mathbf{k}} \\[A(\kappa) - B(\mathbf{k})] \hat{V}_{\mathbf{k}} &= (C(\mathbf{k}) + D(\mathbf{k})) \hat{V}_{\mathbf{k}} \\A(\kappa) &= (\kappa - 2 + \kappa^{-1})/\Delta t^2 \\B(\mathbf{k}) &= -2/\Delta x^2 - 4 \sin^2(\xi_y/2)/\Delta y^2 \\C(\mathbf{k}) &= 2 \cos(\xi_x)/\Delta x^2 \\D(\mathbf{k}) &= \tan(\theta) \sin(\xi_x) \sin(\xi_y)/(\Delta x \Delta y) \\\xi_x &= k_x \Delta x \\\xi_y &= k_y \Delta y\end{aligned}$$

Therefore

$$\begin{aligned}[A(\kappa) - B(\mathbf{k})]^2 \hat{U}_{\mathbf{k}} &= (C(\mathbf{k}) - D(\mathbf{k}))(C(\mathbf{k}) + D(\mathbf{k})) \hat{U}_{\mathbf{k}} \\ &= (C^2(\mathbf{k}) - D^2(\mathbf{k})) \hat{U}_{\mathbf{k}}\end{aligned}$$

Whence

$$\begin{aligned}A(\kappa) &= B(\mathbf{k}) + \left\{ C^2(\mathbf{k}) - D^2(\mathbf{k}) \right\}^{1/2} \\ &= -2/\Delta x^2 - 4 \sin^2(\xi_y/2)/\Delta y^2 + \left\{ (2 \cos(\xi_x)/\Delta x^2)^2 - (\tan(\theta) \sin(\xi_x) \sin(\xi_y)/(\Delta x \Delta y))^2 \right\}^{1/2}\end{aligned}$$

The method will be unstable if the right-hand side of this last expression has a non-zero imaginary part. The method will thus be unstable if

$$|\tan(\theta)| > \frac{|2 \cos(\xi_x)|}{|\sin(\xi_x) \sin(\xi_y)|} \frac{\Delta y}{\Delta x}$$

When $\xi_x = \pi/2$ this condition will hold for any perturbation angle θ with $\tan(\theta) \neq 0$ and $\sin(\xi_y) \neq 0$.

7.2 Artificial diffusion

We can add a second-order artificial diffusion to the DSI scheme

$$\begin{aligned}D_{+t}(\mathbf{E} \cdot \mathbf{n})_{i+\frac{1}{2},j}^{n-\frac{1}{2}} &= \frac{1}{\epsilon} [D_{-y} H_{i+\frac{1}{2},j+\frac{1}{2}}^n] + C_2(\Delta_{+x} \Delta_{-x} + \Delta_{+y} \Delta_{-y})(\mathbf{E} \cdot \mathbf{n})_{i+\frac{1}{2},j}^{n-\frac{1}{2}} \\ D_{+t}(\mathbf{E} \cdot \mathbf{n})_{ij+\frac{1}{2}}^{n-\frac{1}{2}} &= -\frac{1}{\epsilon} [D_{-x} H_{i+\frac{1}{2},j+\frac{1}{2}}^n] + C_2(\Delta_{+x} \Delta_{-x} + \Delta_{+y} \Delta_{-y})(\mathbf{E} \cdot \mathbf{n})_{ij+\frac{1}{2}}^{n-\frac{1}{2}} \\ D_{+t} H_{i+\frac{1}{2},j+\frac{1}{2}}^n &= \frac{1}{\mu} \left[-D_{+x}(\mathbf{E} \cdot \mathbf{p})_{i,j+\frac{1}{2}}^{n+\frac{1}{2}} + D_{+y}(\mathbf{E} \cdot \mathbf{p})_{i+\frac{1}{2},j}^{n+\frac{1}{2}} \right] / \Delta A_{i+\frac{1}{2},j+\frac{1}{2}} \\ &\quad + C_2(\Delta_{+x} \Delta_{-x} + \Delta_{+y} \Delta_{-y}) H_{i+\frac{1}{2},j+\frac{1}{2}}^n\end{aligned}$$

This will stabilize the scheme but will in general add excessive dissipation. A fourth-order dissipation could also be used. It could be that this dissipation could be added locally in order to stabilize the scheme.

8 Stability

First consider the first-order wave equation, $u_t + cu_x = 0$, on a periodic domain discretized with leap-frog,

$$U_i^{n+1} - U_i^{n-1} + \lambda(U_{i+1}^n - U_{i-1}^n) = 0$$

where $\lambda = c\Delta t/h$. We look for solutions of the form $U_j^n = \kappa^n e^{i2\pi\omega x_j}$. The characteristic equation is

$$\kappa^2 + \lambda(e^{i\xi} - e^{-i\xi})\kappa - 1 = 0$$

or

$$\kappa^2 + (2i\lambda \sin(\xi))\kappa - 1 = 0$$

where $\xi = 2\pi\omega h$. Letting $b = \lambda \sin(\xi)$, the roots are

$$\kappa = -ib \pm \sqrt{1 - b^2}$$

If $|b| \leq 1$ then

$$|\kappa|^2 = b^2 + 1 - b^2 = 1$$

and the scheme is neutrally stable.

Now consider the second-order wave equation in 1D, $u_{tt} - c^2 u_{xx} = 0$ discretized with the centred scheme,

$$U_i^{n+1} - 2U_i^n + U_i^{n-1} - \lambda(U_{i+1}^n - 2U_i^n + U_{i-1}^n) = 0$$

where $\lambda = (c\Delta t/h)^2$. The characteristic equation is (symbol)

$$\kappa^2 - 2[1 - \lambda + \lambda \cos(\xi)]\kappa + 1$$

if $b = 1 + \lambda(\cos(\xi) - 1)$ then

$$\kappa = b \pm \sqrt{b^2 - 1}$$

If $|b| \leq 1$ then

$$|\kappa|^2 = b^2 + 1 - b^2 = 1$$

Thus the scheme is stable if

$$\lambda = (c\Delta t/h)^2 \leq 1$$

In two dimensions we get a similar expression with $b = 1 + \lambda_x(\cos(\xi_x) - 1) + \lambda_y(\cos(\xi_y) - 1)$ and we again find that $|\kappa| = 1$ if $|b| \leq 1$. For stability we require $\lambda_x + \lambda_y \leq 1$,

$$(c\Delta t/h_x)^2 + (c\Delta t/h_y)^2 \leq 1$$

or

$$\Delta t \leq \frac{1}{c}[(1/h_x)^2 + (1/h_y)^2]^{-1/2} \quad (29)$$

Consider the general time stepping method

$$V^{n+1} - 2V^n + V^{n-1} = AU_i$$

for a vector $V \in \mathbb{R}^N$ and matrix $A \in \mathbb{R}^{N \times N}$. If A is diagonalizable, $A = S^{-1}\Lambda S$, then we can write the system of equations as a set of decoupled equations,

$$v_m^{n+1} - 2v_m^n + v_m^{n-1} = \lambda_m v_m^n$$

where λ_m are the eigenvalues of A and v_m the eigenvectors. Looking for a solution of the form $v_m^n = \kappa^n$ gives the characteristic equation:

$$\kappa^2 - 2[1 + \frac{1}{2}\lambda_m]\kappa + 1$$

Letting $b = 1 + \frac{1}{2}\lambda_m$ then

$$\kappa = b \pm \sqrt{b^2 - 1}$$

and if b is real and $|b| \leq 1$ then

$$|\kappa|^2 = b^2 + 1 - b^2 = 1$$

Thus the scheme is stable if λ_m is real and $\lambda_m < 0$ and

$$|1 + \frac{1}{2}\lambda_m| \leq 1$$

i.e.

$$-4 \leq \lambda_m \leq 0 \quad (30)$$

8.1 Time step limit with artificial dissipation

Consider the addition of an artificial dissipation term of the form

$$u_{tt} - c^2 \Delta u - \delta(-h^2 \Delta)^p u_t = 0$$

In one dimension this equation is discretized as

$$U_i^{n+1} - 2U_i^n + U_i^{n-1} - \lambda(U_{i+1}^n - 2U_i^n + U_{i-1}^n) - \delta \Delta t (-\Delta_+ \Delta_-)^p (U^n - U^{n-1}) = 0$$

where $\lambda = (c \Delta t / h)^2$. Proceeding with the stability analysis leads to the characteristic equation

$$\kappa^2 - 2[1 - \lambda + \lambda \cos(\xi) - a/2]\kappa + 1 - a = 0$$

where

$$a = \delta \Delta t (4 \sin^2(\xi/2))^p$$

Letting $b = 1 + \lambda(\cos(\xi) - 1) - a/2$ then

$$\kappa = b \pm \sqrt{b^2 + a - 1}$$

If $b^2 + a \leq 1$ then

$$|\kappa|^2 = b^2 + 1 - b^2 - a = 1 - a$$

Thus the scheme is stable if $\delta \geq 0$. If $b^2 + a \leq 1$, then

$$(1 - a/2 - 2\lambda \sin^2(\xi/2))^2 + a \leq 1$$

or

$$\begin{aligned} -\sqrt{1-a} &\leq 1 - a/2 - 2\lambda \sin^2(\xi/2) \leq \sqrt{1-a} \\ 2\lambda \sin^2(\xi/2) &\leq 1 - a/2 + \sqrt{1-a} \end{aligned}$$

Making the assumption that $a \ll 1$ leads to

$$\lambda \leq 1 - a/2 + O(a^2)$$

Writing $a/2 = \beta \Delta t$, and $\lambda = \Delta t^2/\gamma$, then

$$\begin{aligned} \Delta t^2 &\leq \gamma - \beta \gamma \Delta t \\ \Delta t^2 + \beta \gamma \Delta t &\leq \gamma \\ (\Delta t + \beta \gamma/2)^2 &\leq \gamma + \beta^2 \gamma^2/4 \\ \Delta t &\leq \sqrt{\gamma + \beta^2 \gamma^2/4} - \beta \gamma/2 \end{aligned}$$

Thus we have the stability condition

$$\begin{aligned} \Delta t &\leq \sqrt{\gamma + \beta^2 \gamma^2/4} - \beta \gamma/2 \\ &\approx \sqrt{\gamma} - \beta \gamma/2 \end{aligned}$$

where γ is the square of the time step that would be chosen when $\beta = 0$,

$$\gamma = \frac{1}{c^2(h_x^{-2} + h_y^{-2})} = \Delta t_0^2$$

and

$$\beta = \frac{\delta}{2}(4)^p$$

Thus we choose the time step by (**check this**)

$$\Delta t = \Delta t_0 - \frac{\delta}{4}(4)^p \Delta t_0^2$$

9 Analysis of Gedney et. al

In “Numerical Stability of NonorthogonalFDTD Methods” Gedney and Roden[?] write the general scheme (i.e. including the NFDTD [?], DSI schemes) in the form

$$\begin{aligned}\mathbf{b}^n &= \mathbf{b}^{n-1} - \Delta t C_e D_e A_d \mathbf{d}^{n-\frac{1}{2}} \\ \mathbf{d}^{n+\frac{1}{2}} &= \mathbf{d}^{n-\frac{1}{2}} + \Delta t C_h A_b \mathbf{b}^n\end{aligned}$$

Here

- C_e : Contour integral of electric field
- D_e : Matrix of inverse relative permittivity
- A_d : Averaging (projection) operator for the electric field
- C_h : Contour integral of the magnetic field
- A_b : Averaging (projection) operator for the magnetic field

We can eliminate \mathbf{d} or \mathbf{b} to obtain the schemes

$$\mathbf{b}^{n+1} - 2\mathbf{b}^n + \mathbf{b}^{n-1} = -\Delta t^2 C_e D_e A_d C_h A_b \mathbf{b}^n$$

and

$$\mathbf{d}^{n+\frac{3}{2}} - 2\mathbf{d}^{n+\frac{1}{2}} + \mathbf{d}^{n-\frac{1}{2}} = -\Delta t^2 C_h A_b C_e D_e A_d \mathbf{d}^{n+\frac{1}{2}}$$

Define the matrices

$$\begin{aligned}M &= C_h A_b C_e D_e A_d \\ \tilde{M} &= C_e D_e A_d C_h A_b\end{aligned}$$

The scheme will be stable provided the eigenvalues of M are real and non-negative and M has a complete set of eigenvectors. A sufficient condition is that M be symmetric positive definite.

From the general stability argument (30) we know that the time step restriction will be

$$\Delta t^2 \max \lambda(M) < 4$$

To symmetrize M w.r.t. the permittivity matrix D_e Gedney and Roden[?] write

$$M \approx C_h A_b C_e D_e^{\frac{1}{2}} A_d D_e^{\frac{1}{2}}$$

and wave their hands a it about why this is ok. Computations show that it is accurate.

In general it is difficult to choose the projection matrices A_d and A_b to be symmetric.

They show how to built a symmetric operator for a structured grid.

For the general DSI type scheme on unstructured grids they find they can choose

$$A_b \approx \frac{1}{2}(A_b + A_b^T)$$

and this works well for quadrilateral prism elements (i.e. an unstructured grid in 2 dimensions and structured in the 3rd) but not more general elements such as tetrahedra.

10 Energy Estimates

For references see the book by Gustafsson Kreiss and Oliger[?] and the paper by Kreiss, Petersson and Yström[?].

For the second order wave equation

$$w_{tt} = \nabla \cdot (c^2 \nabla w)$$

we can get an energy estimate on a periodic domain from

$$\begin{aligned} (w_t, w_{tt}) &= (w_t, \nabla \cdot (c^2 \nabla w)) \\ \frac{1}{2} \partial_t \|w_t\|^2 &= -(\nabla w_t, c^2 \nabla w) \\ \frac{1}{2} \partial_t \{\|w_t\|^2 + \|c \nabla w\|^2\} &= 0 \end{aligned}$$

and thus $\mathcal{E} = \|w_t\|^2 + \|c \nabla w\|^2$ is constant on a periodic domain.

On a rectangular domain we can use the approximation

$$D_{+t} D_{-t} w_i^n = (D_{+x} D_{-x} + D_{+y} D_{-y}) w_i^n$$

To get an energy estimate (on a periodic domain) we follow[?]

$$\begin{aligned} w^{n+1} + w^{n-1} &= 2w^n + \Delta t^2 A w^n \\ (w^{n+1} - w^{n-1}, w^{n+1} + w^{n-1})_h &= (w^{n+1}, (2I + \Delta t^2 A) w^n) - (w^{n-1}, (2I + \Delta t^2 A) w^n) \\ &= (w^{n+1}, (2I + \Delta t^2 A) w^n) - (w^n, (2I + \Delta t^2 A) w^{n-1}) \quad (\text{using } A = A^*) \end{aligned}$$

Adding $\|w^n\|_h^2$ to both side and re-arranging terms gives

$$\begin{aligned} \|w^{n+1}\|_h^2 + \|w^n\|_h^2 - (w^{n+1}, (2I + \Delta t^2 A) w^n) &= \|w^n\|_h^2 + \|w^{n-1}\|_h^2 - (w^n, (2I + \Delta t^2 A) w^{n-1}) \\ \|w^{n+1} - w^n\|_h^2 - \Delta t^2 (w^{n+1}, Aw^n) &= \|w^n - w^{n-1}\|_h^2 - \Delta t^2 (w^n, Aw^{n-1}) \end{aligned}$$

and thus the discrete energy

$$\mathcal{E}_h^n = \frac{1}{\Delta t^2} \|w^n - w^{n-1}\|^2 - (w^n, Aw^{n-1})$$

remains constant. In order to be an energy norm we want this quantity to be positive definite. We can write \mathcal{E}_h^n in the form

$$\mathcal{E}_h^n = \frac{1}{\Delta t^2} (w^{n+1} - w^n, (I + \frac{\Delta t^2}{4} A)(w^n - w^n)) - \frac{1}{4} (w^{n+1} + w^n, A(w^{n+1} + w^n))$$

and thus

$$\mathcal{E}_h^n \geq \frac{1}{\Delta t^2} \left(1 - \frac{\Delta t^2}{4} |\lambda_{\max}| \right) \|w^{n+1} - w^n\|^2 + \frac{1}{4} |\lambda_{\min}| \|w^{n+1} + w^n\|^2$$

Whence if we choose

$$\frac{\Delta t^2}{4} \max |\lambda_m| \leq 1 - \delta \Delta t^2$$

then \mathcal{E}_h is positive definite with

$$\mathcal{E}_h^n \geq M \{\|w^{n+1} - w^n\|^2 + \|w^{n+1} + w^n\|^2\}$$

where $M = \min(\delta, \frac{1}{4} |\lambda_{\min}|)$.

11 The Non-orthogonal FDTD method of Lee, Palandech and Mittra

The NFDTD method of Lee, Palandech and Mittra[?] is given as follows. Introduce the contravariant components E^i and covariant components E_i from

$$\begin{aligned}\mathbf{E} &= \sum_i E^i \mathbf{x}_{r_i} = \sum_i E^i \mathbf{A}_i \\ \mathbf{E} &= \sum_i E_i \nabla_{\mathbf{x}} r_i = \sum_i \mathbf{A}^i E_i\end{aligned}$$

with $\mathbf{A}^i \cdot \mathbf{A}_j = \delta_{ij}$ and $\mathbf{E} \cdot \mathbf{A}^i = E^i$, $\mathbf{E} \cdot \mathbf{A}_i = E_i$.

Then E^i are the natural faced based values and E_i the natural edge based values.

The face centered values for E^i are advanced in terms of the edge based values for H_i

$$D_{+t} E_{ijk}^{1,n} = \frac{\Delta t}{\epsilon J} \left(D_{+r_2} H_{3,j-\frac{1}{2}}^{n+\frac{1}{2}} - D_{+r_3} H_{2,k-\frac{1}{2}}^{n+\frac{1}{2}} \right)$$

Similarly for H^i from E_i ,

To convert H^i into H_i we use

$$\mathbf{A}_i = \sum_j g_{ij} \mathbf{A}^j \quad , g_{ij} = \mathbf{A}_i \cdot \mathbf{A}_j$$

We approximate

$$H_i = \sum_j g_{ij} H^j$$

as

$$H_1 = g_{11} H^1 + \frac{g_{12}}{4} \left[\sum H_{i \pm \frac{1}{2}, j \pm \frac{1}{2}}^2 \right] + \frac{g_{13}}{4} \left[\sum H_{i \pm \frac{1}{2}, k \pm \frac{1}{2}}^3 \right]$$

This scheme does not result in a symmetric approximation. Gedney and Roden show a way to symmetrize the scheme.

12 Symmetric Difference Approximations on Curvilinear Grids

Here is a conservative approximation to the operator $Lw = \nabla \cdot (a\nabla w)$

$$\begin{aligned}\nabla \cdot (a\nabla w) &= \frac{1}{J} \{ \partial_r(\mathbf{a}_1 \cdot (a\nabla w)) + \partial_s(\mathbf{a}_2 \cdot (a\nabla w)) \} \\ \nabla w &= (r_x w_r + s_x w_s, r_y w_r + s_y w_s) \\ &= (\nabla_{\mathbf{x}} r \cdot \nabla_{\mathbf{r}} w, \nabla_{\mathbf{x}} s \cdot \nabla_{\mathbf{r}} w) \\ \mathbf{a}_m &= J \nabla_{\mathbf{x}} r_m = J(\partial_x r_m, \partial_y r_m) \\ \mathbf{a}_1 &= J(r_x, r_y) \\ \mathbf{a}_2 &= J(s_x, s_y) \\ J &= |\partial_{\mathbf{r}} \mathbf{x}|\end{aligned}$$

The operator can be written in the form

$$Lw = \nabla \cdot (a\nabla w) = \frac{1}{J} \left\{ \frac{\partial}{\partial r_1} \left(A^{11} \frac{\partial w}{\partial r_1} \right) + \frac{\partial}{\partial r_2} \left(A^{22} \frac{\partial w}{\partial r_2} \right) + \frac{\partial}{\partial r_1} \left(A^{12} \frac{\partial w}{\partial r_2} \right) + \frac{\partial}{\partial r_2} \left(A^{21} \frac{\partial w}{\partial r_1} \right) \right\}$$

where

$$\begin{aligned}A^{11} &= aJ(r_x^2 + r_y^2) \\ A^{12} &= aJ(r_x s_x + r_y s_y) \\ A^{21} &= A^{12} \\ A^{22} &= aJ(s_x^2 + s_y^2)\end{aligned}$$

This operator is self-adjoint (with periodic boundary conditions) since

$$\begin{aligned}(v, Lw) &= (v, \frac{1}{J} \left\{ \frac{\partial}{\partial r_1} \left(A^{11} \frac{\partial w}{\partial r_1} \right) + \frac{\partial}{\partial r_2} \left(A^{22} \frac{\partial w}{\partial r_2} \right) + \frac{\partial}{\partial r_1} \left(A^{12} \frac{\partial w}{\partial r_2} \right) + \frac{\partial}{\partial r_2} \left(A^{21} \frac{\partial w}{\partial r_1} \right) \right\}) \\ &= -(\partial_{r_1} v, \left(A^{11} \frac{\partial w}{\partial r_1} \right)) - (\partial_{r_2} v, \left(A^{22} \frac{\partial w}{\partial r_2} \right)) - (\partial_{r_1} v, \left(A^{12} \frac{\partial w}{\partial r_2} \right)) - (\partial_{r_2} v, \left(A^{21} \frac{\partial w}{\partial r_1} \right)) \\ &= (\partial_{r_1} (A^{11} \partial_{r_1} v) + \partial_{r_2} (A^{22} \partial_{r_2} v) + \partial_{r_2} (A^{12} \partial_{r_1} v) + \partial_{r_1} (A^{21} \partial_{r_2} v), w) \\ &= (Lv, w)\end{aligned}$$

where we have used $A^{21} = A^{12}$.

A **second-order accurate** compact discretization to this expression is

$$\begin{aligned}\nabla \cdot (a\nabla w) \approx \frac{1}{J} \left\{ D_{+r_1} \left(A_{i_1-\frac{1}{2}}^{11} D_{-r_1} w \right) + D_{+r_2} \left(A_{i_2-\frac{1}{2}}^{22} D_{-r_2} w \right) + \right. \\ \left. D_{0r_1} (A^{12} D_{0r_2} w) + D_{0r_2} (A^{21} D_{0r_1} w) \right\}\end{aligned}$$

where we can define the cell average values for A^{mn} by

$$\begin{aligned}A_{i_1-\frac{1}{2}}^{11} &\equiv \frac{1}{2} (A_{i_1}^{11} + A_{i_1-1}^{11}) \\ A_{i_2-\frac{1}{2}}^{22} &\equiv \frac{1}{2} (A_{i_2}^{22} + A_{i_2-1}^{22})\end{aligned}$$

The question is whether this discrete operator is symmetric. Taking the discrete inner product of v with

$L_h w$ and integrating by parts gives

$$\begin{aligned}
(v, L_h w)_h &= \sum_{\mathbf{i}} v_{\mathbf{i}} \frac{1}{J} \left\{ D_{+r_1} \left(A_{i_1-\frac{1}{2}}^{11} D_{-r_1} w \right) + D_{+r_2} \left(A_{i_2-\frac{1}{2}}^{22} D_{-r_2} w \right) + \right. \\
&\quad \left. D_{0r_1} (A^{12} D_{0r_2} w) + D_{0r_2} (A^{21} D_{0r_1} w) \right\} J \Delta r \Delta s \\
&= - \sum_{\mathbf{i}} D_{-r_1} v_{\mathbf{i}} \left(A_{i_1-\frac{1}{2}}^{11} D_{-r_1} w \right) + D_{-r_2} v_{\mathbf{i}} \left(A_{i_2-\frac{1}{2}}^{22} D_{-r_2} w \right) + \\
&\quad D_{0r_1} v_{\mathbf{i}} (A^{12} D_{0r_2} w) + D_{0r_2} v_{\mathbf{i}} (A^{21} D_{0r_1} w) J \Delta r \Delta s \\
&= \sum_{\mathbf{i}} \frac{1}{J} \left\{ D_{+r_1} \left(A_{i_1-\frac{1}{2}}^{11} D_{-r_1} v \right) + D_{+r_2} \left(A_{i_2-\frac{1}{2}}^{22} D_{-r_2} v \right) + \right. \\
&\quad \left. D_{0r_1} (A^{12} D_{0r_2} v) + D_{0r_2} (A^{21} D_{0r_1} v) \right\} w_{\mathbf{i}} J \Delta r \Delta s \\
&= (L_h v, w)_h.
\end{aligned}$$

Thus L_h is symmetric. We can obtain an energy estimate for the wave equation $w_{tt} = L_h w$ from

$$\begin{aligned}
(w_t, w_{tt})_h &= (w_t, L_h w)_h \\
&= \sum_{\mathbf{i}} w_t \left\{ D_{+r_1} \left(A_{i_1-\frac{1}{2}}^{11} D_{-r_1} w \right) + D_{+r_2} \left(A_{i_2-\frac{1}{2}}^{22} D_{-r_2} w \right) + \right. \\
&\quad \left. D_{0r_1} (A^{12} D_{0r_2} w) + D_{0r_2} (A^{21} D_{0r_1} w) \right\} \Delta r \Delta s \\
&= - \sum_{\mathbf{i}} D_{-r_1} w_t A_{i_1-\frac{1}{2}}^{11} D_{-r_1} w + D_{-r_2} w_t A_{i_2-\frac{1}{2}}^{22} D_{-r_2} w \\
&\quad + D_{0r_1} w_t A^{12} D_{0r_2} w + D_{0r_2} w_t A^{21} D_{0r_1} w \Delta r \Delta s \\
&= - \partial_t \sum A_{i_1-\frac{1}{2}}^{11} |D_{-r_1} w|^2 + A_{i_2-\frac{1}{2}}^{22} |D_{-r_2} w|^2 + A^{12} (D_{0r_1} w) (D_{0r_2} w) \Delta r \Delta s
\end{aligned}$$

and thus

$$\mathcal{E}_h = \|w_t\|_h^2 + \sum A_{i_1-\frac{1}{2}}^{11} |D_{-r_1} w|^2 + A_{i_2-\frac{1}{2}}^{22} |D_{-r_2} w|^2 + A^{12} (D_{0r_1} w) (D_{0r_2} w) \Delta r \Delta s$$

is constant. This will be a positive operator provided the discrete operator satisfies an ellipticity constraint. We have $A^{11} > 0$, $A^{22} > 0$ and

$$\begin{aligned}
|A^{12}| &= aJ|(r_x s_x + r_y s_y)| \\
&\leq aJ \frac{1}{2} (r_x^2 + s_x^2 + r_y^2 + s_y^2) \\
&\leq \frac{1}{2} (A^{11} + A^{22})
\end{aligned}$$

We also have

$$\begin{aligned}
|D_{0r_1} w|^2 &= \left| \frac{1}{2} (D_{+r_1} w + D_{-r_1} w) \right|^2 \\
&\leq \frac{1}{2} (|D_{+r_1} w|^2 + |D_{-r_1} w|^2)
\end{aligned}$$

and thus

$$\begin{aligned}
|A^{12} (D_{0r_1} w) (D_{0r_2} w)| &\leq |A^{12}| |D_{0r_1} w| |D_{0r_2} w| \\
&\leq \frac{1}{2} |A^{12}| (|D_{0r_1} w|^2 + |D_{0r_2} w|^2) \\
&\leq \frac{1}{4} |A^{12}| (|D_{+r_1} w|^2 + |D_{-r_1} w|^2 + |D_{+r_2} w|^2 + |D_{-r_2} w|^2)
\end{aligned}$$

Therefore

$$\begin{aligned}\mathcal{E}_h &\leq \|w_t\|_h^2 + \sum A_{i_1-\frac{1}{2}}^{11} |D_{-r_1} w|^2 + A_{i_2-\frac{1}{2}}^{22} |D_{-r_2} w|^2 \\ &\quad - \frac{1}{4} |A^{12}| (|D_{+r_1} w|^2 + |D_{-r_1} w|^2 + |D_{+r_2} w|^2 + |D_{-r_2} w|^2) \\ &\leq \|w_t\|_h^2 + \sum \frac{1}{2} A_{i_1-\frac{1}{2}}^{11} |D_{-r_1} w|^2 + \frac{1}{2} A_{i_1+\frac{1}{2}}^{11} |D_{+r_1} w|^2 + \frac{1}{2} A_{i_2-\frac{1}{2}}^{22} |D_{-r_2} w|^2 + \frac{1}{2} A_{i_2+\frac{1}{2}}^{22} |D_{+r_2} w|^2 \\ &\quad - \frac{1}{4} |A^{12}| (|D_{+r_1} w|^2 + |D_{-r_1} w|^2 + |D_{+r_2} w|^2 + |D_{-r_2} w|^2)\end{aligned}$$

and we require (***) check this ***)

$$\frac{1}{4} |A^{12}| (|D_{+r_1} w|^2 + |D_{+r_2} w|^2) < \frac{1}{2} A_{i_1+\frac{1}{2}}^{11} |D_{+r_1} w|^2 + \frac{1}{2} A_{i_2+\frac{1}{2}}^{22} |D_{+r_2} w|^2$$

and

$$\frac{1}{4} |A^{12}| (|D_{-r_1} w|^2 + |D_{-r_2} w|^2) < \frac{1}{2} A_{i_1-\frac{1}{2}}^{11} |D_{-r_1} w|^2 + \frac{1}{2} A_{i_2-\frac{1}{2}}^{22} |D_{-r_2} w|^2$$

and we thus a sufficient condition will be (***) could do better**)

$$|A_{i_1, i_2}^{12}| < 2 \min \left\{ A_{i_1+\frac{1}{2}}^{11}, A_{i_1-\frac{1}{2}}^{11}, A_{i_2+\frac{1}{2}}^{22}, A_{i_2-\frac{1}{2}}^{22} \right\}$$

Now suppose we use a centered approximation in time

$$w^{n+1} - 2w^n + w^{n-1} = \Delta t^2 L_h w^n$$

then, as was shown in a previous section, the discrete energy

$$\mathcal{E}_h^n = \frac{1}{\Delta t^2} \|w^n - w^{n-1}\|^2 - (w^n, L_h w^{n-1})$$

will be constant and positive definite provided $\frac{\Delta t^2}{4} \max |\lambda(l_h)| \leq 1 - \delta \Delta t^2$

Now suppose that we want to solve the wave equation posed as a first order system

$$\begin{aligned}\mathbf{u}_t &= \nabla w \\ w_t &= \nabla \cdot \mathbf{u}\end{aligned}$$

where $\mathbf{u} = (u, v)^T$.

In order to recover the above symmetric approximation for L_h we could use an approximation of the form (***** check this **** not finished ***)

$$\begin{aligned}\partial_t U_{i-\frac{1}{2}, j} &= B_1^{-1} \left(A_{i_1-\frac{1}{2}}^{11} D_{-r_1} W + M_{-r_1} A^{12} D_{0r_2} W \right) \\ \partial_t V_{j, j-\frac{1}{2}} &= B_2^{-2} \left(A_{i_2-\frac{1}{2}}^{22} D_{-r_2} W + M_{-r_2} A^{21} D_{0r_1} W \right) \\ \partial_t W_{i, j} &= \frac{1}{J} \left\{ D_{+r_1} \left(B_1 U_{i-\frac{1}{2}, j} \right) + D_{+r_2} \left(B_2 V_{j, j-\frac{1}{2}} \right) \right\} \\ M_{-r_1} u_i &\equiv \frac{1}{2} (u_{i_1} + u_{i_1-1}) \quad (\text{Averaging operator}) \\ D_{+r_1} M_{-r_1} &= D_{0r_1}\end{aligned}$$

where U and V are approximations to the contravariant components of \mathbf{u} .

Thus the energy estimate can be obtained ??

$$\begin{aligned}
(B_1 U, U_t) &= \sum_{ij} U_{i-\frac{1}{2},j} \left(A_{i_1-\frac{1}{2}}^{11} D_{-r_1} W + M_{-r_1} A^{12} D_{0r_2} W \right) \\
&= \sum_{ij} -D_{+r_1} \left(A_{i_1-\frac{1}{2}}^{11} U_{i-\frac{1}{2},j} \right) W - D_{0r_2} \left(M_{-r_1} A^{12} U_{i-\frac{1}{2},j} \right) W \\
(B_2 V, V_t) &= \sum_{ij} V_{j,j-\frac{1}{2}} \left(A_{i_2-\frac{1}{2}}^{22} D_{-r_2} W + M_{-r_2} A^{21} D_{0r_1} W \right) \\
&= \sum_{ij} -D_{+r_2} \left(A_{i_2-\frac{1}{2}}^{22} V_{j,j-\frac{1}{2}} \right) W - D_{0r_1} \left(M_{-r_2} A^{21} V_{j,j-\frac{1}{2}} \right) W
\end{aligned}$$

13 Discrete Boundary Conditions

For perfect electrical conductors (PEC) the boundary conditions for the electric field are

$$\mathbf{n} \times \mathbf{E} = 0 \quad (31)$$

If we let τ_m , $m = 1, d - 1$ denote the tangent vectors at the boundary then

$$\tau_m \cdot \mathbf{E} = 0$$

Since $\nabla \cdot \mathbf{E} = 0$ we can also use the condition

$$\frac{1}{J} \{ \partial_{r_1} (\mathbf{a}_1 \cdot \mathbf{E}) + \partial_{r_2} (\mathbf{a}_2 \cdot \mathbf{E}) + \partial_{r_3} (\mathbf{a}_3 \cdot \mathbf{E}) \} = 0$$

Recall that

$$\mathbf{a}_m = J \nabla_{\mathbf{x}} r_m$$

Now \mathbf{a}_1 is always proportional to the normal to the boundary $r = \text{constant}$. On an orthogonal grid \mathbf{a}_2 and \mathbf{a}_3 lie in the tangent plane and thus $\mathbf{a}_2 \cdot \mathbf{E}$ and $\mathbf{a}_3 \cdot \mathbf{E}$ can be written as linear combinations of the tangential components of \mathbf{E} , (on a boundary $r = \text{constant}$) then the divergence condition becomes

$$\partial_{r_1} (\mathbf{a}_1 \cdot \mathbf{E}) = 0 \quad \text{at } r = 0.$$

13.1 Boundary conditions for the magnetic field

In two-dimensions we have the equations

$$\begin{aligned}
\partial_t E_x - \frac{1}{\epsilon} \partial_y H_z &= 0 \\
\partial_t E_y + \frac{1}{\epsilon} \partial_x H_z &= 0 \\
\partial_t H_z + \frac{1}{\mu} [\partial_x E_y - \partial_y E_x] &= 0
\end{aligned}$$

Taking the dot product of the tangent with the first two equations gives

$$\begin{aligned}
\epsilon (\tau \cdot (E_x, E_y))_t &= (\tau \cdot (\partial_y H_z, -\partial_x H_z)) \\
&= \partial_n H_z
\end{aligned}$$

Thus we have the PEC boundary condition for the magnetic field

$$\partial_n H_z = 0$$

In the general three-dimensional case we have

$$\begin{aligned}\epsilon(\mathbf{n} \times \mathbf{E})_t &= \mathbf{n} \times (\nabla \times \mathbf{H}) \\ &= \mathbf{n} \cdot (\nabla \mathbf{H}) - (\mathbf{n} \cdot \nabla) \mathbf{H} \\ &= n_j \partial_i H_j - n_j \partial_j H_i \quad (\text{component form}) \quad = \tau_m \cdot (\nabla \times \mathbf{H}) \quad (\tau_m \text{ is a tangent vector})\end{aligned}$$

We also have

$$\begin{aligned}\mu \mathbf{n} \cdot \mathbf{H}_t &= -\mathbf{n} \cdot (\nabla \times \mathbf{E}) \\ &= \nabla \cdot (\mathbf{n} \times \mathbf{E}) - \mathbf{E} \cdot (\nabla \times \mathbf{n}) \\ &= \frac{1}{J} \sum_m \partial_{r_m} \{ \mathbf{a}_m \cdot (\mathbf{n} \times \mathbf{E}) \} - \mathbf{E} \cdot (\nabla \times \mathbf{n})\end{aligned}$$

Thus in 3D the boundary conditions for \mathbf{H} are

$$\begin{aligned}\mathbf{n} \cdot \mathbf{H} &= 0 \\ \mathbf{n} \cdot (\nabla \mathbf{H}) - \partial_n \mathbf{H} &= 0\end{aligned}$$

or

$$\begin{aligned}n_j H_j &= 0 \\ n_j \partial_i H_j - n_j \partial_j H_i &= 0\end{aligned}$$

13.2 Second-order accurate boundary conditions

For a second-order accurate scheme we can use (at the boundary $i = 0$)

$$\begin{aligned}\boldsymbol{\tau}_m \cdot \mathbf{E}_{0,j} &= 0 \\ (\mathbf{a}_1 \cdot \mathbf{E})_{-1,j} &= (\mathbf{a}_1 \cdot \mathbf{E})_{+1,j} \\ \boldsymbol{\tau}_m \cdot \mathbf{E}_{-1,j} &= \boldsymbol{\tau}_m \cdot (I - D_+^2) \mathbf{E}_{-1,j} \equiv g_m \quad (\text{extrapolate}) \\ w_{-1,j} &= w_{+1,j}\end{aligned}$$

We use the extrapolation, $\boldsymbol{\tau}_m \cdot D_+^2 \mathbf{E}_{-1,j} = 0$, since this is consistent with the tangential component being an odd function and thus the second-derivative (second-difference) is expected to be zero.

With our assumption of an orthogonal grid is thus follows that electric field at the ghost point is given by

$$\mathbf{E}_{-1,j} = (\mathbf{a}_1 \cdot \mathbf{E})_{+1,j} \frac{\mathbf{a}_1}{\|\mathbf{a}_1\|^2} + g_m \boldsymbol{\tau}_m$$

13.3 Fourth-order accurate boundary conditions

Since $\boldsymbol{\tau}_m \cdot \mathbf{E} = 0$ along the boundary it follows that $\boldsymbol{\tau}_m \cdot \mathbf{E}_{tt} = 0$ and thus

$$\boldsymbol{\tau}_m \cdot \Delta \mathbf{E} = 0 \quad \text{on the boundary}$$

Taking two time derivatives of the divergence equation

$$\partial_{r_1} (\mathbf{a}_1 \cdot \mathbf{E}_{tt}) + \partial_{r_2} (\mathbf{a}_2 \cdot \mathbf{E}_{tt}) + \partial_{r_3} (\mathbf{a}_3 \cdot \mathbf{E}_{tt}) = 0$$

And using the fact that $\partial_{r_2} (\mathbf{a}_2 \cdot \mathbf{E}_{tt})$ and $\partial_{r_3} (\mathbf{a}_3 \cdot \mathbf{E}_{tt})$ are zero on the boundary (If \mathbf{a}_m , $m = 2, 3$ are in the tangent plane, which is true on an orthogonal grid) it follows that the following condition holds on the boundary,

$$\partial_r (\mathbf{a}_1 \cdot \Delta \mathbf{E})(0, r_2, r_3) = 0 \tag{32}$$

Now on an orthogonal grid the Laplacian can be written as

$$\Delta = \sum_{m,n=1}^d c_{mn} \partial_{r_m} \partial_{r_n} + \sum c_m \partial_{r_m} \quad (33)$$

$$= c_{11} \partial_{r_1}^2 + c_{22} \partial_{r_2}^2 + c_{33} \partial_{r_3}^2 + c_{12} \partial_{r_1} \partial_{r_2} + c_{13} \partial_{r_1} \partial_{r_3} + c_{23} \partial_{r_2} \partial_{r_3} + c_1 \partial_{r_1} + c_2 \partial_{r_2} + c_3 \partial_{r_3} \quad (34)$$

(where we have neglected the term $c_{12} \partial_r \partial_s$). Whence equation (32) can be written out in detail as

$$\partial_r (\mathbf{a}_1 \cdot \Delta \mathbf{E}) = \mathbf{a}_1 \cdot \left(\sum_{m,n=1}^d c_{mn} \partial_r \partial_{r_m} \partial_{r_n} + \sum c_m \partial_r \partial_{r_m} \right) \quad (35)$$

$$+ \sum_{m,n=1}^d \partial_r(c_{mn}) \partial_{r_m} \partial_{r_n} + \sum \partial_r(c_m) \partial_{r_m} \Big) + \partial_r \mathbf{a}_1 \cdot \Delta \mathbf{u} \quad (36)$$

$$= \mathbf{a}_1 \cdot \left(c_{11} \mathbf{u}_{rrr} + c_{22} \mathbf{u}_{rss} + c_{33} \mathbf{u}_{rr_3 r_3} + c_1 \mathbf{u}_{rr} + c_2 \mathbf{u}_{rs} + c_3 \mathbf{u}_{rr_3} \right) \quad (37)$$

$$\partial_r c_{11} \mathbf{u}_{rr} + \partial_r c_{22} \mathbf{u}_{ss} + \partial_r c_{33} \mathbf{u}_{r_3 r_3} + \partial_r c_{10} \mathbf{u}_r + \partial_r c_{01} \mathbf{u}_s + \partial_r c_3 \mathbf{u}_{r_3} \Big) \quad (38)$$

$$+ \partial_r \mathbf{a}_1 \cdot \Delta \mathbf{u} = 0 \quad (\text{on the boundary, } r = 0) \quad (39)$$

We wish to avoid a numerical boundary that includes mixed derivative terms such as those involving \mathbf{u}_{rs} or \mathbf{u}_{rss} in the above expression. These mixed derivatives would make the boundary condition non-local by coupling adjacent points. We can, however, find expressions for these mixed derivative expressions in terms of non-mixed derivatives.

13.3.1 Two dimensions

First consider the two-dimensional case. Taking the r - and s -derivatives of the divergence equation gives

$$\begin{aligned} \partial_r^2(\mathbf{a}_1 \cdot \mathbf{u}) + \partial_r \partial_s(\mathbf{a}_2 \cdot \mathbf{u}) &= 0 \\ \partial_r \partial_s(\mathbf{a}_1 \cdot \mathbf{u}) + \partial_s^2(\mathbf{a}_2 \cdot \mathbf{u}) &= 0 \end{aligned}$$

or

$$\begin{aligned} \mathbf{a}_2 \cdot \mathbf{u}_{rs} &= -\{\partial_r^2(\mathbf{a}_1 \cdot \mathbf{u}) + \partial_r \partial_s(\mathbf{a}_2) \mathbf{u} + \partial_r(\mathbf{a}_2) \mathbf{u}_s + \partial_s(\mathbf{a}_2) \mathbf{u}_r\} \\ \mathbf{a}_1 \cdot \mathbf{u}_{rs} &= -\{\partial_s^2(\mathbf{a}_2 \cdot \mathbf{u}) + \partial_r \partial_s(\mathbf{a}_1) \mathbf{u} + \partial_r(\mathbf{a}_1) \mathbf{u}_s + \partial_s(\mathbf{a}_1) \mathbf{u}_r\} \end{aligned}$$

Since $\mathbf{a}_1 \cdot \mathbf{a}_2 \neq 0$, we can solve these expressions for \mathbf{u}_{rs} ,

$$\mathbf{u}_{rs} = \mathbf{F}_1(\mathbf{u}_r, \mathbf{u}_s, \mathbf{u}_{rr}, \mathbf{u}_{ss}) \quad (40)$$

Now $\partial_s(\nabla \cdot \mathbf{u}) = 0$ implies

$$\mathbf{a}_1 \cdot \mathbf{u}_{rs} = -\left(\partial_s \mathbf{a}_1 \cdot \mathbf{u}_r + \partial_s(\partial_r \mathbf{a}_1 \cdot \mathbf{u}) + \partial_s^2(\mathbf{a}_2 \cdot \mathbf{u}) + \partial_s \partial_{r_3}(\mathbf{a}_3 \cdot \mathbf{u})\right)$$

This last expression can be differentiated with respect to s to give an equation for

$$\mathbf{a}_1 \cdot \mathbf{u}_{rss} = -\left(\partial_s \mathbf{a}_1 \cdot \mathbf{u}_{rs} + \partial_s^2 \mathbf{a}_1 \cdot \mathbf{u}_r + \partial_s^2(\partial_r \mathbf{a}_1 \cdot \mathbf{u}) + \partial_s^3(\mathbf{a}_2 \cdot \mathbf{u}) + \partial_s^2 \partial_{r_3}(\mathbf{a}_3 \cdot \mathbf{u})\right) \quad (41)$$

Combining equations (37), (40), and (41) allows us to rewrite the boundary condition (37) without any mixed derivatives,

$$\partial_r(\mathbf{a}_1 \cdot \Delta \mathbf{E}) = \mathbf{b}_3 \cdot \mathbf{u}_{rrr} + \mathbf{b}_2 \cdot \mathbf{u}_{rr} + \mathbf{b}_1 \cdot \mathbf{u}_r = G(\mathbf{u}_s, \mathbf{u}_{ss}, \mathbf{u}_{sss}) \quad (42)$$

Magnetic field in two dimensions:

In two-dimensions the boundary condition for the magnetic field, w , is

$$\begin{aligned}\partial_n w &= \mathbf{n} \cdot (\nabla w) \\ &= (n_1, n_2) \cdot (r_x w_r + s_x w_s, r_y w_r + s_y w_s) \\ &= (n_1 r_x + n_2 r_y) w_r + (n_1 s_x + n_2 s_y) w_s\end{aligned}$$

On a boundary $r = 0$, $\mathbf{n} = \nabla_{\mathbf{x}} r / \|\nabla_{\mathbf{x}} r\|$ and then

$$\partial_n w = \frac{(r_x^2 + r_y^2)}{\|\nabla_{\mathbf{x}} r\|} w_r + \frac{(r_x s_x + r_y s_y)}{\|\nabla_{\mathbf{x}} r\|} w_s$$

Thus the Neumann boundary condition for w can be written as

$$w_r = -\frac{\nabla_{\mathbf{x}} r \cdot \nabla_{\mathbf{x}} s}{\|\nabla_{\mathbf{x}} r\|^2} w_s$$

On an orthogonal grid the right-hand-side is zero. Assume now that the grid is orthogonal and $w_r(0, s) = 0$, then

$$\begin{aligned}\partial_t^2 w_r &= \partial_r \Delta w \\ &= \partial_r \{ c_{11} \partial_r^2 w + c_{22} \partial_s^2 w + c_{10} \partial_r w + c_{01} \partial_s w \} \\ &= c_{11} \partial_r^3 w + c_{22} \partial_r \partial_s^2 w + c_{10} \partial_r^2 w + c_{01} \partial_r \partial_s w \\ &\quad + (\partial_r c_{11}) \partial_r^2 w + (\partial_r c_{22}) \partial_s^2 w + (\partial_r c_{10}) \partial_r w + (\partial_r c_{01}) \partial_s w\end{aligned}$$

giving the BC

$$c_{11} \partial_r^3 w + (c_{10} + \partial_r c_{11}) \partial_r^2 w = -\{(\partial_r c_{22}) \partial_s^2 w + (\partial_r c_{01}) \partial_s w\} \quad \text{at } r = 0$$

We are thus led to the discrete boundary conditions for the fourth-order accurate scheme

$$\begin{aligned}(\boldsymbol{\tau}_m \cdot \mathbf{E})_{0,j} &= 0 \\ \boldsymbol{\tau}_m \cdot \Delta_{2h} \mathbf{E}_{0,j} &= 0 \\ \boldsymbol{\tau}_m \cdot \mathbf{E}_{-2,j} &= \boldsymbol{\tau}_m \cdot (I - D_+^4) \mathbf{E}_{-2,j} \equiv g_m \quad (\text{extrapolate}) \\ D_{0r}(1 - (\Delta r)^2 / 6D_{+r}D_{-r})(\mathbf{a}_1 \cdot \mathbf{E})_{0,j} &= 0 \\ \mathbf{b}_3 \cdot (D_{0r}D_{+r}D_{-r} \mathbf{E}) + \mathbf{b}_2 \cdot \mathbf{u}_{rr} + \mathbf{b}_1 \cdot \mathbf{u}_r &= G(\mathbf{u}_s, \mathbf{u}_{ss}, \mathbf{u}_{sss}) \\ D_{0r}(1 - (\Delta r)^2 / 6D_{+r}D_{-r})w_{0,j} &= 0 \\ c_{11} D_{0r}D_{+r}D_{-r} w + (c_{10} + \partial_r c_{11}) D_{+r}D_{-r} w &= -\{(\partial_r c_{22}) D_{+s}D_{-s} w + (\partial_r c_{01}) D_{0s} w\}\end{aligned}$$

13.3.2 Three dimensions

Now consider the three-dimensional situation which is more complicated. We need expressions for the mixed derivatives taht appear in the expression for $\partial_{r_1}(\mathbf{a}_1 \cdot \Delta \mathbf{u}) = 0$, equation (35),

$$\mathbf{a}_1 \cdot \mathbf{u}_{rs}, \tag{43}$$

$$\mathbf{a}_1 \cdot \mathbf{u}_{rr_3}, \tag{44}$$

$$\mathbf{a}_1 \cdot \mathbf{u}_{rss}, \tag{45}$$

$$\mathbf{a}_1 \cdot \mathbf{u}_{rr_3r_3}, \tag{46}$$

The divergence equation implies

$$\mathbf{a}_1 \cdot \mathbf{u}_r = -\{(\partial_r \mathbf{a}_1) \cdot \mathbf{u} + \partial_{r_2}(\mathbf{a}_2 \cdot \mathbf{u}) + \partial_{r_3}(\mathbf{a}_3 \cdot \mathbf{u})\}$$

Taking the r , s , and r_3 -derivatives of the divergence equation gives

$$\begin{aligned}\partial_r^2(\mathbf{a}_1 \cdot \mathbf{u}) + \partial_r \partial_s(\mathbf{a}_2 \cdot \mathbf{u}) + \partial_r \partial_{r_3}(\mathbf{a}_3 \cdot \mathbf{u}) &= 0 \\ \partial_r \partial_s(\mathbf{a}_1 \cdot \mathbf{u}) + \partial_s^2(\mathbf{a}_2 \cdot \mathbf{u}) + \partial_s \partial_{r_3}(\mathbf{a}_3 \cdot \mathbf{u}) &= 0 \\ \partial_r \partial_{r_3}(\mathbf{a}_1 \cdot \mathbf{u}) + \partial_s \partial_{r_3}(\mathbf{a}_2 \cdot \mathbf{u}) + \partial_{r_3}^2(\mathbf{a}_3 \cdot \mathbf{u}) &= 0\end{aligned}$$

In this 3d case the first equation only gives a relation for

$$\mathbf{a}_2 \cdot \mathbf{u}_{rs} + \mathbf{a}_3 \cdot \mathbf{u}_{rr_3} = -\{\partial_r^2(\mathbf{a}_1 \cdot \mathbf{u}) + \dots\}$$

as opposed to the 2d case where this equation determined the tangential component of \mathbf{u}_{rs} . This means the 3d case is more involved.

From $\partial_{r_2}(\nabla \cdot \mathbf{u}) = 0$ and $\partial_{r_3}(\nabla \cdot \mathbf{u}) = 0$ we get the normal components of the mixed derivatives,

$$\begin{aligned}\mathbf{a}_1 \cdot \mathbf{u}_{rs} &= -\{\partial_{r_2}\mathbf{a}_1 \cdot \mathbf{u}_r + \partial_{r_2}((\partial_r \mathbf{a}_1) \cdot \mathbf{u}) + \partial_{r_2}^2(\mathbf{a}_2 \cdot \mathbf{u}) + \partial_{r_2} \partial_{r_3}(\mathbf{a}_3 \cdot \mathbf{u})\} \\ \mathbf{a}_1 \cdot \mathbf{u}_{rr_3} &= -\{\partial_{r_3}\mathbf{a}_1 \cdot \mathbf{u}_r + \partial_{r_3}((\partial_r \mathbf{a}_1) \cdot \mathbf{u}) + \partial_{r_2} \partial_{r_3}(\mathbf{a}_2 \cdot \mathbf{u}) + \partial_{r_3}^2(\mathbf{a}_3 \cdot \mathbf{u})\}\end{aligned}$$

and thus we have $\mathbf{a}_1 \cdot \mathbf{u}_{rs}$ and $\mathbf{a}_1 \cdot \mathbf{u}_{rr_3}$ defined in terms of tangential derivatives.

From $\partial_{r_2}^2(\nabla \cdot \mathbf{u}) = 0$ and $\partial_{r_3}^2(\nabla \cdot \mathbf{u}) = 0$ we also get

$$\begin{aligned}\mathbf{a}_1 \cdot \mathbf{u}_{rss} &= -\{\partial_{r_2}\mathbf{a}_1 \cdot \mathbf{u}_{rs} + \partial_{r_2}(\partial_{r_2}\mathbf{a}_1 \cdot \mathbf{u}_r + \partial_{r_2}((\partial_r \mathbf{a}_1) \cdot \mathbf{u}) + \partial_{r_2}^2(\mathbf{a}_2 \cdot \mathbf{u}) + \partial_{r_2} \partial_{r_3}(\mathbf{a}_3 \cdot \mathbf{u}))\} \\ \mathbf{a}_1 \cdot \mathbf{u}_{rr_3r_3} &= -\{\partial_{r_3}\mathbf{a}_1 \cdot \mathbf{u}_{rr_3} + \partial_{r_3}(\partial_{r_3}\mathbf{a}_1 \cdot \mathbf{u}_r + \partial_{r_3}((\partial_r \mathbf{a}_1) \cdot \mathbf{u}) + \partial_{r_2} \partial_{r_3}(\mathbf{a}_2 \cdot \mathbf{u}) + \partial_{r_3}^2(\mathbf{a}_3 \cdot \mathbf{u}))\}\end{aligned}$$

The only difficult terms on the RHS of these last two expressions are $\partial_{r_2}\mathbf{a}_1 \cdot \mathbf{u}_{rs}$ and $\partial_{r_3}\mathbf{a}_1 \cdot \mathbf{u}_{rr_3}$.

In two-dimensions we could solve explicitly for \mathbf{u}_{rs} just from the divergence equation and it's derivatives. In three-dimensions we need more information. Since we know $\mathbf{a}_1 \cdot \mathbf{u}_{rs}$ we can compute \mathbf{u}_{rs} if we know $\boldsymbol{\tau}_m \cdot \mathbf{u}_{rs}$ for $m = 1, 2$.

Now letting $\boldsymbol{\tau} = \boldsymbol{\tau}_m$ then

$$\boldsymbol{\tau} \cdot \mathbf{u}_{rs} = (\boldsymbol{\tau} \cdot \mathbf{u}_r)_s - \boldsymbol{\tau}_s \cdot \mathbf{u}_r$$

The boundary conditions for $\boldsymbol{\tau} \cdot \mathbf{u}$ will allow us to compute $\boldsymbol{\tau} \cdot \mathbf{u}_r(r, s, r_3)$ on the boundary and at all ghost points and thus we can determine an approximation to $(\boldsymbol{\tau} \cdot \mathbf{u}_r)_s$. For example a second-order approximation should be sufficient,

$$\begin{aligned}(\boldsymbol{\tau} \cdot \mathbf{u}_r)_s(0, r_2, r_3) &:= G^{rs}(s, r_3) \\ &\approx D_{0s}(\boldsymbol{\tau}_i \cdot (D_{0r} \mathbf{U}_i))\end{aligned}$$

Thus by first computing the tangential components we then can determine $(\boldsymbol{\tau} \cdot \mathbf{u}_r)_s(0, s, r_3)$ and thus we can assume that we know $\boldsymbol{\tau} \cdot \mathbf{u}_{rs}$ in terms of $\boldsymbol{\tau}_s \cdot \mathbf{u}_r$ and a known function:

$$\begin{aligned}\boldsymbol{\tau} \cdot \mathbf{u}_{rs} &= -\boldsymbol{\tau}_s \cdot \mathbf{u}_r + G^{rs} \\ G^{rs}(s, r_3) &= (\boldsymbol{\tau} \cdot \mathbf{u}_r)_s(0, s, r_3) \quad (\text{known}) \text{ from tangential components}\end{aligned}$$

Similiarly we get

$$\begin{aligned}\boldsymbol{\tau} \cdot \mathbf{u}_{rr_3} &= -\boldsymbol{\tau}_{r_3} \cdot \mathbf{u}_r + G^{rr_3} \\ G^{rr_3}(s, r_3) &= (\boldsymbol{\tau} \cdot \mathbf{u}_r)_{r_3}(0, s, r_3) \quad (\text{known}) \text{ from tangential components}\end{aligned}$$

Combining these results allows us to rewrite the boundary condition (37) in the form

$$\partial_r(\mathbf{a}_1 \cdot \Delta \mathbf{E}) = \mathbf{b}_3 \cdot \mathbf{u}_{rrr} + \mathbf{b}_2 \cdot \mathbf{u}_{rr} + \mathbf{b}_1 \cdot \mathbf{u}_r = G(\mathbf{u}_s, \mathbf{u}_{ss}, \mathbf{u}_{r_3}, \mathbf{u}_{r_3r_3}, \mathbf{u}_{sr_3}, (\boldsymbol{\tau} \cdot \mathbf{u}_r)_s, (\boldsymbol{\tau} \cdot \mathbf{u}_r)_{r_3}) \quad (47)$$

We are thus led to the discrete boundary conditions for the fourth-order accurate scheme in three-dimensions

$$(\boldsymbol{\tau}_m \cdot \mathbf{E})_{0,j} = 0 \quad m = 1, 2 \quad (48)$$

$$\boldsymbol{\tau}_m \cdot \Delta_{2h} \mathbf{E}_{0,j} = 0 \quad m = 1, 2 \quad (49)$$

$$\boldsymbol{\tau}_m \cdot \mathbf{E}_{-2,j} = \boldsymbol{\tau}_m \cdot (I - D_+^4) \mathbf{E}_{-2,j} \equiv g_m, \quad m = 1, 2 \quad (\text{extrapolate}) \quad (50)$$

$$D_{0r}(1 - (\Delta r)^2 / 6D_{+r}D_{-r})(\mathbf{a}_1 \cdot \mathbf{E})_{0,j} = 0 \quad (51)$$

$$\mathbf{b}_3 \cdot (D_{0r}D_{+r}D_{-r} \mathbf{E}) + \mathbf{b}_2 \cdot \mathbf{u}_{rr} + \mathbf{b}_1 \cdot \mathbf{u}_r = G(\mathbf{u}_s, \mathbf{u}_{ss}, \mathbf{u}_{r3}, \mathbf{u}_{r3r3}, \mathbf{u}_{sr3}, (\boldsymbol{\tau} \cdot \mathbf{u}_r)_s, (\boldsymbol{\tau} \cdot \mathbf{u}_r)_{r3}) \quad (52)$$

To summarize, the first three equations can be used to determine the tangential components on the boundary and two ghost lines,

$$\boldsymbol{\tau}_m \cdot \mathbf{E}_{i_1, i_2, i_3} \quad i_1 = 0, -1, -2$$

The last two equations then determine the normal components on the two ghost lines,

$$\mathbf{a}_1 \cdot \mathbf{E}_{i_1, i_2, i_3} \quad i_1 = -1, -2$$

13.4 Sixth- and higher-order accurate boundary conditions

For sixth and higher order accurate boundary conditions we proceed in the same fashion as for the fourth order case.

By differentiating the boundary conditions $2m$ times with respect to time and using the interior PDE, is follows that for $m = 0, 1, 2, 3 \dots$,

$$\begin{aligned} \boldsymbol{\tau} \cdot \Delta^m \mathbf{E}_{0,j} &= 0 \\ \partial_r(\mathbf{a}_1 \cdot \Delta^m \mathbf{E})_{0,j} &= 0 \end{aligned}$$

The Laplacian squared is

$$\begin{aligned} \Delta^2 &= \left(c_{11} \partial_r^2 + c_{22} \partial_s^2 + c_{10} \partial_r + c_{01} \partial_s \right)^2 \\ &= d_{1111} \partial_r^4 + d_{2222} \partial_s^4 + d_{1122} \partial_r^2 \partial_s^2 + d_{1112} \partial_r^3 \partial_s + d_{1222} \partial_r \partial_s^3 \\ &\quad + d_{111} \partial_r^3 + d_{222} \partial_s^3 + d_{112} \partial_r^2 \partial_s + d_{122} \partial_r \partial_s^2 \\ &\quad + d_{11} \partial_r^2 + d_{12} \partial_r \partial_s + d_{22} \partial_s^2 + d_{10} \partial_r + d_{01} \partial_s + c_{10} \partial_r + c_{01} \partial_s \end{aligned}$$

We would like to determine expressions at $r = 0$ for the mixed-derivatives that appear in this equation. We already know \mathbf{u}_{rs} .

We make use of

$$\partial_s(\boldsymbol{\tau} \cdot \mathbf{u}_{tt})(0, s) = 0$$

to give

$$\begin{aligned} \partial_s(\boldsymbol{\tau} \cdot \mathbf{u}_{tt})(0, s) &= \partial_s(\boldsymbol{\tau} \cdot \Delta \mathbf{u})(0, s) \\ &= \boldsymbol{\tau} \cdot \left\{ c_{11} \mathbf{u}_{rrs} + c_{10} \mathbf{u}_{rs} + c_{22} \partial_s^3 \mathbf{u} + c_{01} \partial_s^2 \mathbf{u} \right. \\ &\quad \left. + \partial_s(c_{11}) \partial_r^2 \mathbf{u} + \partial_s(c_{22}) \partial_s^2 \mathbf{u} + \partial_s(c_{10}) \partial_r \mathbf{u} + \partial_s(c_{01}) \partial_s \mathbf{u} \right\} \end{aligned}$$

Whence we know

$$\boldsymbol{\tau} \cdot \mathbf{u}_{rrs} = F_{112}(\mathbf{u}_{rr}, \mathbf{u}_r, \mathbf{u}_{sss}, \mathbf{u}_{ss}, \mathbf{u}_s) \quad (53)$$

In the same manner, from $\partial_s^2(\boldsymbol{\tau} \cdot \mathbf{u}_{tt})(0, s) = 0$ we can determine

$$\boldsymbol{\tau} \cdot \mathbf{u}_{rrss} = F_{1122}(\mathbf{u}_{rr}, \mathbf{u}_r, \mathbf{u}_{ssss}, \mathbf{u}_{sss}, \mathbf{u}_{ss}, \mathbf{u}_s) \quad (54)$$

We also need $\boldsymbol{\tau} \cdot \partial_r^3 \partial_s \mathbf{u}$ and $\boldsymbol{\tau} \cdot \partial_r \partial_s^2 \mathbf{u}$

To get $\boldsymbol{\tau} \cdot \partial_r^3 \partial_s \mathbf{u}$ we use the divergence condition (cf. $v_{xxxy} = -u_{xxxx}$),

$$\begin{aligned}\partial_r^3(\delta) &= \partial_r^4(\mathbf{a}_1 \cdot \mathbf{u}) + \partial_r^3 \partial_s(\mathbf{a}_2 \cdot \mathbf{u}) \\ \partial_r^2 \partial_s(\delta) &= \partial_r^3 \partial_s(\mathbf{a}_1 \cdot \mathbf{u}) + \partial_r^2 \partial_s^2(\mathbf{a}_2 \cdot \mathbf{u})\end{aligned}$$

gives

$$\begin{aligned}\mathbf{a}_2 \cdot (\partial_r^3 \partial_s \mathbf{u}) &= -\{\partial_r^4(\mathbf{a}_1 \cdot \mathbf{u}) + \partial_r^3 \partial_s(\mathbf{a}_2) \mathbf{u} + \partial_s(\mathbf{a}_2) \partial_r^3 \mathbf{u} + \dots\} \\ \mathbf{a}_1 \cdot (\partial_r^3 \partial_s \mathbf{u}) &= -\{\partial_r^2 \partial_s^2(\mathbf{a}_2 \cdot \mathbf{u}) \partial_r^3 \partial_s(\mathbf{a}_1) \mathbf{u} + \partial_r^3(\mathbf{a}_1) \partial_s \mathbf{u} + \dots\}\end{aligned}$$

giving

$$\partial_r^3 \partial_s \mathbf{u} = \mathbf{F}_{1112}(\partial_r \mathbf{u}, \partial_s \mathbf{u}, \dots)$$

Discrete boundary conditions for the sixth-order accurate scheme are

$$\begin{aligned}(\boldsymbol{\tau}_m \cdot \mathbf{E})_{0,j} &= 0 \\ \boldsymbol{\tau}_m \cdot \Delta_{4h} \mathbf{E}_{0,j} &= 0 \\ \boldsymbol{\tau}_m \cdot \Delta_{2h}^2 \mathbf{E}_{0,j} &= 0 \\ \boldsymbol{\tau}_m \cdot \mathbf{E}_{-3,j} &= \boldsymbol{\tau}_m \cdot (I - D_+^7) \mathbf{E}_{-3,j} \equiv g_m \quad (\text{extrapolate}) \\ D_{0r} \left(1 - \frac{(\Delta r)^2}{6} D_{+r} D_{-r} \pm \frac{(\Delta r)^4}{120} D_{+r}^2 D_{-r}^2\right) (\mathbf{a}_1 \cdot \mathbf{E})_{0,j} &= 0 \\ D_{0r} (\mathbf{a}_1 \cdot \Delta_{4h} E v)_{0,j} - \frac{(\Delta r)^2}{6} D_{+r} D_{-r} (\mathbf{a}_1 \cdot \Delta_{2h} E v)_{0,j} &= 0 \\ D_{0r} (\mathbf{a}_1 \cdot \Delta_{2h}^2 E v)_{0,j} &= 0\end{aligned}$$

where Δ_{2h} is a second order accurate approximation to the Laplacian operator.

13.5 Boundary conditions for the magnetic field

For the magnetic field we have

$$\begin{aligned}\mathbf{n} \cdot \mathbf{H} &= 0 \\ \nabla \cdot \mathbf{H} &= 0\end{aligned}$$

13.6 Extended boundaries in two-dimensions

Consider a corner on a two-dimensional orthogonal curvilinear grid at $\mathbf{r} = 0$. We need to determine values along the extended boundaries (i.e. $s = 0, r < 0$ and $r = 0, s < 0$).

We have

$$\begin{aligned}\mathbf{a}_1 \cdot \mathbf{u}(r, 0, t) &= 0, && (\text{tangential component on } s = 0) \\ \mathbf{a}_2 \cdot \mathbf{u}(0, s, t) &= 0, && (\text{tangential component on } r = 0) \\ \mathbf{u}(0, 0, t) &= \partial_t^m \mathbf{u}(0, 0, t) = 0, && (\text{all time derivatives are zero at } \mathbf{r} = 0, m = 0, 1, 2, \dots) \\ \Delta \mathbf{u}(0, 0, t) &= 0\end{aligned}$$

where as usual $\mathbf{a}_1 = J\nabla_{\mathbf{x}}r$ and $\mathbf{a}_2 = J\nabla_{\mathbf{x}}s$.

For second-order we can thus solve the four equations

$$\begin{aligned}c_{11}D_{+r}D_{-r}\mathbf{U}_i + c_{22}D_{+s}D_{-s}\mathbf{U}_i + c_1D_{0r}\mathbf{U}_i + c_2D_{0s}\mathbf{U}_i &= 0 \\ (\mathbf{a}_1 \cdot \mathbf{U})_{-1,0} &= 0 \\ (\mathbf{a}_2 \cdot \mathbf{U})_{0,-1} &= 0\end{aligned}$$

to determine the four unknown components of the vectors $\mathbf{U}_{-1,0}$ and $\mathbf{U}_{0,-1}$.

Note that for the second-order approximation, since $\mathbf{U}_{0,0} = 0$ the extended boundary points are not even used. The question is whether the above second-order approximation is good enough for the fourth-order accurate method.

13.7 Corners in two-dimensions

Given the values on the extended boundaries we can then determine the values at the ghost points that lie outside corners. By Taylor series

$$u(r_1, r_2) = u(0, 0) + \mathcal{D}_1(r_1, r_2) + \mathcal{D}_2(r_1, r_2) + \mathcal{D}_3(r_1, r_2) + \mathcal{D}_4(r_1, r_2) + O(|\mathbf{r}|^6)$$

where

$$\mathcal{D}_1(r_1, r_2) = (r_1 \partial_{r_1} + r_2 \partial_{r_2})u(0, 0)$$

$$\mathcal{D}_2(r_1, r_2) = \frac{1}{2}(r_1^2 \partial_{r_1}^2 + r_2^2 \partial_{r_2}^2 + 2r_1 r_2 \partial_{r_1} \partial_{r_2})u(0, 0)$$

$$\mathcal{D}_3(r_1, r_2) = \frac{1}{3!}(r_1^3 \partial_r^3 + r_2^3 \partial_{r_2}^3 + 3r_1^2 r_2 \partial_{r_1}^2 \partial_{r_2} + 3r_1 r_2^2 \partial_{r_1} \partial_{r_2}^2 + r_2^3 \partial_{r_2}^3)u(0, 0)$$

$$\mathcal{D}_4(r_1, r_2) = \frac{1}{4!}(r_1^4 \partial_r^4 + 4r_1^3 r_2 \partial_{r_1}^3 \partial_{r_2} + 6r_1^2 r_2^2 \partial_{r_1}^2 \partial_{r_2}^2 + 4r_1 r_2^3 \partial_{r_1} \partial_{r_2}^3 + r_2^4 \partial_{r_2}^4)u(0, 0)$$

Whence

$$u(-r_1, -r_2) = 2u(0, 0) - u(r_1, r_2) + 2\mathcal{D}_2(r_1, r_2) + 2\mathcal{D}_4(r_1, r_2) + O(|\mathbf{r}|^6) \quad (55)$$

(56)

For second order at the corner we use the approximation

$$u(-r_1, -r_2) \approx 2u(0, 0) - u(r_1, r_2) + 2\mathcal{D}_2(r_1, r_2) + O(|\mathbf{r}|^4) \quad (57)$$

$$\mathcal{D}_2(r_1, r_2) = \frac{1}{2}(r_1^2 \partial_{r_1}^2 + r_2^2 \partial_{r_2}^2 + 2r_1 r_2 \partial_{r_1} \partial_{r_2})u(0, 0) \quad (58)$$

where the mixed derivatives, $\partial_{r_1} \partial_{r_2} u(0, 0)$, are obtained from equation (??).

For fourth-order accuracy we use

$$u(-r_1, -r_2) \approx 2u(0, 0) - u(r_1, r_2) + 2\mathcal{D}_2(r_1, r_2) + 2\mathcal{D}_4(r_1, r_2) + O(|\mathbf{r}|^6) \quad (59)$$

(60)

All non-mixed derivatives, $\partial_r^3 u$, $\partial_s^3 u$ etc. can be computed from the boundary values which are assumed known at this point.

The mixed derivatives $\partial_{r_1} \partial_{r_2} u(0, 0)$, are obtained from equation (??).

We also need approximations for $\partial_{r_1}^3 \partial_{r_2} u$, $\partial_{r_1}^2 \partial_{r_2}^2 u$ and $\partial_{r_1} \partial_{r_2}^3 u$.

13.8 Extended boundaries in three-dimensions

Consider the edge $\mathbf{r} = (0, 0, r_3)$, $r_3 \in [0.1]$ of an orthogonal grid in three dimensions.

We need to determine values of the ghost points along the extended boundaries (i.e. $r_2 = 0$, $r_1 < 0$ and $r_1 = 0$, $r_2 < 0$).

The following conditions hold on a PEC boundary

$$\begin{aligned}\mathbf{a}_1 \cdot \mathbf{u}(r, 0, 0, t) &= \mathbf{a}_3 \cdot \mathbf{u}(r, 0, 0, t) = 0, && (\text{tangential component on } r_2 = 0) \\ \mathbf{a}_2 \cdot \mathbf{u}(0, s, 0, t) &= \mathbf{a}_3 \cdot \mathbf{u}(0, s, 0, t) = 0, && (\text{tangential component on } r_1 = 0) \\ \mathbf{a}_1 \cdot \partial_t^m \mathbf{u}(0, 0, t) &= 0, && (m = 0, 1, 2, \dots) \\ \mathbf{a}_2 \cdot \partial_t^m \mathbf{u}(0, 0, t) &= 0, && (m = 0, 1, 2, \dots)\end{aligned}$$

For second-order accuracy we can thus solve the six equations

$$\begin{aligned}\mathbf{a}_1 \cdot L_h^{(2)} \mathbf{U}_{0,0,i_3} &= 0 \\ \mathbf{a}_2 \cdot L_h^{(2)} \mathbf{U}_{0,0,i_3} &= 0 \\ (\mathbf{a}_1 \cdot \mathbf{U})_{-1,0,i_3} &= 0, \quad (\mathbf{a}_3 \cdot \mathbf{U})_{-1,0,i_3} = 0 \\ (\mathbf{a}_2 \cdot \mathbf{U})_{0,-1,i_3} &= 0, \quad (\mathbf{a}_3 \cdot \mathbf{U})_{0,-1,i_3} = 0\end{aligned}$$

to determine the six unknown components of the vectors $\mathbf{U}_{-1,0,i_3}$ and $\mathbf{U}_{0,-1,i_3}$. Here $L_h^{(2)}$ is a second-order accurate approximation to the Laplacian,

$$L_h^{(2)} \mathbf{U}_i = (c_{11} D_{+r} D_{-r} \mathbf{U}_i + c_{22} D_{+s} D_{-s} \mathbf{U}_i + c_{33} D_{+t} D_{-t} \mathbf{U}_i + c_1 D_{0r} \mathbf{U}_i + c_2 D_{0s}) + c_3 D_{0t} \mathbf{U}_i$$

For fourth-order accuracy we use a fourth-order approximation to the equation and extrapolate

$$\begin{aligned}\mathbf{a}_1 \cdot L_h^{(4)} \mathbf{U}_{0,0,i_3} &= 0 \\ \mathbf{a}_2 \cdot L_h^{(4)} \mathbf{U}_{0,0,i_3} &= 0 \\ (\mathbf{a}_1 \cdot \mathbf{U})_{i_1,0,i_3} &= (\mathbf{a}_3 \cdot \mathbf{U})_{i_1,0,i_3} = 0 \quad i_1 = -1, -2 \\ \Delta_{+r}^4 (\mathbf{a}_2 \cdot \mathbf{U})_{-2,0,i_3} &= 0 \\ (\mathbf{a}_2 \cdot \mathbf{U})_{0,i_2,i_3} &= (\mathbf{a}_3 \cdot \mathbf{U})_{0,i_2,i_3} = 0 \quad i_2 = -1, -2 \\ \Delta_{+s}^4 (\mathbf{a}_1 \cdot \mathbf{U})_{0,-2,i_3} &= 0\end{aligned}$$

These 12 equations determine the 12 unknown components of the vectors $\mathbf{U}_{-1,0,i_3}$, $\mathbf{U}_{-2,0,i_3}$, $\mathbf{U}_{0,-1,i_3}$ and $\mathbf{U}_{0,-2,i_3}$. Since the “tangential components” are known, these 12 equations can be reduced to the solution of 4 equations for the unknown “normal” components.

13.9 Ghost points outside edges in three-dimensions

By Taylor series in r_1 and r_2 (leaving r_3 fixed) gives

$$u(r_1, r_2, r_3) = u(0, 0, r_3) + \mathcal{D}_1(u, r_1, r_2, r_3) + \mathcal{D}_2(u, r_1, r_2, r_3) + \mathcal{D}_3(u, r_1, r_2, r_3) + \mathcal{D}_4(u, r_1, r_2, r_3) + O(|\mathbf{r}|^6)$$

where

$$\begin{aligned}\mathcal{D}_1(u, r_1, r_2, r_3) &= (r_1 \partial_{r_1} + r_2 \partial_{r_2})u(0, 0, r_3) \\ \mathcal{D}_2(u, r_1, r_2, r_3) &= \frac{1}{2}(r_1^2 \partial_{r_1}^2 + 2r_1 r_2 \partial_{r_1} \partial_{r_2} + r_2^2 \partial_{r_2}^2)u(0, 0, r_3) \\ \mathcal{D}_3(u, r_1, r_2, r_3) &= \frac{1}{3!}(r_1^3 \partial_r^3 + r_2^3 \partial_{r_2}^3 + 3r_1^2 r_2 \partial_{r_1}^2 \partial_{r_2} + 3r_1 r_2^2 \partial_{r_1} \partial_{r_2}^2 + r_2^3 \partial_{r_2}^3)u(0, 0, r_3) \\ \mathcal{D}_4(u, r_1, r_2, r_3) &= \frac{1}{4!}(r_1^4 \partial_r^4 + 4r_1^3 r_2 \partial_{r_1}^3 \partial_{r_2} + 6r_1^2 r_2^2 \partial_{r_1}^2 \partial_{r_2}^2 + 4r_1 r_2^3 \partial_{r_1} \partial_{r_2}^3 + r_2^4 \partial_{r_2}^4)u(0, 0, r_3)\end{aligned}$$

We can thus derive the following two formulae for the ghost points,

$$u(-r_1, -r_2, r_3) = 2u(0, 0, r_3) - u(r_1, r_2, r_3) + 2\mathcal{D}_2(u, r_1, r_2, r_3) + 2\mathcal{D}_4(u, r_1, r_2, r_3) + O(|\mathbf{r}|^6) \quad (61)$$

$$u(-r_1, -r_2, r_3) = u(r_1, r_2, r_3) - 2\mathcal{D}_1(u, r_1, r_2, r_3) - 2\mathcal{D}_3(u, r_1, r_2, r_3) + O(|\mathbf{r}|^5) \quad (62)$$

The first formula, equation (61) is appropriate for odd functions and the second is appropriate for even functions.

Consider an edge $\mathbf{r} = (0, 0, r_3)$. On a rectangular grid (perhaps rotated) the components $\mathbf{a}_1 \cdot \mathbf{u}$ and $\mathbf{a}_2 \cdot \mathbf{u}$ will be odd functions while the component $\mathbf{a}_3 \cdot \mathbf{u}$ will be even. It is thus appropriate to use equation (61) for $\mathbf{a}_1 \cdot \mathbf{u}$ and $\mathbf{a}_2 \cdot \mathbf{u}$ but use equation (62) for $\mathbf{a}_3 \cdot \mathbf{u}$.

For second order at the ghost points outside the edge parallel to r_3 we use the approximation

$$\mathbf{a}_m \cdot \mathbf{u}(-r_1, -r_2, r_3) \approx 2\mathbf{a}_m \cdot \mathbf{u}(0, 0, r_3) - \mathbf{a}_m \cdot \mathbf{u}(r_1, r_2, r_3) \quad m = 1, 2 \quad (63)$$

$$\mathbf{a}_3 \cdot \mathbf{u}(-r_1, -r_2, r_3) \approx \mathbf{a}_3 \cdot \mathbf{u}(r_1, r_2, r_3) - \mathbf{a}_3 \cdot \mathcal{D}_1(\mathbf{u}, r_1, r_2, r_3) \quad (64)$$

Along the edge $\mathbf{r} = (0, 0, r_3)$ all the derivatives of $\mathbf{a}_3 \cdot \mathbf{u}$ are zero and thus $\mathbf{a}_3 \cdot \mathbf{u}_r = (\mathbf{a}_3 \cdot \mathbf{u})_r - (\partial_r \mathbf{a}_3) \cdot \mathbf{u} = 0$. This implies $\mathbf{a}_3 \cdot \mathcal{D}_1(\mathbf{u}, r_1, r_2, r_3)$ is zero on the edge and thus we may more simply use

$$\mathbf{a}_3 \cdot \mathbf{u}(-r_1, -r_2, r_3) \approx \mathbf{a}_3 \cdot \mathbf{u}(r_1, r_2, r_3) \quad (65)$$

For fourth-order accuracy we use the approximations

$$\mathbf{a}_m \cdot \mathbf{u}(-r_1, -r_2, r_3) \approx 2\mathbf{a}_m \cdot \mathbf{u}(0, 0, r_3) - \mathbf{a}_m \cdot \mathbf{u}(r_1, r_2, r_3) + 2\mathbf{a}_m \cdot \mathcal{D}_2(\mathbf{u}, r_1, r_2, r_3) \quad m = 1, 2 \quad (66)$$

$$\mathbf{a}_3 \cdot \mathbf{u}(-r_1, -r_2, r_3) \approx \mathbf{a}_3 \cdot \mathbf{u}(r_1, r_2, r_3) - 2\mathbf{a}_3 \cdot \mathcal{D}_1(\mathbf{u}, r_1, r_2, r_3) - 2\mathbf{a}_3 \cdot \mathcal{D}_3(\mathbf{u}, r_1, r_2, r_3) \quad (67)$$

The mixed derivatives $\mathbf{a}_1 \cdot \mathbf{u}_{rs}$ and $\mathbf{a}_2 \cdot \mathbf{u}_{rs}$ can be obtained from the divergence equation

$$\mathbf{a}_1 \cdot \mathbf{u}_{rs} = -\{\} \quad (68)$$

$$\mathbf{a}_2 \cdot \mathbf{u}_{rs} = -\{\} \quad (69)$$

The mixed derivatives $\mathbf{a}_3 \cdot \mathbf{u}_{rrs}$ and $\mathbf{a}_3 \cdot \mathbf{u}_{rss}$ are also needed. From the equation we have

$$c_{11}\mathbf{u}_{rrs} = -\partial_s \{c_{22}\mathbf{u}_{ss} + c_{33}\mathbf{u}_{tt} + c_1\mathbf{u}_r + c_2\mathbf{u}_s + c_3\mathbf{u}_t\} \quad (70)$$

$$= -\{\dots c_1\mathbf{u}_{rs} + \dots\} \quad (71)$$

$$c_{22}\mathbf{u}_{rss} = -\partial_r \{c_{11}\mathbf{u}_{rr} + c_{33}\mathbf{u}_{tt} + c_1\mathbf{u}_r + c_2\mathbf{u}_s + c_3\mathbf{u}_t\} \quad (72)$$

$$= -\{\dots c_2\mathbf{u}_{rs} + \dots\} \quad (73)$$

$$(74)$$

This gives $\mathbf{a}_3 \cdot \mathbf{u}_{rrs}$ but requires $\mathbf{a}_3 \cdot \mathbf{u}_{rs}$. We *could* use a first order approximation for $\mathbf{a}_3 \cdot \mathbf{u}_{rs}$:

$$\mathbf{a}_3 \cdot \mathbf{u}_{rs} \approx \mathbf{a}_3 \cdot D_{+r} D_{+s} \mathbf{U}_{0,0,i_3} \quad (75)$$

OR we could use the second order approximation

$$u_{rs}(r, s) = \{8u(r, s) - u(2r, 2s) - 7u(0, 0) - 6(ru_r + su_s) - 2(r^2u_{rr} + s^su_{ss})\}/(4rs) + O(r^2)$$

ANOTHER way: First compute $\mathbf{a}_3 \cdot \mathbf{U}_{-1,0,i_3}$ from a second order approximation to

$$\mathbf{a}_3 \cdot \{c_{11}\mathbf{u}_{rr} + c_1\mathbf{u}_r\} = -av_3 \cdot \{c_{22}\mathbf{u}_{ss} + c_{33}\mathbf{u}_{tt} + c_2\mathbf{u}_s + c_3\mathbf{u}_t\} \quad (76)$$

(77)

and compute $\mathbf{a}_3 \cdot \mathbf{U}_{0,-1,i_3}$ from a second order approximation to

$$\mathbf{a}_3 \cdot \{c_{22}\mathbf{u}_{ss} + c_2\mathbf{u}_s\} = -av_3 \cdot \{c_{11}\mathbf{u}_{ss} + c_{33}\mathbf{u}_{tt} + c_1\mathbf{u}_r + c_3\mathbf{u}_t\} \quad (78)$$

(79)

Then we can approximate $\mathbf{a}_3 \cdot \mathbf{u}_{rrs}$ and $\mathbf{a}_3 \cdot \mathbf{u}_{rss}$ to second order

$$\mathbf{a}_3 \cdot \mathbf{u}_{rrs} \approx \mathbf{a}_3 \cdot D_{+r}^2 D_{+s} \mathbf{U}_{0,0,i_3} \quad (80)$$

This last equation contains the unknown value $\mathbf{a}_3 \cdot \mathbf{U}_{-1,-1,i_3}$ which we need to move to the left hand side...

13.10 Corners in three-dimensions

Given the values on the extended boundaries we can then determine the values at the ghost points that lie outside corners (i.e. the vertices of the unit cube). By Taylor series

$$u(r_1, r_2, r_3) = u(0, 0) + \mathcal{D}_1(r_1, r_2, r_3) + \mathcal{D}_2(r_1, r_2, r_3) + \mathcal{D}_3(r_1, r_2, r_3) + \mathcal{D}_4(r_1, r_2, r_3) + O(|\mathbf{r}|^6)$$

where

$$\mathcal{D}_1(r_1, r_2, r_3) = (r_1 \partial_{r_1} + r_2 \partial_{r_2} + r_3 \partial_{r_3})u(0, 0)$$

$$\mathcal{D}_2(r_1, r_2, r_3) = \frac{1}{2!}(r_1^2 \partial_{r_1}^2 + r_2^2 \partial_{r_2}^2 + r_3^2 \partial_{r_3}^2 + 2r_1 r_2 \partial_{r_1} \partial_{r_2} + 2r_1 r_3 \partial_{r_1} \partial_{r_3} + 2r_2 r_3 \partial_{r_2} \partial_{r_3})u(0, 0)$$

Whence we derive the expression

$$u(-r_1, -r_2, -r_3) = 2u(0, 0, 0) - u(r_1, r_2, r_3) + 2\mathcal{D}_2(r_1, r_2, r_3) + 2\mathcal{D}_4(r_1, r_2, r_3) + O(|\mathbf{r}|^6) \quad (81)$$

(82)

On a rectangular grid, all components of \mathbf{u} are odd functions about the corner and thus the above formula is the appropriate one to use since it reduces to the condition $u(-r_1, -r_2, -r_3) = 2u(0, 0, 0) - u(r_1, r_2, r_3)$ on a rectangular grid.

For second-order accuracy at the corner we use the approximation

$$u(-r_1, -r_2, -r_3) \approx 2u(0, 0, 0) - u(r_1, r_2, r_3) + O(|\mathbf{r}|^2) \quad (83)$$

(84)

For fourth-order accuracy at the corner we use the approximation

$$u(-r_1, -r_2, -r_3) \approx 2u(0, 0, 0) - u(r_1, r_2, r_3) + 2\mathcal{D}_2(r_1, r_2, r_3) + O(|\mathbf{r}|^4) \quad (85)$$

(86)

where all the second derivatives in \mathcal{D}_2 can be computed from the values on the extended boundaries.

14 Boundary conditions at material interfaces in 2D

In this section we derive conditions at a material interface that can be used to implement higher-order accurate centered discretizations.

Consider the two-dimensional problem

$$\epsilon(x)u_t = w_y \quad (87)$$

$$\epsilon(x)v_t = -w_x \quad (88)$$

$$w_t = u_y - v_x \quad (89)$$

$$(\epsilon(x)u)_x + (\epsilon(x)v)_y = 0 \quad (90)$$

The permittivity, $\epsilon(x)$ is assumed to be piecewise constant with a possible jump at $x = 0$. We assume that the solution to these equations remains bounded.

The above equations can be combined to show that the following second-order wave equations are satisfied,

$$\epsilon(x)u_{tt} = \partial_x\left(\frac{1}{\epsilon}(\epsilon u)_x\right) + u_{yy} \quad (91)$$

$$\epsilon(x)v_{tt} = v_{xx} + v_{yy} - \frac{\epsilon_x}{\epsilon}u_y \quad (92)$$

$$\epsilon(x)w_{tt} = w_{yy} + \epsilon\partial_x\left(\frac{1}{\epsilon}w_x\right) \quad (93)$$

Integrating equations (90), (89) and (88) from $x = 0_-$ to $x = 0_+$ implies the first three interface conditions,

$$[\epsilon u] = 0 \quad (94)$$

$$[v] = 0 \quad (95)$$

$$[w] = 0 \quad (96)$$

Here $[v] = v(0_+, y, t) - v(0_-, y, t)$ is the jump in v across the interface. Thus the tangential component of the electric field is continuous but the normal component may jump.

In the next step, conditions on the first (normal) derivative, u_x , v_x are obtained. We use the fact that if $[v] = 0$ then the jump in any time derivatives is also zero, $[\partial_t^m v] = 0$.

$$[(\epsilon u)_x + (\epsilon(x)v_y)] = 0 \quad (\text{from equation (90)}) \quad (97)$$

$$[v_x - u_y] = 0 \quad (\text{from equation (89) with } [w_t] = 0) \quad (98)$$

$$[w_x/\epsilon] = 0 \quad (\text{from equation (88) with } [v_t] = 0) \quad (99)$$

Note that we could also use $[u_x + v_y] = 0$ since when ϵ is piecewise constant, $u_x + v_y = 0$ for $x \neq 0$. Also note that we write the divergence equation, $(\epsilon u)_x + (\epsilon(x)v_y) = 0$, as a jump condition even though the divergence is identically zero on either side. The reason for this will be explained later.

The jump conditions for u_{xx} , v_{xx} and w_{xx} are

$$[u_{xx} + u_{yy}] = 0 \quad (\text{from equation (91) with } [\epsilon u_{tt}] = 0) \quad (100)$$

$$[(v_{xx} + v_{yy})/\epsilon] = 0 \quad (\text{from equation (92) with } [v_{tt}] = 0) \quad (101)$$

$$[(w_{xx} + w_{yy})/\epsilon] = 0 \quad (\text{from equation (93) with } [w_{tt}] = 0) \quad (102)$$

Note that $[\partial_x(\frac{1}{\epsilon}(\epsilon u)_x) + u_{yy}] = 0$ implies $[u_{xx} + u_{yy}] = 0$ if ϵ is piecewise constant.

The jump conditions for u_{xxx} , v_{xxx} and w_{xxx} are

$$[\Delta u_x + \Delta v_y] = 0 \quad (\text{from equation (90)}) \quad (103)$$

$$[(v_{xxx} + v_{xyy} - u_{xxy} - u_{yyy})/\epsilon] = 0 \quad (\text{from } [v_{xtt} - u_{ytt}] = 0) \quad (104)$$

$$[(w_{xxx} + w_{xyy})/\epsilon^2] = 0 \quad (\text{from } [w_{xtt}/\epsilon] = 0) \quad (105)$$

The fourth derivatives are obtained from

$$[\Delta^2 u/\epsilon] = 0 \quad (\text{from equation (91) with } [\epsilon u_{tttt}] = 0) \quad (106)$$

$$[\Delta^2 v/\epsilon^2] = 0 \quad (\text{from equation (92) with } [v_{tttt}] = 0) \quad (107)$$

$$[\Delta^2 w/\epsilon^2] = 0 \quad (\text{from equation (93) with } [w_{tttt}] = 0) \quad (108)$$

In general, for $m = 0, 1, 2, \dots$ the jump conditions on the even derivatives ∂_x^{2m} are

$$[\Delta^m u/\epsilon^{m-1}] = 0 \quad (109)$$

$$[\Delta^m v/\epsilon^m] = 0 \quad (110)$$

$$[\Delta^m w/\epsilon^m] = 0 \quad (111)$$

while the conditions on the odd derivatives are, for $m = 0, 1, 2, \dots$,

$$[\Delta^m (u_x + v_y)] = 0 \quad (112)$$

$$[(\Delta^m (v_x - u_y))/\epsilon^m] = 0 \quad (113)$$

$$[(\Delta^m w_x)/\epsilon^{m+1}] = 0 \quad (114)$$

For a general interface oriented with normal \mathbf{n} and tangent $\boldsymbol{\tau}$, the jump conditions will be, for $m = 0, 1, 2, \dots$,

$$[\mathbf{n} \cdot \Delta^m \mathbf{u}/\epsilon^{m-1}] = 0 \quad (115)$$

$$[\boldsymbol{\tau} \cdot \Delta^m \mathbf{u}/\epsilon^m] = 0 \quad (116)$$

$$[\Delta^m w/\epsilon^m] = 0 \quad (117)$$

and

$$[\Delta^m (u_x + v_y)] = 0 \quad (118)$$

$$[(\Delta^m (v_x - u_y))/\epsilon^m] = 0 \quad (119)$$

$$[(\Delta^m w_n)/\epsilon^{m+1}] = 0 \quad (120)$$

15 Boundary conditions at material interfaces in 3D

Consider the three-dimensional problem

$$\epsilon(\mathbf{x})\mathbf{E}_t = \nabla \times \mathbf{H} \quad (121)$$

$$\mu(\mathbf{x})\mathbf{H}_t = -\nabla \times \mathbf{E} \quad (122)$$

$$\nabla \cdot (\epsilon(\mathbf{x})\mathbf{E}) = 0 \quad (123)$$

$$\nabla \cdot (\mu(\mathbf{x})\mathbf{H}) = 0 \quad (124)$$

The dielectric permittivity, ϵ , and magnetic permeability, μ are assumed to be piecewise constant with a possible jump across a smooth interface \mathcal{S} , with normal $\mathbf{n}(\mathbf{x})$. It is assumed that the solution to these equations remains bounded. Note that our assumptions of piecewise constant coefficients imply that on each side of the interface the electric and magnetic fields satisfy

$$\mathbf{E}_{tt} = \frac{1}{\epsilon\mu} \Delta \mathbf{E} \quad (125)$$

$$\mathbf{H}_{tt} = \frac{1}{\epsilon\mu} \Delta \mathbf{H} \quad (126)$$

$$\nabla \cdot \mathbf{E} = 0 \quad (127)$$

$$\nabla \cdot \mathbf{H} = 0 \quad (128)$$

The basic jump conditions at a material interface are

$$[\epsilon \mathbf{n} \cdot \mathbf{E}] = 0 \quad [\mu \mathbf{n} \cdot \mathbf{H}] = 0 \quad (129)$$

$$[\tau \cdot \mathbf{E}] = 0 \quad [\tau \cdot \mathbf{H}] = 0 \quad (130)$$

Here τ represents a tangent to the material interface. Since there are two linearly independent tangents, τ_m , $m = 1, 2$, there will be two linearly independent conditions $[\tau_m \cdot \mathbf{E}] = 0$, $m = 1, 2$. Jump conditions on the first spatial derivatives are obtained from the divergence relations (123-124) and equations (121-122) combined with $[\tau \cdot \mathbf{E}_t] = 0$, $[\tau \cdot \mathbf{H}_t] = 0$,

$$[\nabla \cdot (\mathbf{E})] = 0 \quad [\nabla \cdot (\mathbf{H})] = 0 \quad (131)$$

$$[\mu^{-1} \tau \cdot \nabla \times \mathbf{E}] = 0 \quad [\epsilon^{-1} \tau \cdot \nabla \times \mathbf{H}] = 0 \quad (132)$$

Note that it is also true that $[\nabla \cdot (\epsilon \mathbf{E})] = 0$ (or indeed for any piecewise constant ν , it is true that $[\nabla \cdot (\nu \mathbf{E})] = 0$)

Jump conditions on the second spatial derivatives follow from taking two time derivatives of equations (129-130), and using the vector wave equations (125-126) to replace the time derivatives by space derivatives,

$$[\epsilon \mathbf{n} \cdot \Delta \mathbf{E}/(\epsilon\mu)] = 0 \quad [\mu \mathbf{n} \cdot \Delta \mathbf{H}/(\epsilon\mu)] = 0 \quad (133)$$

$$[\tau \cdot \Delta \mathbf{E}/(\mu\epsilon)] = 0 \quad [\tau \cdot \Delta \mathbf{H}/(\mu\epsilon)] = 0 \quad (134)$$

By continuing to take time derivatives it follows that for $m = 0, 1, 2, 3, \dots$,

$$[\epsilon \mathbf{n} \cdot \Delta^m \mathbf{E}/(\epsilon\mu)^m] = 0 \quad [\mu \mathbf{n} \cdot \Delta^m \mathbf{H}/(\epsilon\mu)^m] = 0 \quad (135)$$

$$[\tau \cdot \Delta^m \mathbf{E}/(\mu\epsilon)^m] = 0 \quad [\tau \cdot \Delta^m \mathbf{H}/(\mu\epsilon)^m] = 0 \quad (136)$$

$$[\nabla \cdot (\Delta^m \mathbf{E})] = 0 \quad [\nabla \cdot (\Delta^m \mathbf{H})] = 0 \quad (137)$$

$$[\mu^{-1} \tau \cdot \nabla \times \Delta^m \mathbf{E}/(\mu\epsilon)^m] = 0 \quad [\epsilon^{-1} \tau \cdot \nabla \times \Delta^m \mathbf{H}/(\mu\epsilon)^m] = 0 \quad (138)$$

These interface jump conditions impose conditions for each spatial derivative of the solution.

Another way to write the jump conditions (135) through (138) that doesn't involve the tangent vectors τ is as

$$\left[(\mathbf{E} + ((\epsilon - 1)\mathbf{n} \cdot \mathbf{E}) \mathbf{n}) / (\epsilon\mu)^m \right] = 0, \quad (139)$$

$$\left[(\mu^{-1}(\nabla \times \Delta^m \mathbf{E} - (\mathbf{n} \cdot \nabla \times \Delta^m \mathbf{E}) \mathbf{n}) + \nabla \cdot (\Delta^m \mathbf{E}) \mathbf{n}) / (\epsilon\mu)^m \right] = 0, \quad (140)$$

and

$$[(\mathbf{H} + ((\mu - 1)\mathbf{n} \cdot \mathbf{H}) \mathbf{n}) / (\epsilon\mu)^m] = 0, \quad (141)$$

$$[(\epsilon^{-1}(\nabla \times \Delta^m \mathbf{H} - (\mathbf{n} \cdot \nabla \times \Delta^m \mathbf{H}) \mathbf{n}) + \nabla \cdot (\Delta^m \mathbf{H}) \mathbf{n}) / (\epsilon\mu)^m] = 0. \quad (142)$$

The former equations follow by taking the dot product of the above equations with \mathbf{n} or $\boldsymbol{\tau}$. This latter form may be convenient for discretizing the equations since there is no need to define tangent vectors.

15.1 Discrete boundary conditions for material interfaces

The material interface is assumed to lie along the boundary between two grids as shown in figure ...

All discrete approximations impose the basic interface condition

$$\begin{aligned} [\epsilon \mathbf{n} \cdot \mathbf{E}] &= 0 \\ [\boldsymbol{\tau} \cdot \mathbf{E}] &= 0 \end{aligned}$$

A second-order accurate approximation will use one ghost line on each side of the interface. The values of \mathbf{E} at these two ghost line values are determined by imposing the following conditions:

$$\begin{aligned} [\nabla_{2h} \cdot (\mathbf{E})] &= 0 \\ [\mu^{-1} \boldsymbol{\tau} \cdot \nabla_{2h} \times \mathbf{E}] &= 0 \\ [\epsilon \mathbf{n} \cdot \Delta_{2h} \mathbf{E} / (\epsilon\mu)] &= 0 \\ [\boldsymbol{\tau} \cdot \Delta_{2h} \mathbf{E} / (\mu\epsilon)] &= 0 \end{aligned}$$

Here ∇_{2h} , $\nabla \times_{2h}$, and Δ_{2h} are second-order accurate centered difference approximations.

A fourth-order accurate approximation will use two ghost lines on each side of the interface. The values at the ghost points can be determined using fourth-order accurate approximations to the interface conditions for the first and second derivatives

$$\begin{aligned} [\nabla_{4h} \cdot (\mathbf{E})] &= 0 \\ [\mu^{-1} \boldsymbol{\tau} \cdot \nabla_{2h} \times \mathbf{E}] &= 0 \\ [\epsilon \mathbf{n} \cdot \Delta_{2h} \mathbf{E} / (\epsilon\mu)] &= 0 \\ [\boldsymbol{\tau} \cdot \Delta_{2h} \mathbf{E} / (\mu\epsilon)] &= 0 \end{aligned}$$

together with second-order accurate approximations to the interface conditions for the third and fourth derivatives,

$$\begin{aligned} [(\nabla \cdot \Delta)_{2h} (\mathbf{E})] &= 0 \\ [\mu^{-1} \boldsymbol{\tau} \cdot (\nabla \times \Delta)_{2h} \mathbf{E} / (\epsilon\mu)] &= 0 \\ [\epsilon \mathbf{n} \cdot (\Delta^2)_{2h} \mathbf{E} / (\epsilon\mu)^2] &= 0 \\ [\boldsymbol{\tau} \cdot (\Delta^2)_{2h} \mathbf{E} / (\epsilon\mu)^2] &= 0 \end{aligned}$$

15.2 Reflection and Transmission for a planar material interface

Consider an interface at $x = 0$ between two materials. Assume that for $x < 0$, $\epsilon = \epsilon_1$ and $c = c_1 = \epsilon_1^{-1/2}$ while for $x > 0$ $\epsilon = \epsilon_2$ and $c = c_2 = \epsilon_2^{-1/2}$. For an incident plane wave of the form

$$\begin{aligned}\mathbf{u}^I &= \mathbf{a} e^{i(\mathbf{k} \cdot \mathbf{x} - \omega t)} \\ \mathbf{a} &= (-k_2, k_1)/\|\mathbf{k}\| \quad (\text{since } \nabla \cdot \mathbf{u} = 0)\end{aligned}$$

the solution will consist of a reflected wave and refracted (transmitted) wave in addition to the incident wave. The solution is given by

$$\begin{aligned}\mathbf{u}(\mathbf{x}, t) &= \mathbf{a} e^{i(k_1 x + k_2 y - \omega t)} + R \mathbf{b} e^{i(-k_1 x + k_2 y - \omega t)} \quad \text{for } x < 0 \\ &= \tau \mathbf{d} e^{i(\kappa_1 x + \kappa_2 y - \omega t)} \quad \text{for } x > 0\end{aligned}$$

where R is the reflection coefficient, τ is the transmission coefficient and where $\mathbf{b} = (-k_2, -k_1)/\|\mathbf{k}\|$ and $\mathbf{d} = (-\kappa_2, \kappa_1)/\|\boldsymbol{\kappa}\|$.

We have the conditions, $[\epsilon u] = 0$, $[v] = 0$ and $\omega = c_1 \|\mathbf{k}\| = c_2 \|\boldsymbol{\kappa}\|$. These imply that ** check these**

$$\begin{aligned}\kappa_2 &= k_2 \\ \kappa_1 &= \sqrt{(c_1/c_2)^2(k_1^2 + k_2^2) - k_2^2} \\ \tau &= \frac{2c_2 \cos(\theta_1)}{c_2 \cos(\theta_2) + c_1 \cos(\theta_1)} \\ R &= \frac{c_1 \cos(\theta_1) - c_2 \cos(\theta_2)}{c_2 \cos(\theta_2) + c_1 \cos(\theta_1)} \\ \cos(\theta_1) &= k_1/\|\mathbf{k}\| \quad (\theta_1 \text{ is the angle of incidence}) \\ \cos(\theta_2) &= \kappa_1/\|\boldsymbol{\kappa}\| \quad (\theta_2 \text{ is the angle of reflection}) \\ \sin(\theta_1)/c_1 &= \sin(\theta_2)/c_2 \quad (\text{Snell's law, from } \kappa_2 = k_2)\end{aligned}$$

Note that when

$$\frac{k_1^2}{k_2^2} < \left(\frac{c_2}{c_1}\right)^2 - 1$$

then κ_1 is imaginary. This corresponds to total internal reflection. This solution is still valid (check this!) provided we take the branch of the square root with $\text{Im}(\kappa_1) \geq 0$. The solution has an evanescent wave that decays exponentially into the second region. If we take $\kappa_1 = i\alpha$ with $\alpha \geq 0$ then the refracted wave is

$$\mathbf{u}(\mathbf{x}, t) = \tau \mathbf{d} e^{-\alpha x} e^{i(\kappa_2 y - \omega t)} \quad \text{for } x > 0$$

16 Absorbing Boundary Conditions

In this section we discuss absorbing boundary conditions (ABC's).

16.1 Engquist-Majda one-way wave equations

Consider the wave equation

$$u_{tt} = u_{xx} + u_{yy} + u_{zz}$$

We consider a boundary at $x = 0$. The wave equation can be formally factored using pseudo-differential operators

$$(D_x - D_t \sqrt{1 - S^2})(D_x + D_t \sqrt{1 - S^2}) = 0$$

where

$$S^2 = (D_y^2 + D_z^2)/D_t^2$$

The operator $G^- = D_x - D_t \sqrt{1 - S^2}$ only supports waves moving to the left. Applying G^- to a wave function U will absorb waves moving to left (at any angle). To see this consider a wave that moves in the negative x -direction

$$U(\mathbf{x}, t) = e^{i(\mathbf{k} \cdot \mathbf{x} + \omega t)}$$

with $k_x > 0$ and $\omega = \sqrt{\mathbf{k} \cdot \mathbf{k}} > 0$.

In Fourier space

$$\begin{aligned} \mathcal{F}\{G^- U\} &= ik_x - i\omega \sqrt{1 - (k_y^2 + k_z^2)/\omega^2} \\ &= ik_x - i\sqrt{\omega^2 - k_y^2 + k_z^2} \\ &= ik_x - i|k_x| \\ &= 0 \end{aligned}$$

thus giving $D_t G^- U = 0$.

We will apply $G^- = D_x - D_t \sqrt{1 - S^2}$ as a non-reflecting boundary condition. If applied exactly it will absorb (treat exactly without reflection) all outgoing plane waves. It will not handle evanescent modes.

Aside: Evanescent waves When a plane wave hits a material interface there will be a reflected wave and a refracted wave (transmitted wave). If the refracted ray bends toward the normal we have what is called external reflection. If it bends away from the normal it is called internal reflection. At a critical angle θ_c the refracted wave is parallel to the interface. For angles greater than θ_c there is no refracted wave and we have total internal reflection. There is however an evanescent wave that travels parallel to the boundary and decays exponentially into the second medium. The evanescent wave ensures that the tangential component of the electric field is continuous across the interface.

If the wave approaching the boundary is nearly normal incidence then $k_x^2 \gg k_y^2 + k_z^2$ and thus

$$\widehat{S^2} = (k_y^2 + k_z^2)/\omega^2 = (k_y^2 + k_z^2)/(k_x^2 + k_y^2 + k_z^2) \ll 1$$

Thus S^2 is thought of as being small and we approximate

$$\sqrt{1 - S^2} \approx p_0 + p_2 S^2$$

Whence

$$\begin{aligned} D_t G^- &\approx D_t D_x - D_t^2 (p_0 + p_2 S^2) \\ &\approx D_t D_x - p_0 D_t^2 - p_2 (D_y^2 + D_z^2) \\ &= D_t D_x - p_0 D_x^2 - (p_0 + p_2)(D_y^2 + D_z^2) \end{aligned}$$

For $p_0 = 1$, $p_2 = -1/2$ this gives the approximate (second-order) Engquist-Majda ABC,

$$L_2^{em}u = \partial_t \partial_x u - \partial_t^2 u + \frac{1}{2}(\partial_y^2 + \partial_z^2)u = 0 \quad (143)$$

$$= \partial_t \partial_x u - \partial_x^2 u - \frac{1}{2}(\partial_y^2 + \partial_z^2)u = 0 \quad (144)$$

which is exact for waves impinging on the boundary in the normal direction (angle of incidence of zero). Mur's scheme is a discretization of the above BC – Mur centered his scheme at $t + \Delta/2$ and $\Delta x/2$ to give a second order approximation using only two time levels.

We can use a better approximation

$$\sqrt{1 - S^2} \approx \frac{p_0 + p_2 S^2}{q_0 + q_2 S^2}$$

This give a third-order boundary condition

$$L_3^{em}u = \partial_x(q_0 \partial_t^2 + q_2(\partial_y^2 + \partial_z^2)) - \partial_t(p_0 \partial_t^2 + p_2(\partial_y^2 + \partial_z^2)) \quad (145)$$

$$= q_0 \partial_x \partial_t^2 + q_2 \partial_x(\partial_y^2 + \partial_z^2) - p_0 \partial_t^3 - p_2 \partial_t(\partial_y^2 + \partial_z^2) \quad (146)$$

Engquist and Majda suggested $p_0 = q_0 = 1$ and $p_2 = -3/4$, $q_2 = -1/4$ which is the Padé approximation (minimizing the error near $S = 0$).

Trefethen and Halpern considered other possibilities such as a Chebyshev or least squares. One could choose the coefficients to make the approximation exact at other angles.

16.2 Second-order accurate discretization

Consider Engquist-Majda ABC,

$$\partial_t \partial_x u = \alpha \partial_x^2 u + \beta(\partial_y^2 + \partial_z^2)u \quad (147)$$

where, for example $\alpha = c$ and $\beta = \frac{1}{2}c$, will give a second-order accurate approximation. We can discretize this equation with the centered second-order accurate approximation

$$D_0^t D_0^x U_{ij}^n = \alpha D_+^x D_-^x U_{ij}^n + \beta(D_+^y D_-^y + D_+^z D_-^z)U_{ij}^n \quad (148)$$

This equation will give the ghost point value U_{-1j}^{n+1} given interior and boundary values at time t^{n+1} and old values at time t^n .

Here is another second-order approximation, centred at $t^{n+\frac{1}{2}}$ that uses only two time levels,

$$D_+^t D_0^x U_{ij}^n = \mathcal{A}_+^t \left(\alpha D_+^x D_-^x U_{ij}^n + \beta(D_+^y D_-^y + D_+^z D_-^z)U_{ij}^n \right) \quad (149)$$

$$\mathcal{A}_+^t f^n = \frac{1}{2}(f^{n+1} + f^n) \quad (150)$$

The value at the ghost point U_{-1j}^{n+1} in equation (149) can be explicitly solved for given interior and boundary values at time t^{n+1} and old values at time t^n .

This gives the approximation

$$\left(\frac{1}{2\Delta t \Delta x} + \frac{\alpha}{2\Delta x^2} \right) U_{-1j}^{n+1} = D_+^t D_0^x U_{ij}^n + \frac{1}{2\Delta t \Delta x} U_{-1j}^{n+1} \quad (151)$$

$$- \mathcal{A}_+^t \left(\alpha D_+^x D_-^x U_{ij}^n - \beta(D_+^y D_-^y + D_+^z D_-^z)U_{ij}^n \right) + \frac{\alpha}{2\Delta x^2} U_{-1j}^{n+1} \quad (152)$$

or

$$\left(1 + \alpha \frac{\Delta t}{\Delta x} \right) U_{-1j}^{n+1} = 2\Delta t \Delta x \left[D_+^t D_0^x U_{ij}^n + \frac{1}{2\Delta t \Delta x} U_{-1j}^{n+1} \right] \quad (153)$$

$$- \mathcal{A}_+^t \left(\alpha D_+^x D_-^x U_{ij}^n - \beta(D_+^y D_-^y + D_+^z D_-^z)U_{ij}^n \right) + \frac{\alpha}{2\Delta x^2} U_{-1j}^{n+1} \quad (154)$$

Note: The right-hand-side of the above expression does not depend on U_{-1j}^{n+1} .

16.3 Fourth-order accuracy

For fourth-order accuracy we have two ghost points and need an additional numerical boundary condition. We could use the normal derivative of one of the above approximations,

$$\partial_x L_2^{em} u = D_t D_x^2 - p_0 D_x^3 - (p_0 + p_2) D_x (D_y^2 + D_z^2)$$

It might be appropriate to use the first order approximation $L_1^{em} = \partial_t - \partial_x$ times the second-order

$$L_1^{em} L_2^{em} u = (\partial_t - \partial_x) \left[D_t D_x - p_0 D_x^2 - (p_0 + p_2) (D_y^2 + D_z^2) \right]$$

16.4 Absorbing boundary conditions on a curvilinear grid

Consider a rotated rectangular grid. The wave equation in transformed coordinates is

$$\begin{aligned} u_{tt} &= (r_x^2 + r_y^2 + r_z^2) u_{rr} + (s_x^2 + s_y^2 + s_z^2) u_{ss} + \dots \\ &= D_n^2 u + \Delta_\tau u \\ D_n &= \|\nabla_{\mathbf{x}} r\| \partial_r \end{aligned}$$

where D_n is the normal derivative to a boundary $r = \text{const}$. Following the same argument as before we can derive the (second-order) Engquist-Majda ABC as

$$\partial_t D_n u = \alpha D_n^2 u + \beta \Delta_\tau u$$

Now consider a general curvilinear grid. The wave equation in transformed coordinates is

$$\begin{aligned} u_{tt} &= Lu \\ &= (r_x^2 + r_y^2 + r_z^2) u_{rr} + (s_x^2 + s_y^2 + s_z^2) u_{ss} + 2(r_x s_x + r_y s_y + r_z s_z) u_{rs} \\ &\quad + (r_{xx} + r_{yy} + r_{zz}) u_r + (s_{xx} + s_{yy} + s_{zz}) u_s + \dots \\ &= D_n^2 u + \Delta_\tau u \\ D_n &= \|\nabla_{\mathbf{x}} r\| \partial_r \\ \Delta_\tau &= (L - D_n^2) u \end{aligned}$$

where we have arbitrarily chosen D_n to be an approximation to the normal derivative. This gives the ABC

$$\partial_t D_n u = \alpha D_n^2 u + \beta \Delta_\tau u$$

which may reasonably accurate for a nearly orthogonal grid.

A more accurate approximation for non-orthogonal grids could be to set D_n to the actual normal derivative:

$$\begin{aligned} D_n &= \mathbf{n} \cdot \nabla = \frac{\nabla_{\mathbf{x}} r}{|\nabla_{\mathbf{x}} r|} \cdot \nabla_{\mathbf{x}} \\ &= |\nabla_{\mathbf{x}} r| \partial_r + (\mathbf{n} \cdot \nabla s) \partial_s \end{aligned}$$

16.5 Non-reflecting Boundary Conditions and Incident Fields

The non-reflecting boundary conditions were derived assuming that there are no incoming waves, just waves leaving the domain. We can treat the case of an incident field arriving from outside the computational domain in a couple of ways.

Approach I: In this approach we write the total electric field in the neighbourhood of the boundary as the sum of a given incident field $\mathbf{E}^i(\mathbf{x}, t)$ and a scattered field $\mathbf{E}^s(\mathbf{x}, t)$,

$$\mathbf{E}(\mathbf{x}, t) = \mathbf{E}^i(\mathbf{x}, t) + \mathbf{E}^s(\mathbf{x}, t).$$

We assume that the incident field is an exact solution of Maxwell's equations near the boundary. We can apply the non-reflecting boundary condition to $\mathbf{E}^s(\mathbf{x}, t)$ by subtracting $\mathbf{E}^i(\mathbf{x}, t)$ from the total field. In the discrete case, at each time step we can subtract $\mathbf{E}^i(\mathbf{x}, t)$ from $\mathbf{E}(\mathbf{x}, t)$ on a few points near the boundary, apply the NRBC, and then add back $\mathbf{E}^i(\mathbf{x}, t)$.

Approach II: In this approach we change the NRBC or ABC to account for the incident field. Given the NRBC,

$$\mathcal{L}\mathbf{E}^s = 0, \quad (155)$$

by substituting $\mathbf{E}^s(\mathbf{x}, t) = \mathbf{E}(\mathbf{x}, t) - \mathbf{E}^i(\mathbf{x}, t)$ we get the new condition for the total field

$$\mathcal{L}\mathbf{E} = \mathcal{L}\mathbf{E}^i \quad (156)$$

For example,

$$\partial_t \partial_x \mathbf{E} - (\alpha \partial_x^2 \mathbf{E} + \beta (\partial_y^2 + \partial_z^2) \mathbf{E}) = \partial_t \partial_x \mathbf{E}^i - (\alpha \partial_x^2 \mathbf{E}^i + \beta (\partial_y^2 + \partial_z^2) \mathbf{E}^i) \quad (157)$$

Note: We could potentially set the RHS to $G^- \mathbf{E}^i$ if $\mathcal{L} \approx G^-$.

17 Radiation Boundary Conditions

In this section we discuss radiation boundary conditions.

17.0.1 Non-local exact boundary conditions for a periodic strip

Consider the solution of a problem on the strip $[x_a, x_b] \times [y_a, y_b]$ with an artificial boundary at $x = x_a$ and $x = x_b$ and periodic boundaries in y .

The non-local exact boundary conditions are imposed at $x = x_a$ and $x = x_b$ as

$$u_t + u_n + H(u) = 0$$

where the kernel $H(u)$ is determined by routines supplied by Tom Hagstrom.

To discretize this BC we use a Taylor series approximation to determine the ghost point value $u(h, t + \Delta t)$ in terms of derivatives centered at $u(0, t)$,

$$\begin{aligned} u(h, t + dt) &= u(0, t) + \Delta t u_t(0, t) + h u_x(0, t) + \frac{\Delta t^2}{2} u_{tt}(0, t) + \Delta t h u_{tx}(0, t) + h^2 u_{xx}(0, t) \\ &\quad + \frac{\Delta t^3}{3!} u_{ttt}(0, t) + \frac{3\Delta t^2}{3!} h u_{ttx}(0, t) + \frac{3\Delta t h^2}{3!} u_{txx}(0, t) + \frac{h^3}{3!} u_{txx}(0, t) + \dots \end{aligned}$$

The time derivatives in the Taylor series are determined from the boundary condition and the equation,

$$\begin{aligned} u_t &= -u_n - H(u) \\ u_{tt} &= \Delta u \\ u_{tn} + u_{nn} + H(u_n) &= 0 \end{aligned}$$

Here we use the fact that $u_n = \pm u_x$ and that u_x, u_{xx}, \dots are also solutions of the wave equation.

17.0.2 Non-local exact boundary conditions for an annular boundary

Consider the solution of Maxwell's equation in the region $\mathbf{D}(R, \mathbf{x}_0)$, a disk of radius R and centre \mathbf{x}_0 ,

$$\mathbf{D}(R, \mathbf{x}_0) = \{|\mathbf{x} - \mathbf{x}_0| < R\}.$$

The non-local exact boundary conditions imposed at $r \equiv |\mathbf{x} - \mathbf{x}_0| = R$ are of the form

$$\frac{1}{c} u_t + u_r + \frac{1}{2R} u + H(u) = 0$$

where $u_r = u_n = \mathbf{n} \cdot \nabla u$ and where the kernel $H(u)$ is determined by routines supplied by Tom Hagstrom.

To discretize this BC we use a Taylor series approximation to determine the ghost point value $u(x + \Delta x, y + \Delta y, t + dt)$ in terms of solution and its derivatives centered at the boundary $u(\mathbf{x}, t)$,

$$\begin{aligned} u(x + \Delta x, y + \Delta y, t + dt) &= u(\mathbf{x}, t) + \Delta t u_t(\mathbf{x}, t) + \Delta x u_x(0, t) + \Delta y u_y(\mathbf{x}, t) \\ &\quad + \frac{1}{2} \left(\Delta t^2 u_{tt} + 2\Delta t (\Delta x u_{tx} + \Delta y u_{ty}) + \Delta x^2 u_{xx} + 2\Delta x \Delta y u_{xy} + \Delta y^2 u_{yy} \right) \\ &\quad + \frac{1}{3!} \left(\Delta t^3 u_{ttt} + 3\Delta t^2 (\Delta x u_{ttx} + \Delta y u_{tty}) + 3\Delta t (\Delta x^2 u_{txx} + 2\Delta x \Delta y u_{xy} \Delta y^2 u_{tyy}) \right. \\ &\quad \left. + \Delta x^3 u_{xxx} + 3\Delta x^2 \Delta y u_{xxy} + 3\Delta x \Delta y^2 u_{xyy} + \Delta y^3 u_{yyy} \right) + \dots \end{aligned}$$

The terms with pure spatial derivatives at time t can be computed directly using centred approximations.

The terms that involve time derivatives are given by

$$\begin{aligned}
u_t &= -c(u_n + \frac{1}{2R}u + H(u)) \\
u_{tx} &= -c((u_x)_n + \frac{1}{2R}u_x + H(u_x)) \\
u_{ty} &= -c((u_y)_n + \frac{1}{2R}u_y + H(u_y)) \\
u_{tt} &= c^2(\Delta u) \\
u_{txx} &= -c((u_{xx})_n + \frac{1}{2R}u_{xx} + H(u_{xx})) \\
u_{txy} &= -c((u_{xy})_n + \frac{1}{2R}u_{xy} + H(u_{xy})) \\
u_{tyy} &= -c((u_{yy})_n + \frac{1}{2R}u_{yy} + H(u_{yy})) \\
u_{ttt} &= c^2(u_{txx} + u_{tyy}) \\
&\vdots
\end{aligned}$$

Here we use the fact that u_x, u_y, u_{xx}, u_{xy} are also solutions to the wave equation.

Note that u_r is not a solution of the wave equation and so we cannot use a Taylor expansion in r alone.

18 Higher-order accurate self-adjoint approximations on curvilinear grids

We can define higher-order accurate symmetric approximations to the operator $\nabla \cdot (a\nabla)u$. For this purpose we use the following approximations,

$$\begin{aligned}\frac{\partial u}{\partial x}(x + h/2) &= D_+ \left[1 + \sum_{n=1}^{\infty} \alpha_n h^{2n} (D_+ D_-)^n \right] u(x + h/2) \\ &= D_+ \left[I - \frac{h^2}{24} D_+ D_- + \frac{3}{640} h^4 (D_+ D_-)^2 - \frac{5}{7168} h^6 (D_+ D_-)^3 + \dots \right] u \\ \frac{\partial u}{\partial x}(x) &= D_0 \left[1 + \sum_{n=1}^{\infty} \beta_n h^{2n} (D_+ D_-)^n \right] u(x) \\ &= D_0 \left[I - \frac{h^2}{6} D_+ D_- + \frac{h^4}{30} (D_+ D_-)^2 - \frac{h^6}{140} (D_+ D_-)^3 + \dots \right] u\end{aligned}$$

The coefficients in these approximations can be determined by Taylor series. A more convenient approach however is illustrated for the first expression as follows. We begin by making the ansatz,

$$\frac{\partial u}{\partial x}(x + h/2) = D_+ \left[1 + \sum_{n=1}^{\infty} \alpha_n h^{2n} (D_+ D_-)^n \right] u(x + h/2)$$

Substituting $u(x + h/2) = e^{i\omega(x+h/2)}$ into this expression and using

$$\begin{aligned}D_+ e^{i\omega(x+h/2)} &= \frac{2i}{h} \sin(\xi/2) e^{i\omega(x+h/2)} \\ h^2 D_+ D_- e^{i\omega(x+h/2)} &= -4 \sin^2(\xi/2) e^{i\omega(x+h/2)} \\ \xi &= \omega h\end{aligned}$$

gives the equation

$$y = \sin(y) \left[1 + \sum_{n=1}^{\infty} \alpha_n (-4 \sin^2(y))^n \right]$$

where $y = \xi/2$. Expanding $\sin(y)$ in a Taylor series and equating powers of y gives (using a symbolic manipulation package such as maple, for example)

$$\alpha_1 = -\frac{1}{6}, \quad \alpha_2 = \frac{3}{640}, \quad \alpha_3 = -\frac{5}{7168}, \quad \alpha_4 = \frac{35}{294912}$$

We now define the approximation

$$\frac{\partial}{\partial r} \left(a \frac{\partial}{\partial r} \right) u = \left\{ D_+ \left[1 + \sum_{n=1}^M \alpha_n h^{2n} (D_+ D_-)^n \right] \right\} a(r-h/2) \left\{ D_- + \left[1 + \sum_{n=1}^M \alpha_n h^{2n} (D_+ D_-)^n \right] \right\} u + O(h^{2M+2}).$$

We will also need approximations for $a(r - h/2)$,

$$\begin{aligned}a_{i-1/2} &= \frac{1}{2}(a_i + a_{i-1}) + O(h^2) \\ &= \frac{9}{16}(a_i + a_{i-1}) - \frac{1}{16}(a_{i+1} + a_{i-2}) + O(h^4) \\ &= \frac{75}{128}(a_i + a_{i-1}) - \frac{25}{256}(a_{i+1} + a_{i-2}) + \frac{3}{16}(a_{i+2} + a_{i-3}) + O(h^6) \\ &= \frac{1225}{2048}(a_i + a_{i-1}) - \frac{245}{2048}(a_{i+1} + a_{i-2}) + \frac{49}{2048}(a_{i+2} + a_{i-3}) - \frac{5}{2048}(a_{i+3} + a_{i-4}) + O(h^8)\end{aligned}$$

The fourth, sixth and eighth order approximations are based on the following expansion:

$$\begin{aligned}
\frac{\partial}{\partial r} \left(a \frac{\partial}{\partial r} \right) u &= D_+ (a_{i-1/2}^{(0)} D_-) u_i \\
&\quad - \frac{1}{24} h^2 \left[D_+ (a_{i-1/2}^{(1)} D_+ + D_-^2) + D_+^2 D_- (a_{i-1/2}^{(1)} D_-) \right] u_i \\
&\quad + \frac{1}{24^2} h^4 \left[D_+^2 D_- (a_{i-1/2}^{(2)} D_+ + D_-^2) \right] u_i + \frac{3}{640} h^4 \left[D_+ (a_{i-1/2}^{(2)} D_+^2 D_-^3) + D_+^3 D_-^2 (a_{i-1/2}^{(2)} D_-) \right] u_i \\
&\quad - \frac{5}{7168} h^6 \left[D_+^4 D_-^3 (a_{i-1/2}^{(3)} D_-) + D_+ (a_{i-1/2}^{(3)} D_+^3 D_-^4) \right] u_i \\
&\quad - \frac{3}{640 \cdot 24} h^6 \left[D_+^2 D_- (a_{i-1/2}^{(3)} D_+^2 D_-^3) + D_+^3 D_-^2 (a_{i-1/2}^{(3)} D_+ D_-^2) \right] u_i \\
&\quad + O(h^8)
\end{aligned}$$

To keep the formulae compact we use different orders of approximation for $a_{i-1/2}$ denoted by $a_{i-1/2}^{(m)}$. Here is a fourth-order approximation,

$$\begin{aligned}
\frac{\partial}{\partial r} \left(a \frac{\partial}{\partial r} \right) u &\approx D_+ (a_{i-1/2}^{(0)} D_-) u_i \\
&\quad - \frac{1}{24} h^2 \left[D_+ (a_{i-1/2}^{(1)} D_+ + D_-^2) + D_+^2 D_- (a_{i-1/2}^{(1)} D_-) \right] u_i \\
a_{i-1/2}^{(0)} &= \frac{9}{16} (a_i + a_{i-1}) - \frac{1}{16} (a_{i+1} + a_{i-2}) \\
a_{i-1/2}^{(1)} &= \frac{1}{2} (a_i + a_{i-1})
\end{aligned}$$

Here is a sixth-order approximation

$$\begin{aligned}
\frac{\partial}{\partial r} \left(a \frac{\partial}{\partial r} \right) u &\approx D_+ (a_{i-1/2}^{(0)} D_-) u_i \\
&\quad - \frac{1}{24} h^2 \left[D_+ (a_{i-1/2}^{(1)} D_+ + D_-^2) + D_+^2 D_- (a_{i-1/2}^{(1)} D_-) \right] u_i \\
&\quad + \frac{1}{24^2} h^4 \left[D_+^2 D_- (a_{i-1/2}^{(2)} D_+ + D_-^2) \right] u_i + \frac{3}{640} h^4 \left[D_+ (a_{i-1/2}^{(2)} D_+^2 D_-^3) + D_+^3 D_-^2 (a_{i-1/2}^{(2)} D_-) \right] u_i \\
a_{i-1/2}^{(0)} &= \frac{75}{128} (a_i + a_{i-1}) - \frac{25}{256} (a_{i+1} + a_{i-2}) + \frac{3}{16} (a_{i+2} + a_{i-3}) \\
a_{i-1/2}^{(1)} &= \frac{9}{16} (a_i + a_{i-1}) - \frac{1}{16} (a_{i+1} + a_{i-2}) \\
a_{i-1/2}^{(2)} &= \frac{1}{2} (a_i + a_{i-1})
\end{aligned}$$

Here is an eight-order approximation

$$\begin{aligned}
\frac{\partial}{\partial r} \left(a \frac{\partial}{\partial r} \right) u &\approx D_+ (a_{i-1/2}^{(0)} D_-) u_i \\
&\quad - \frac{1}{24} h^2 \left[D_+ (a_{i-1/2}^{(1)} D_+ D_-^2) + D_+^2 D_- (a_{i-1/2}^{(1)} D_-) \right] u_i \\
&\quad + \frac{1}{24^2} h^4 \left[D_+^2 D_- (a_{i-1/2}^{(2)} D_+ D_-^2) \right] u_i + \frac{3}{640} h^4 \left[D_+ (a_{i-1/2}^{(2)} D_+^2 D_-^3) + D_+^3 D_-^2 (a_{i-1/2}^{(2)} D_-) \right] u_i \\
&\quad - \frac{5}{7168} h^6 \left[D_+^4 D_-^3 (a_{i-1/2}^{(3)} D_-) + D_+ (a_{i-1/2}^{(3)} D_+^3 D_-^4) \right] u_i \\
&\quad - \frac{3}{640 \cdot 24} h^6 \left[D_+^2 D_- (a_{i-1/2}^{(3)} D_+^2 D_-^3) + D_+^3 D_-^2 (a_{i-1/2}^{(3)} D_+ D_-^2) \right] u_i \\
a_{i-1/2}^{(0)} &= \frac{1225}{2048} (a_i + a_{i-1}) - \frac{245}{2048} (a_{i+1} + a_{i-2}) + \frac{49}{2048} (a_{i+2} + a_{i-3}) - \frac{5}{2048} (a_{i+3} + a_{i-4}) \\
a_{i-1/2}^{(1)} &= \frac{75}{128} (a_i + a_{i-1}) - \frac{25}{256} (a_{i+1} + a_{i-2}) + \frac{3}{16} (a_{i+2} + a_{i-3}) \\
a_{i-1/2}^{(2)} &= \frac{9}{16} (a_i + a_{i-1}) - \frac{1}{16} (a_{i+1} + a_{i-2}) \\
a_{i-1/2}^{(3)} &= \frac{1}{2} (a_i + a_{i-1})
\end{aligned}$$

We also need to approximate the mixed derivative terms

$$\frac{\partial}{\partial r} \left(b \frac{\partial}{\partial s} \right) u$$

We proceed in a similiar fashion to above using

$$\frac{\partial}{\partial r} \left(b \frac{\partial}{\partial s} \right) u = D_{0r} \left[1 + \sum_{n=1}^{\infty} \beta_n h_r^{2n} (D_{+r} D_{-r})^n \right] \left\{ b D_{0s} \left[1 + \sum_{n=1}^{\infty} \beta_n h_s^{2n} (D_{+s} D_{-s})^n \right] \right\} u$$

which can be expanded as

$$\begin{aligned}
\frac{\partial}{\partial r} \left(b \frac{\partial}{\partial s} \right) u &= D_{0r} (b D_{0s}) u \\
&\quad - \frac{1}{6} \left[h_s^2 D_{0r} (b D_{0s} D_{+s} D_{-s}) + h_r^2 D_{0r} D_{+r} D_{-r} (b D_{0s}) \right] u \\
&\quad + \frac{1}{30} \left[h_s^4 D_{0r} (b D_{0s} D_{+s}^2 D_{-s}^2) + h_r^2 D_{0r} D_{+r}^2 D_{-r}^2 (b D_{0s}) \right] u \\
&\quad + \frac{1}{6 \cdot 6} h_r^2 h_s^2 \left[D_{0r} D_{+r} D_{-r} (b D_{0s} D_{+s} D_{-s}) \right] u \\
&\quad - \frac{1}{140} \left[h_s^6 D_{0r} (b D_{0s} D_{+s}^3 D_{-s}^3) + h_r^6 D_{0r} D_{+r}^3 D_{-r}^3 (b D_{0s}) \right] u \\
&\quad - \frac{1}{6 \cdot 30} \left[h_r^2 h_s^4 D_{0r} D_{+r} D_{-r} (b D_{0s} D_{+s}^2 D_{-s}^2) + h_r^4 h_s^2 D_{0r} D_{+r}^2 D_{-r}^2 (b D_{0s} D_{+s} D_{-s}) \right] u \\
&\quad + O(h^8)
\end{aligned}$$

19 Higher-order accurate time stepping for the second-order wave equation

In this section we derive approximations for time-stepping the second-order equation

$$u_{tt} = f(u, x, t) \tag{158}$$

Integrating the equation from 0 to t gives

$$u_t(t) - u_t(0) = \int_0^t f(\tau) d\tau$$

which can be integrated again from 0 to Δ ,

$$u(\Delta) - u(0) + u_t(0)\Delta = \int_0^\Delta (\Delta - \tau)f(\tau) d\tau$$

Combining this with the equation integrated from $-\Delta$ to 0 results in

$$u(\Delta) - 2u(0) + u(-\Delta) = \int_0^\Delta (\Delta - \tau)f(\tau) d\tau + \int_{-\Delta}^0 (\Delta + \tau)f(\tau) d\tau \quad (159)$$

Equation (159) is the basis for generating time-stepping methods of the Störmer family. To generate explicit methods we write f as a polynomial

$$f = l_{m0}(x)f_0 + l_{m1}f_{-1} + \dots + l_{mm}f_{-m} + O(h^{m+1}) \quad (160)$$

$f_i = f(i\Delta)$, and where l_{mi} is the i^{th} Lagrange polynomial of order m which passes through the points $0, -\Delta, -2\Delta, \dots$,

$$l_{m,i} = \frac{\prod_{j \neq i} (x - (-j\Delta))}{\prod_{j \neq i} ((-i\Delta)x - (-j\Delta))}$$

Substituting the polynomial approximation (160) for f into equation (159) leads to methods of the form

$$\begin{aligned} u(\Delta) - 2u(0) + u(-\Delta) &= \Delta^2 \sum_{i=0} \gamma_i f(-i\Delta) \\ &\approx \Delta^2 \{f_0\} \quad (\text{order 2}) \\ &\approx \Delta^2 \left\{ \frac{13}{12}f_0 - \frac{1}{6}f_{-1} + \frac{1}{12}f_{-2} \right\} \quad (\text{order 3}) \\ &\approx \Delta^2 \left\{ \frac{7}{6}f_0 - \frac{5}{12}f_{-1} + \frac{1}{3}f_{-2} - \frac{1}{12}f_{-3} \right\} \quad (\text{order 4}) \\ &\approx \Delta^2 \left\{ \frac{299}{240}f_0 - \frac{176}{240}f_{-1} + \frac{194}{240}f_{-2} - \frac{96}{240}f_{-3} + \frac{19}{240}f_{-4} \right\} \quad (\text{order 5}) \\ &\approx \Delta^2 \left\{ \frac{317}{240}f_0 - \frac{266}{240}f_{-1} + \frac{374}{240}f_{-2} - \frac{276}{240}f_{-3} + \frac{109}{240}f_{-4} - \frac{18}{240}f_{-5} \right\} \quad (\text{order 6}) \end{aligned}$$

20 Higher-order time stepping with the Modified Equation approach

The modified equation approach is based on the taylor series expression

$$u^{n\pm 1} = u^n + \Delta t \partial_t u + \frac{\Delta t^2}{2} \partial_t^2 u + \frac{\Delta t^3}{3!} \partial_t^3 u + \frac{\Delta t^4}{4!} \partial_t^4 u + \dots$$

giving

$$u^{n+1} - 2u^n + u^{n-1} = 2 \frac{\Delta t^2}{2!} \partial_t^2 u + 2 \frac{\Delta t^4}{4!} \partial_t^4 u + 2 \frac{\Delta t^6}{6!} \partial_t^6 u + \dots$$

If we are solving the (forced) second-order wave equation

$$u_{tt} = c^2 \Delta u + f$$

then

$$\begin{aligned} \partial_t^4 u &= (c^2 \Delta)^2 u + c^2 \Delta f + f_{tt} \\ \partial_t^6 u &= (c^2 \Delta)^3 u + (c^2 \Delta)^2 f + c^2 \Delta f_{tt} + \partial_t^4 f \\ \partial_t^8 u &= (c^2 \Delta)^4 u + (c^2 \Delta)^3 f + (c^2 \Delta)^2 f_{tt} + c^2 \Delta \partial_t^4 f + \partial_t^6 f \end{aligned}$$

then we can derive the expression

$$\begin{aligned} u^{n+1} - 2u^n + u^{n-1} &= 2 \frac{\Delta t^2}{2!} (c^2 \Delta u + f) \\ &\quad + 2 \frac{\Delta t^4}{4!} \left\{ (c^2 \Delta)^2 u + c^2 \Delta f + f_{tt} \right\} \\ &\quad + 2 \frac{\Delta t^6}{6!} \left\{ (c^2 \Delta)^3 u + (c^2 \Delta)^2 f + c^2 \Delta f_{tt} + \partial_t^4 f \right\} \\ &\quad + 2 \frac{\Delta t^8}{8!} \left\{ (c^2 \Delta)^4 u + (c^2 \Delta)^3 f + (c^2 \Delta)^2 f_{tt} + c^2 \Delta \partial_t^4 f + \partial_t^6 f \right\} + \dots \end{aligned}$$

Here's a fourth-order accurate approximation

$$U^{n+1} - 2U^n + U^{n-1} = \Delta t^2 (c^2 \Delta_{4h} U + f) \quad (161)$$

$$+ \frac{\Delta t^4}{12} ((c^2 \Delta_{2h})^2 U + c^2 \Delta f + f_{tt}) \quad (162)$$

where Δ_{mh} is a m^{th} -order approximation.

Here's a sixth-order scheme,

$$\begin{aligned} U^{n+1} - 2U^n + U^{n-1} &= \Delta t^2 (c^2 \Delta_{6h} U + f) \\ &\quad + \frac{\Delta t^4}{12} ((c^2 \Delta_{4h})^2 U + c^2 \Delta f + f_{tt}) \\ &\quad + \frac{\Delta t^6}{360} ((c^2 \Delta_{2h})^3 U + (c^2 \Delta)^2 f + c^2 \Delta f_{tt} + \partial_t^4 f) \end{aligned}$$

Here's a eighth-order scheme,

$$\begin{aligned} U^{n+1} - 2U^n + U^{n-1} &= \Delta t^2 (c^2 \Delta_{8h} U + f) \\ &\quad + \frac{\Delta t^4}{12} ((c^2 \Delta_{6h})^2 U + c^2 \Delta f + f_{tt}) \\ &\quad + \frac{\Delta t^6}{360} ((c^2 \Delta_{4h})^3 U + (c^2 \Delta)^2 f + c^2 \Delta f_{tt} + \partial_t^4 f) \\ &\quad + \frac{\Delta t^8}{20160} ((c^2 \Delta_{2h})^4 U + F_4) \end{aligned}$$

20.1 Modified Equation Time Stepping and Complex Index of Refraction

Consider the case of Maxwell's equations in a lossy media (complex index of refraction)

$$\begin{aligned} u_{tt} &= c^2 \Delta u - \sigma(\mathbf{x}) u_t + f, \\ u_{tt} + \sigma(\mathbf{x}) u_t &= c^2 \Delta u + f. \end{aligned}$$

where σu_t is the loss term with σ the electric conductivity Let us derive a fourth-order accurate modified equation approximation. Using

$$\frac{u^{n+1} - u^{n-1}}{2\Delta t} = u_t + \frac{\Delta t^2}{6} \partial_t^3 u + O(\Delta t^4)$$

it follows that (we will treat the σu_t term implicitly)

$$\begin{aligned} \frac{u^{n+1} - 2u^n + u^{n-1}}{\Delta t^2} + \sigma \frac{u^{n+1} - u^{n-1}}{2\Delta t} &= [u_{tt} + \sigma u_t] + \frac{\Delta t^2}{12} [\partial_t^4 u + 2\sigma \partial_t^3 u] + O(\Delta t^4) \\ &= [c^2 \Delta u + f] + \frac{\Delta t^2}{12} [(\partial_t^2 + \sigma \partial_t)^2 u - \sigma^2 \partial_t^2 u] + O(\Delta t^4) \\ &= [c^2 \Delta u + f] + \frac{\Delta t^2}{12} [(\partial_t^2 + \sigma \partial_t)^2 u - \sigma^2 (c^2 \Delta u - \sigma u_t + f)] + O(\Delta t^4) \end{aligned}$$

Now (there will some extra terms here if σ depends on t)

$$\begin{aligned} (\partial_t^2 + \sigma \partial_t)^2 u &= (\partial_t^2 + \sigma \partial_t) [c^2 \Delta u + f] \\ &= c^2 \Delta [c^2 \Delta u + f] + f_{tt} + \sigma f_t \\ &= c^4 \Delta^2 u + c^2 \Delta f + f_{tt} + \sigma f_t \end{aligned}$$

and whence

$$\frac{u^{n+1} - 2u^n + u^{n-1}}{\Delta t^2} + \sigma \left[1 - \frac{(\sigma \Delta t)^2}{12} \right] \frac{u^{n+1} - u^{n-1}}{2\Delta t} = c^2 \left[1 - \frac{(\sigma \Delta t)^2}{12} \right] \Delta u + \frac{\Delta t^2}{12} c^4 \Delta^2 u \quad (163)$$

$$+ \left[1 - \frac{(\sigma \Delta t)^2}{12} \right] f + \frac{\Delta t^2}{12} [c^2 \Delta f + f_{tt} + \sigma f_t] + O(\Delta t^4). \quad (164)$$

This approximation requires relatively simple changes to the method with $\sigma = 0$, equation (162). We probably need

$$\sigma \Delta t < \sqrt{12}$$

for this scheme to be stable, but maybe not (?).

20.2 Modified Equation Time Stepping and Divergence Cleaning

A possible way to damp the divergence in the solution to Maxwell's equations is to solve the following coupled systems for \mathbf{E} and \mathbf{H}

$$\mathbf{E}_{tt} = c^2 \Delta \mathbf{E} + \mathbf{f}_E - \alpha(\mathbf{E}_t - \epsilon^{-1} \nabla \times \mathbf{H} - \mathbf{g}_E), \quad (165)$$

$$\mathbf{H}_{tt} = c^2 \Delta \mathbf{H} + \mathbf{f}_H - \alpha(\mathbf{H}_t + \mu^{-1} \nabla \times \mathbf{E} - \mathbf{g}_H), \quad (166)$$

where $\alpha > 0$ is a positive damping constant. Then the divergence of the electric (or magnetic) field, $\delta = \nabla \cdot \mathbf{E}$, satisfies the damped wave equation

$$\delta_{tt} = c^2 \Delta \delta - \alpha \delta_t.$$

Ignoring boundaries, this equation will damp all spatial modes (except the constant mode) to zero as $t \rightarrow \infty$.

To approximate equations (165)-(166) with the modified equation method we can either proceed directly or instead start from modified equation approximations for the second-order and first order systems (which seems easier):

$$\mathbf{E}_{tt} = c^2 \Delta \mathbf{E} + \mathbf{f}_E, \quad (167)$$

$$\mathbf{H}_{tt} = c^2 \Delta \mathbf{H} + \mathbf{f}_H, \quad (168)$$

$$\mathbf{E}_t = \epsilon^{-1} \nabla \times \mathbf{H} + \mathbf{g}_E, \quad (169)$$

$$\mathbf{H}_t = -\mu^{-1} \nabla \times \mathbf{E} + \mathbf{g}_H. \quad (170)$$

Fourth-order modified equation approximations are

$$\frac{\mathbf{E}^{n+1} - 2\mathbf{E}^n + \mathbf{E}^{n-1}}{\Delta t^2} = c^2 \Delta_{4h} \mathbf{E} + \mathbf{f}_E + \frac{\Delta t^2}{12} ((c^2 \Delta_{2h})^2 \mathbf{E} + c^2 \Delta \mathbf{f}_E + \mathbf{f}_{E,tt}), \quad (171)$$

$$\frac{\mathbf{E}^{n+1} - \mathbf{E}^{n-1}}{2\Delta t} = \partial_t \mathbf{E} + \frac{\Delta t^2}{6} \partial_t^3 \mathbf{E} \quad (172)$$

$$= \epsilon^{-1} \nabla \times \mathbf{H} + \epsilon^{-1} c^2 \frac{\Delta t^2}{6} \nabla \times \Delta \mathbf{H} + \mathbf{g}_E + \epsilon^{-1} \frac{\Delta t^2}{6} [c^2] + \dots (\mathbf{f}_H, \mathbf{g}_E) \dots \quad (173)$$

which can be combined

$$\frac{\mathbf{E}^{n+1} - 2\mathbf{E}^n + \mathbf{E}^{n-1}}{\Delta t^2} + \alpha \frac{\mathbf{E}^{n+1} - \mathbf{E}^{n-1}}{2\Delta t} = \quad (174)$$

$$(c^2 \Delta_{4h} \mathbf{E} + \mathbf{f}_E) + \frac{\Delta t^2}{12} ((c^2 \Delta_{2h})^2 \mathbf{E} + c^2 \Delta \mathbf{f}_E + \mathbf{f}_{E,tt}) \quad (175)$$

$$+ \alpha \left[\epsilon^{-1} \nabla \times \mathbf{H} + \epsilon^{-1} c^2 \frac{\Delta t^2}{6} \nabla \times \Delta \mathbf{H} + \dots \right] \quad (176)$$

For **Cartesian grids** (or rectangular tensor product grids), if we define the discrete divergence and discrete curl operators using the same fourth order approximations

$$\text{div}_{4h} \mathbf{E} = \nabla_{4h} \cdot \mathbf{E} = (D_{4x}, D_{4y}, D_{4z}) \cdot \mathbf{E}, \quad (177)$$

$$\text{curl}_{4h} \mathbf{E} = \nabla_{4h} \times \mathbf{E} = (D_{4x}, D_{4y}, D_{4z}) \times \mathbf{E}, \quad (178)$$

then it will follow that the divergence of the curl will be zero for the discrete operators

$$\text{div}_{4h} \text{curl}_{4h} \mathbf{u} = \nabla_{4h} \cdot \nabla_{4h} \times \mathbf{u} = 0, \quad (179)$$

since all the discrete approximates commute, $D_{4x} D_{4y} = D_{4y} D_{4x}$. Unfortunately, if we use the fourth order approximation curl_{4h} in the approximation to $c^2 \nabla \times \Delta \mathbf{H}$, we will end up with at least a 7 point stencil. If we use a 5 point stencil to approximate $c^2 \nabla \times \Delta \mathbf{H}$ then it will no longer be true that the discrete divergence of this approximation will be zero. The equation for the discrete divergence of the electric field, $\delta_{4h} = \nabla_{4h} \cdot \mathbf{E}$, would then have a source term in it and δ_{4h} would not converge to zero in time.

To avoid this we can instead use the approximation

$$\partial_t^3 \mathbf{E} = c^2 \partial_t \Delta \mathbf{E} \quad (180)$$

$$= c^2 \left[\frac{\Delta \mathbf{E}^n - \Delta \mathbf{E}^{n-1}}{\Delta t} + \Delta t \partial_t^2 \Delta \mathbf{E} \right] + O(\Delta t^2) \quad (181)$$

$$= c^2 \left[\frac{\Delta \mathbf{E}^n - \Delta \mathbf{E}^{n-1}}{\Delta t} + c^2 \Delta t \Delta^2 \mathbf{E}^n \right] + O(\Delta t^2) \quad (182)$$

With this approximation the discrete divergence should go to zero.

For **curvilinear grids**, some care is required in approximating the divergence and curl so that the discrete div of the discrete curl is zero. In this case it is important to approximate both the div and curl with consistent *conservative* approximations. At the continuous level the continuous approximations are

$$\begin{aligned} \nabla \cdot \mathbf{f} &= \frac{1}{J} \sum_{m=1}^d \frac{\partial}{\partial r_m} (J \nabla_{\mathbf{x}} r_m \cdot \mathbf{f}), \\ \nabla \times \mathbf{f} &= \sum_m \frac{1}{J} \frac{\partial \mathbf{x}}{\partial r_m} \left[\frac{\partial}{\partial r_{m+1}} \left(\frac{\partial \mathbf{x}}{\partial r_{m+2}} \cdot \mathbf{f} \right) - \frac{\partial}{\partial r_{m+2}} \left(\frac{\partial \mathbf{x}}{\partial r_{m+1}} \cdot \mathbf{f} \right) \right], \end{aligned}$$

where the subscripts $m+1, m+2$ are to be taken modulo d . Note that

$$\nabla_{\mathbf{x}} r_m \cdot \frac{\partial \mathbf{x}}{\partial r_n} = \sum_k \frac{\partial r_m}{\partial x_k} \frac{\partial x_k}{\partial r_n} = \frac{\partial r_m}{\partial r_n} = \delta_{mn}. \quad (183)$$

Thus

$$\begin{aligned} \nabla \cdot (\nabla \times \mathbf{f}) &= \frac{1}{J} \sum_{m=1}^d \frac{\partial}{\partial r_m} (J \nabla_{\mathbf{x}} r_m \cdot (\nabla \times \mathbf{f})) \\ &= \frac{1}{J} \sum_{m=1}^d \frac{\partial}{\partial r_m} \left[\frac{\partial}{\partial r_{m+1}} \left(\frac{\partial \mathbf{x}}{\partial r_{m+2}} \cdot \mathbf{f} \right) - \frac{\partial}{\partial r_{m+2}} \left(\frac{\partial \mathbf{x}}{\partial r_{m+1}} \cdot \mathbf{f} \right) \right] \\ &= 0 \end{aligned}$$

In the discrete case we define difference approximations for the unit cube derivatives

$$D_{r_m} \approx \frac{\partial}{\partial r_m}$$

(say a centered second or fourth order accurate approximation) and then define discrete conservative approximations to div and curl as

$$\begin{aligned} \nabla_h \cdot \mathbf{f} &\equiv \frac{1}{J} \sum_{m=1}^d D_{r_m} (J \nabla_{\mathbf{x}} r_m \cdot \mathbf{f}), \\ \nabla_h \times \mathbf{f} &\equiv \sum_m \frac{1}{J} \frac{\partial \mathbf{x}}{\partial r_m} \left[D_{r_{m+1}} \left(\frac{\partial \mathbf{x}}{\partial r_{m+2}} \cdot \mathbf{f} \right) - D_{r_{m+2}} \left(\frac{\partial \mathbf{x}}{\partial r_{m+1}} \cdot \mathbf{f} \right) \right]. \end{aligned}$$

These approximations will satisfy $\nabla_h \cdot (\nabla_h \times \mathbf{f}) = 0$ provided (183) is satisfied at the discrete level since

$$\begin{aligned} \nabla_h \cdot (\nabla_h \times \mathbf{f}) &= \frac{1}{J} \sum_{m=1}^d D_{r_m} (J \nabla_{\mathbf{x}} r_m \cdot (\nabla_h \times \mathbf{f})) \\ &= \frac{1}{J} \sum_{m=1}^d D_{r_m} \left[D_{r_{m+1}} \left(\frac{\partial \mathbf{x}}{\partial r_{m+2}} \cdot \mathbf{f} \right) - D_{r_{m+2}} \left(\frac{\partial \mathbf{x}}{\partial r_{m+1}} \cdot \mathbf{f} \right) \right] \\ &= 0. \end{aligned}$$

Here we have used the fact that D_{r_m} commutes with D_{r_n} , $D_{r_m}D_{r_n} = D_{r_n}D_{r_m}$.

For general **curvilinear grids**, it will **not** be true that the divergence of the Laplacian is equal to the Laplacian of the divergence. The equation for the discrete divergence of \mathbf{E} for the second-order accurate scheme will be

$$\begin{aligned}\frac{\delta_h^{n+1} - 2\delta_h^n + \delta_h^{n-1}}{\Delta t^2} + \alpha \frac{\delta_h^{n+1} - \delta_h^{n-1}}{2\Delta t} &= c^2 \nabla_h \cdot \Delta_h \mathbf{E} \\ &= c^2 \Delta_h \delta_h + c^2 (\nabla_h \cdot \Delta_h \mathbf{E} - \Delta_h \nabla_h \cdot \mathbf{E}), \\ &= c^2 \Delta_h \delta_h + c^2 O(h^2).\end{aligned}$$

The divergence satisfies a damped wave equation with a forcing function of $O(h^2)$. In this case we expect that $\delta_h = O(c^2 h^2 / \alpha)$. We can thus reduce the divergence by increasing α , although we likely want to keep α smaller than $O(1/\Delta t)$. Note that if the term $\alpha \nabla_h \cdot \nabla_h \times \mathbf{H}$ had not been exactly zero then we could only expect $\delta_h = O(h^2)$ (without the exact factor of $1/\alpha$) and there would have been less of a benefit of increasing α (This needs to be verified numerically).

For the fourth-order accurate scheme we have

$$\begin{aligned}\frac{\delta_h^{n+1} - 2\delta_h^n + \delta_h^{n-1}}{\Delta t^2} + \alpha \frac{\delta_h^{n+1} - \delta_h^{n-1}}{2\Delta t} &= c^2 (1 + \alpha \Delta t / (6\epsilon)) \nabla_h \cdot \Delta_h \mathbf{E}^n + \frac{c^4 \Delta t^2}{12} (1 + \alpha \Delta t / \epsilon) \nabla_h \cdot \Delta_{2h}^2 \mathbf{E}^n \\ &\quad - c^2 \alpha \Delta t / (6\epsilon) \nabla_h \cdot \Delta_{2h} \mathbf{E}^{n-1}\end{aligned}$$

or

$$\begin{aligned}\frac{\delta_h^{n+1} - 2\delta_h^n + \delta_h^{n-1}}{\Delta t^2} + \alpha \frac{\delta_h^{n+1} - \delta_h^{n-1}}{2\Delta t} &= c^2 (1 + \alpha \Delta t / (6\epsilon)) \Delta_h \delta_h^n + \frac{c^4 \Delta t^2}{12} (1 + \alpha \Delta t / \epsilon) \Delta_{2h}^2 \delta_h^n \\ &\quad - c^2 \alpha \Delta t / (6\epsilon) \Delta_{2h} \delta_h^{n-1} + O(c^2 h^4 + c^4 \Delta t^2 h^2) (1 + \alpha \Delta t)\end{aligned}$$

In this case we expect that $\delta_h = O(c^2 h^4 + c^4 \Delta t^2 h^2) (1 + \alpha \Delta t) / \alpha$.

The divergence equation is of the form

$$y_{tt} + \alpha y_t + k^2 y = f$$

where $y \approx \delta$ and k is the wave-number of a spatial mode. The solution of the homogenous ODE is

$$\begin{aligned}y &= A e^{\lambda_1 t} + B e^{\lambda_2 t}, \\ \lambda_m &= -\frac{\alpha}{2} \pm \sqrt{(\alpha/2)^2 - k^2}, \\ \lambda_m &\sim -\frac{\alpha}{2} \pm i\beta \quad \text{if } \alpha < 2k \text{ (high frequencies)}, \\ &\sim -\frac{\alpha}{2} \pm \frac{\alpha}{2} (1 - 2k^2/\alpha^2) \quad \text{if } \alpha > 2k \text{ (low frequencies)}.\end{aligned}$$

The general solution is

$$\begin{aligned}y &= A e^{\lambda_1 t} + B e^{\lambda_2 t} + \frac{1}{\lambda_2 - \lambda_1} \int_0^t (e^{\lambda_2(t-\tau)} - e^{\lambda_1(t-\tau)}) f(\tau) d\tau, \\ &= A e^{\lambda_1 t} + B e^{\lambda_2 t} + \frac{1}{2\sqrt{(\alpha/2)^2 - k^2}} \int_0^t (e^{\lambda_2(t-\tau)} - e^{\lambda_1(t-\tau)}) f(\tau) d\tau.\end{aligned}$$

Thus high frequencies will be damped at a rate $e^{-(\alpha/2)t}$ while low frequencies should be $O(f/\alpha)$.

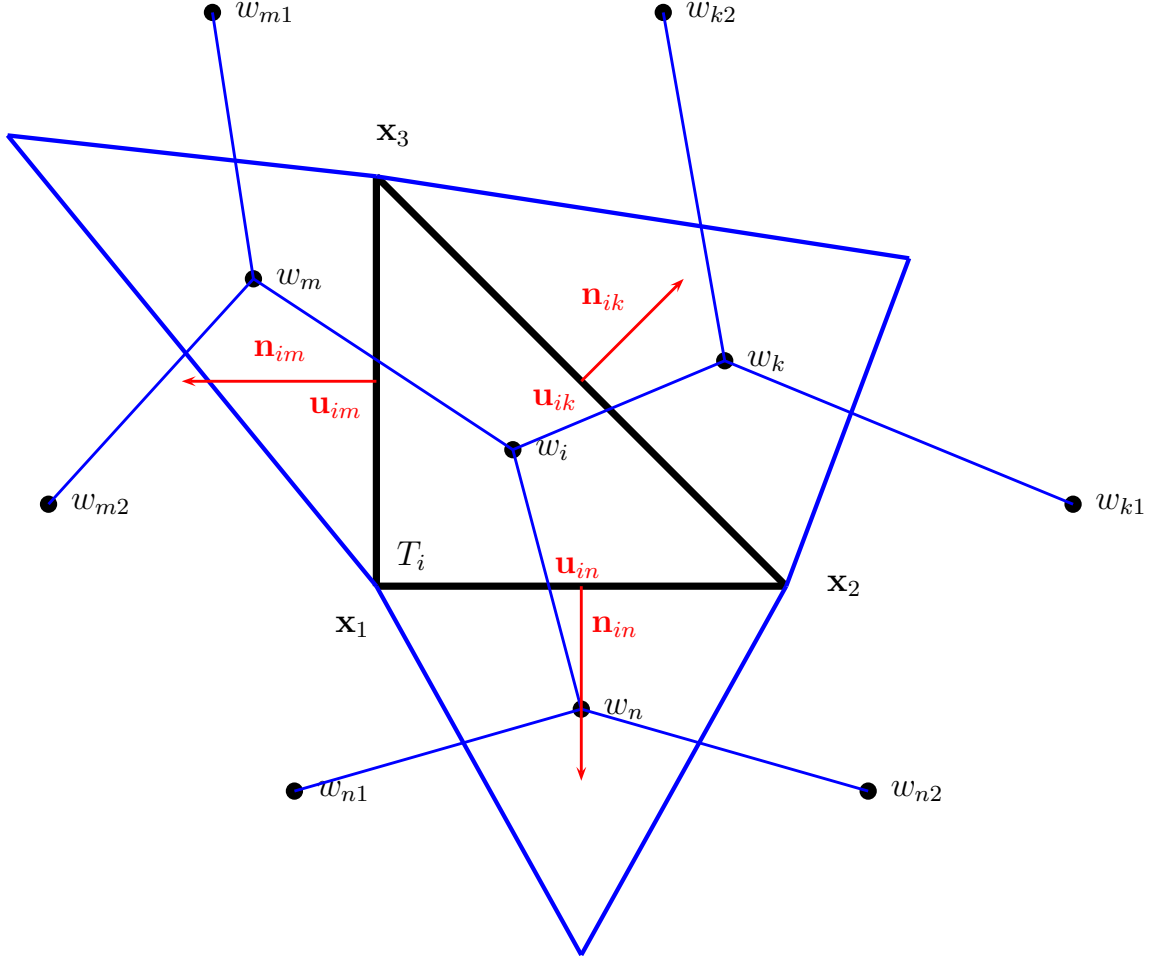


Figure 2: Discretization on a triangular grid.

21 Symmetric approximations on triangular grids

Consider the wave equation written as a first order system,

$$\begin{aligned}\mathbf{u}_t &= \nabla w \\ w_t &= \nabla \cdot \mathbf{u}\end{aligned}$$

where w satisfies the second order wave equation, $w_{tt} = \Delta w$.

Approach 1: Look for a symmetric discretization of the first order system. Use the approximations

$$\begin{aligned}w_t &= \nabla \cdot \mathbf{u} \approx \sum_j \mathbf{n}_{ij} \cdot \mathbf{u}_{ij} \Delta s_{ij} \\ \frac{\partial}{\partial t} \mathbf{n}_{ij} \cdot \mathbf{u}_{ij} &= \mathbf{n}_{ij} \cdot \nabla w \approx \sum_{k \in M_{ij}} \gamma_{ijk} (w_i - w_k)\end{aligned}$$

where M_{ij} is some set of neighbours of w_i and w_j .

Approach 2: Look for a symmetric discretization of the laplacian on a triangular grid. The discretization for w_i at the centroid of triangle T_i will be of the form

$$\Delta w_i \approx \sum_{j \in N_i} \alpha_{ij} (w_i - w_j)$$

where N_i is the set of neighbours of w_i . The approximation will be symmetric if $\alpha_{ij} = \alpha_{ji}$.

22 Exact Solutions

22.1 Eigenfunctions of a 2D disk

Let $(u, v, w) = (E_x, E_y, H_z)$. Then the TE_Z equations are

$$\begin{aligned} u_{tt} &= \Delta u \\ v_{tt} &= \Delta v \\ w_{tt} &= \Delta w \\ \nabla \cdot (u, v) &= 0 \\ \mathbf{n} \times \mathbf{u} &= 0, \partial_n w = 0 \quad \text{for } \mathbf{x} \in \partial D \end{aligned}$$

We look for solutions on the unit disk, $D_1 = \{(x, y) | x^2 + y^2 \leq 1\}$. with a time dependence $e^{-i\omega t}$, $\mathbf{u}(x, y, t) = \mathbf{u}(x, y)e^{-i\omega t}$. The magnetic field will satisfy the eigenvalue problem

$$\begin{aligned} \frac{1}{r} \partial_r(r \partial_r w) + \frac{1}{r^2} \partial_\theta^2 w &= -\omega^2 w \\ \partial_r w &= 0 \quad \text{for } r = 1 \end{aligned}$$

The eigenvalues and eigenvectors will be enumerated by a pair of integers, (n, p) with

$$w_{p,n}(x, y, t) = J_n(\omega_{p,n}r) \cos(n\theta) \cos(\omega_{p,n}t) \quad n = 0, 1, 2, \dots, p = 1, 2, \dots$$

where for a fixed n , $\omega_{p,n}$ is the p -th zero of the derivative of the Bessel function

$$J'_n(\omega_{p,n}) = 0$$

For $n = 0$ we do not include the root $\omega_{1,n} = 0$. Given $w_{p,n}$ we can determine $(u_{p,n}, v_{p,n})$ from the relations

$$\begin{aligned} u_t &= w_y \\ v_t &= -w_x \end{aligned}$$

Thus

$$\begin{aligned} u_{p,n}(x, y, t) &= \frac{1}{\omega_{p,n}} \left\{ \omega_{p,n} J'_n(\omega_{p,n}r) \sin(\theta) \cos(n\theta) - \frac{n}{r} J_n(\omega_{p,n}r) \cos(\theta) \sin(n\theta) \right\} \sin(\omega_{p,n}t) \\ v_{p,n}(x, y, t) &= -\frac{1}{\omega_{p,n}} \left\{ \omega_{p,n} J'_n(\omega_{p,n}r) \cos(\theta) \cos(n\theta) + \frac{n}{r} J_n(\omega_{p,n}r) \sin(\theta) \sin(n\theta) \right\} \sin(\omega_{p,n}t) \end{aligned}$$

where we have used

$$r_x = \cos(\theta), \quad r_y = \sin(\theta), \quad \theta_x = -\frac{\sin(\theta)}{r}, \quad \theta_y = \frac{\cos(\theta)}{r}$$

We can check that the boundary condition $\mathbf{n} \times \mathbf{u} = 0$ is satisfied. The tangent vector is $\boldsymbol{\tau} = \hat{\theta} = (-\sin(\theta), \cos(\theta))$ and thus

$$\begin{aligned} (-\sin(\theta), \cos(\theta)) \cdot (u, v) &= -\frac{1}{\omega_{p,n}} \left\{ \omega_{p,n} J'_n(\omega_{p,n}r) \cos(n\theta) \right\} \sin(\omega_{p,n}t) \\ &= 0 \quad \text{at } r = 1 \end{aligned}$$

We also note that $J_n(z)$ has the series expansion

$$J_n(z) = \left(\frac{1}{2}z\right)^n \sum_{k=0}^{\infty} \frac{(-\frac{1}{4}z^2)^k}{k!(n+k)!}$$

which is useful when evaluating $J_n(\omega_{p,n}r)/r$ for small values of r .

22.2 Eigenfunctions of a 3D cylinder

Consider the cylindrical domain of length d in the axial direction, $C(d) = \{\mathbf{x} \in \mathbb{R}^3 \mid x^2 + y^2 \leq 1, z \in [0, d]\}$. Let $\mathbf{u} = (u, v, w) = (E_x, E_y, E_z)$. Maxwell's equations are

$$\begin{aligned} u_{tt} &= \Delta u \\ v_{tt} &= \Delta v \\ w_{tt} &= \Delta w \\ \nabla \cdot (\mathbf{u}) &= 0 \\ \mathbf{n} \times \mathbf{u} &= 0 \quad \text{for } \mathbf{x} \in \partial C(d) \end{aligned}$$

Note that combining the boundary condition with the divergence condition implies $w_z(x, y, 0) = w_z(x, y, 1) = 0$.

To begin with consider the cylinder, $C(\pi)$, of length $d = \pi$. If we look for eigenfunctions of the form $w(r, \theta, z, t) = w(r, \theta) \cos(kz) e^{-i\omega t}$ we are led to the following problem for $w(r, \theta)$,

$$\begin{aligned} \frac{1}{r} \partial_r(r \partial_r w) + \frac{1}{r^2} \partial_\theta^2 w &= -(\omega^2 - k^2)w \\ w &= 0 \quad \text{for } r = 1 \end{aligned}$$

Thus the eigenfunctions for w are enumerated by the 3 integers (n, p, k) with

$$\begin{aligned} w_{p,n,k}(r, \theta, z, t) &= J_n(\lambda_{p,n}r) \cos(n\theta) \cos(kz) \cos(\omega_{p,n,k}t) \\ \omega_{p,n,k} &= \sqrt{k^2 + \lambda_{p,n}^2} \quad n = 0, 1, 2, \dots, p = 1, 2, \dots, k = 1, 2, 3, \dots \end{aligned}$$

where for a fixed n , $\lambda_{p,n}$ is the p -th zero of the Bessel function

$$J_n(\lambda_{p,n}) = 0$$

To determine u and v we look for a solution of the form

$$\begin{aligned} u(r, \theta, z) &= Aw_x \tan(kz) = A\partial_x \{J_n(\lambda_{p,n}r) \cos(n\theta)\} \sin(kz) \\ u(r, \theta, z) &= Aw_y \tan(kz) = A\partial_y \{J_n(\lambda_{p,n}r) \cos(n\theta)\} \sin(kz) \end{aligned}$$

This ansatz will satisfy the boundary condition at $z = 0, 1$. It will also satisfy the boundary condition $\boldsymbol{\tau} \cdot (\mathbf{u}, v) = 0$ at $r = 1$ which can be seen from

$$\begin{aligned} \partial_\theta w &= x_\theta w_x + y_\theta w_y \\ &= \frac{1}{r}(-\sin(\theta)w_x + \cos(\theta)w_y) \\ &= \frac{1}{r}\boldsymbol{\tau} \cdot (w_x, w_y) \end{aligned}$$

If $w(1, \theta) = 0$ then $\partial_\theta w(1, \theta) = 0$ and $\boldsymbol{\tau} \cdot (w_x, w_y)(1, \theta) = 0$. It also follows that

$$\begin{aligned} u_x + v_y + w_z &= A(w_{xx} + w_{yy}) \tan(kz) + w_z \\ &= -\lambda^2 A w \tan(kz) - kw \tan(kz) \\ &= -(\lambda^2 A + k)w \tan(kz) \end{aligned}$$

Thus for the divergence of \mathbf{u} to be zero we require

$$A = -\frac{k}{\lambda^2}$$

This leads us to the following expressions for the eigenfunctions of the domain $C(d)$,

$$\begin{aligned}
u_{p,n,k}(r, \theta, z, t) &= -\frac{(k\pi/d)}{\lambda^2} \left\{ \lambda J'_n(\lambda r) \cos(\theta) \cos(n\theta) + \frac{n}{r} J_n(\lambda r) \sin(\theta) \sin(n\theta) \right\} \sin(k\pi z/d) \cos(\omega t) \\
v_{p,n,k}(r, \theta, z, t) &= -\frac{(k\pi/d)}{\lambda^2} \left\{ \lambda J'_n(\lambda r) \sin(\theta) \cos(n\theta) - \frac{n}{r} J_n(\lambda r) \cos(\theta) \sin(n\theta) \right\} \sin(k\pi z/d) \cos(\omega t) \\
w_{p,n,k}(r, \theta, z, t) &= J_n(\lambda r) \cos(n\theta) \cos(k\pi z/d) \cos(\omega t) \\
\lambda &= \lambda_{p,n}, \quad \text{with } J_n(\lambda_{p,n}) = 0, \\
\omega &= \omega_{p,n,k} = \sqrt{(k\pi/d)^2 + \lambda_{p,n}^2} \\
n &= 0, 1, 2, 3, \dots, \quad p = 1, 2, 3, \dots, \quad k = 1, 2, 3, \dots
\end{aligned}$$

22.3 Scattering of a plane wave by a dielectric cylinder

Consider a TE_Z plane wave that is incident upon a dielectric cylinder of radius a ,

$$\begin{aligned} u^I &= 0 \\ v^I &= \frac{\omega}{k} e^{i(kx - \omega t)} \\ w^I &= e^{i(kx - \omega t)} \end{aligned}$$

Define

$$\begin{aligned} \epsilon_i &= \text{dielectric permittivity for the region inside the cylinder} \\ \epsilon_o &= \text{dielectric permittivity for the region outside the cylinder} \\ m &= \sqrt{\epsilon_i/\epsilon_o} = c_o/c_i \quad \text{relative index of refraction?} \end{aligned}$$

The solution for the magnetic field in terms of the incident, scattered field and dielectric field is of the form (see for example Balanis[?] or van de Hulst[?]),

$$\begin{aligned} w^I &= \sum_{n=-\infty}^{\infty} i^n J_n(kr) e^{in\theta} \quad (\text{incident plane wave}) \\ w^S &= \sum_{n=-\infty}^{\infty} i^n a_n H_n(kr) e^{in\theta} \quad (\text{scattered field for } r > a) \\ w^D &= \sum_{n=-\infty}^{\infty} i^n b_n J_n(mkr) e^{in\theta} \quad (\text{dielectric field for } r < a) \\ H_n &\equiv H_n^{(2)} = J_n - iY_n \end{aligned}$$

Imposing the interface jump conditions $[w] = 0$ and $[w_r/\epsilon] = 0$ at $r = a$ determines the coefficients a_n and b_n

$$\begin{aligned} d_n &= mH'_n(ka) J_n(mka) - H_n(ka) J'_n(mka) \quad (\text{determinant}) \\ a_n &= [J_n(ka) J'_n(mka) - mJ'_n(ka) J_n(mka)]/d_n \\ b_n &= m[J_n(ka) H'_n(ka) - J'_n(ka) H_n(ka)]/d_n \end{aligned}$$

Note that since $J_{-n} = (-1)^n J_n$, and $H_{-n} = (-1)^n H_n$ it follows that $a_{-n} = a_n$ and $b_{-n} = b_n$. Using the Wronskian condition $J_n(x)Y'_n(x) - J'_n(x)Y_n(x) = \frac{2}{\pi x}$ the expression for b_n becomes

$$b_n = \frac{-2im}{\pi k a d_n}$$

The asymptotic form of J_n and Y_n for large n are

$$\begin{aligned} J_n(x) &\sim \frac{1}{2\pi n}^{1/2} \left[\frac{ex}{2n} \right]^n \\ Y_n(x) &\sim -\frac{2}{\pi n}^{1/2} \left[\frac{ex}{2n} \right]^{-n} \end{aligned}$$

Note that Y_n grows like $n^{n-1/2}$ as $n \rightarrow \infty$.

22.4 Scattering by a dielectric sphere

23 Scattering by a dielectric sphere

In this section we compute the solution to a plane wave that scatters from a di-electric sphere. The exact solution to this problem can be determined as a Mie series. We first derive this solution. The discussion here follows *Light Scattering by Small Particles* by van de Hulst [?]. It is assumed in this discussion that the magnetic permeability is one, $\mu = 1$.

Let k be the wave number of the incident field and m the refractive index, $m = c_{\text{vacuum}}/c_{\text{medium}}$. The incident field is (note signs),

$$\begin{aligned}\mathbf{E} &= \hat{\mathbf{i}} e^{-ikz+i\omega t} \\ \mathbf{H} &= \hat{\mathbf{j}} e^{-ikz+i\omega t}\end{aligned}$$

Note that the solution for a perfectly conducting sphere follows from the limit $m \rightarrow \infty$. The scalar wave equation

$$\Delta\psi + m^2 k^2 \psi = 0$$

has solutions of the form

$$\begin{aligned}\psi_{ln} &= e^{il\phi} P_n^l(\cos(\theta)) z_n(mkr), \\ P_n^l &= \text{Legendre polynomial}, \\ z_n(\rho) &= \sqrt{\frac{\pi}{2\rho}} Z_{n+1/2}(\rho), \quad (\text{spherical Bessel function}), \\ Z_{n+1/2}(\rho) &= \text{Bessel function},\end{aligned}$$

for integers $n \geq l \geq 0$. Note that $\omega = m_1 k_1$ in medium 1 and $\omega = m_2 k_2$ in medium 2. Solutions to the vector wave equations of Maxwell's equations can be found from solutions to the scalar wave equation as follows. If ψ satisfies the scalar wave equation then vectors \mathbf{M}_ψ and \mathbf{N}_ψ

$$\begin{aligned}\mathbf{M}_\psi &\equiv \nabla \times (r\psi), \\ mk\mathbf{N}_\psi &\equiv \nabla \times (\mathbf{M}_\psi)\end{aligned}$$

satisfy the vector wave equations

$$\begin{aligned}\Delta\mathbf{M}_\psi + m^2 k^2 \mathbf{M}_\psi &= 0, \\ \Delta\mathbf{N}_\psi + m^2 k^2 \mathbf{N}_\psi &= 0,\end{aligned}$$

and

$$\begin{aligned}mk\mathbf{N}_\psi &= \nabla \times (\mathbf{M}_\psi), \\ mk\mathbf{M}_\psi &\equiv \nabla \times (\mathbf{N}_\psi).\end{aligned}$$

The spherical polar components are given by

$$M_r = 0, \quad mkN_r = \partial_r^2(r\psi) + m^2 k^2 r\psi, \quad (184)$$

$$M_\theta = \frac{1}{r \sin(\theta)} \partial_\phi(r\psi), \quad mkN_\theta = \frac{1}{r} \partial_r \partial_\theta(r\psi), \quad (185)$$

$$M_\phi = -\frac{1}{r} \partial_\theta(r\psi), \quad mkN_\phi = \frac{1}{r \sin(\theta)} \partial_r \partial_\phi(r\psi). \quad (186)$$

Given two solutions u and v to the scalar wave equation, Maxwell's equations

$$\begin{aligned}\nabla \times \mathbf{E} &= -ik\mathbf{H}, \\ \nabla \times \mathbf{H} &= ikm^2 \mathbf{E},\end{aligned}$$

are satisfied by

$$\mathbf{E} = \mathbf{M}_v + i\mathbf{N}_u, \quad (187)$$

$$\mathbf{H} = m(-\mathbf{M}_u + i\mathbf{N}_v). \quad (188)$$

Now consider a sphere with refractive index $m_1 = m$ inside and $m_2 = 1$ outside. In terms of spherical harmonics, the incident wave is

$$u^i = e^{i\omega t} \cos(\phi) \sum_{n=1}^{\infty} (-i)^n \frac{2n+1}{n(n+1)} P_n^1(\cos(\theta)) j_n(kr),$$

$$v^i = e^{i\omega t} \sin(\phi) \sum_{n=1}^{\infty} (-i)^n \frac{2n+1}{n(n+1)} P_n^1(\cos(\theta)) j_n(kr).$$

The scattered field outside the sphere is

$$u^s = e^{i\omega t} \cos(\phi) \sum_{n=1}^{\infty} -a_n (-i)^n \frac{2n+1}{n(n+1)} P_n^1(\cos(\theta)) h_n^{(2)}(kr),$$

$$v^s = e^{i\omega t} \sin(\phi) \sum_{n=1}^{\infty} -b_n (-i)^n \frac{2n+1}{n(n+1)} P_n^1(\cos(\theta)) h_n^{(2)}(kr),$$

and the transmitted wave inside the dielectric sphere is

$$u^d = e^{i\omega t} \cos(\phi) \sum_{n=1}^{\infty} m c_n (-i)^n \frac{2n+1}{n(n+1)} P_n^1(\cos(\theta)) j_n(mkr),$$

$$v^d = e^{i\omega t} \sin(\phi) \sum_{n=1}^{\infty} m d_n (-i)^n \frac{2n+1}{n(n+1)} P_n^1(\cos(\theta)) j_n(mkr).$$

where

$$h_n^{(1)} = j_n + iy_n,$$

$$h_n^{(2)} = j_n - iy_n.$$

Introduce the Riccati-Bessel functions, (*note* χ_n is the opposite sign to that used by van de Hulst)

$$\psi_n(z) = z j_n(z) = \sqrt{\pi z/2} J_{n+1/2}(z),$$

$$\chi_n(z) = z y_n(z) = -\sqrt{\pi z/2} Y_{n+1/2}(z),$$

$$\zeta_n(z) = z j_n^{(2)}(z) = \psi_n(z) - i \chi_n(z).$$

Application of the interface equations gives

$$a_n = \frac{\psi'_n(mka)\psi_n(ka) - m \psi_n(mka)\psi'_n(ka)}{\psi'_n(mka)\zeta_n(ka) - m \psi_n(mka)\zeta'_n(ka)},$$

$$b_n = \frac{m\psi'_n(mka)\psi_n(ka) - \psi_n(mka)\psi'_n(ka)}{m\psi'_n(mka)\zeta_n(ka) - \psi_n(mka)\zeta'_n(ka)},$$

$$c_n = \frac{i}{\psi'_n(mka)\zeta_n(ka) - m \psi_n(mka)\zeta'_n(ka)},$$

$$d_n = \frac{i}{m\psi'_n(mka)\zeta_n(ka) - \psi_n(mka)\zeta'_n(ka)}.$$

We can now determine expressins for the full field components of \mathbf{E} from the solutions u and v by computing the sphere -polar components of the auxillary functions \mathbf{N}_u , \mathbf{N}_v , \mathbf{M}_u and \mathbf{M}_v . First note that the spherical Bessel equation for $R = R(r)$,

$$(r^2 R')' + (n(n+1) + m^2 k^2 r^2)R = 0,$$

has solutions $R(r) = j_n(mkr)$ and $R = y_n(mkr)$. Noting that $(r^2 R')' = r(rR)''$ it follows that

$$\begin{aligned} r \left[(rR)'' + m^2 k^2 r R \right] &= r(rR)'' + m^2 k^2 r^2 R \\ &= -n(n+1)R \end{aligned}$$

and thus from (184),

$$N_r(j_n(mkr)) = \frac{-n(n+1)}{mkr} j_n(mkr)$$

The components of the electric field can be determined from the expressions for (u, v) along with (187) and (184)-(184). The total field outside the sphere is ***check me ***

$$E_r^t = -e^{i\omega t} \frac{i \cos(\phi)}{(kr)^2} \sum_{n=1}^{\infty} (-i)^n (2n+1) P_n^1(\cos(\theta)) (\psi_n(kr) - a_n \zeta_n(kr)), \quad (189)$$

$$E_\theta^t = e^{i\omega t} \frac{\cos(\phi)}{(kr)} \sum_{n=1}^{\infty} (-i)^n \frac{2n+1}{n(n+1)} \left\{ \frac{P_n^1}{\sin(\theta)} [\psi_n(kr) - b_n \zeta_n(kr)] + i \partial_\theta P_n^1 [\psi'_n(kr) - a_n \zeta'_n(kr)] \right\}, \quad (190)$$

$$E_\phi^t = -e^{i\omega t} \frac{\sin(\phi)}{(kr)} \sum_{n=1}^{\infty} (-i)^n \frac{2n+1}{n(n+1)} \left\{ \partial_\theta P_n^1 [\psi_n(kr) - b_n \zeta_n(kr)] + i \frac{P_n^1}{\sin(\theta)} [\psi'_n(kr) - a_n \zeta'_n(kr)] \right\}. \quad (191)$$

The field inside the sphere is

$$E_r^d = -e^{i\omega t} \frac{i \cos(\phi)}{(mkr)^2} \sum_{n=1}^{\infty} (-i)^n (2n+1) P_n^1(\cos(\theta)) m c_n \psi_n(mkr), \quad (192)$$

$$E_\theta^d = e^{i\omega t} \frac{\cos(\phi)}{mkr} \sum_{n=1}^{\infty} (-i)^n \frac{2n+1}{n(n+1)} \left\{ \frac{P_n^1}{\sin(\theta)} m d_n \psi_n(mkr) + i \partial_\theta P_n^1 m c_n \psi'_n(mkr) \right\}, \quad (193)$$

$$E_\phi^d = -e^{i\omega t} \frac{\sin(\phi)}{mkr} \sum_{n=1}^{\infty} (-i)^n \frac{2n+1}{n(n+1)} \left\{ \partial_\theta P_n^1 m d_n \psi_n(mkr) + i \frac{P_n^1}{\sin(\theta)} m c_n \psi'_n(mkr) \right\}. \quad (194)$$

23.1 Numerical results for scattering from a dielectric sphere

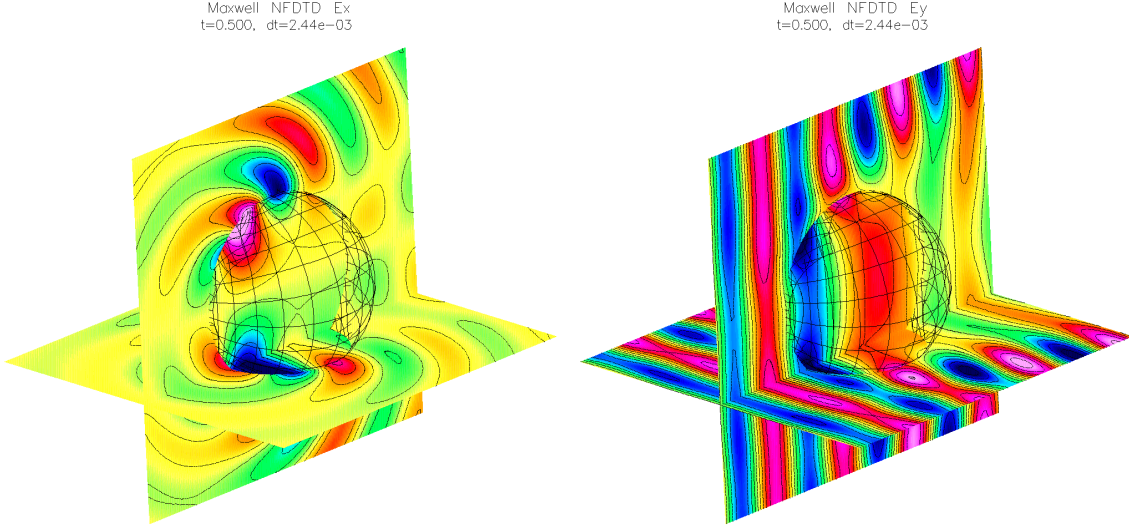


Figure 3: Scattering of a plane wave by a dielectric sphere at $t = .5$ with $k_x = 1$, $\epsilon_1 = .25$ (inside), $\epsilon_2 = 1$ (outside). The fields for E_x and E_y are shown.

The solution is computed numerically for a grid with radius 1. The grids are generated with the `solidSphereInABox.cmd` command file. The initial conditions are taken as the exact solution at times $t = -\Delta t$ and $t = 0$. The exact solution is imposed on the outer boundaries of the domain. The solution is integrated to time $t = .5$. Figure 3 shows the computed solution. The wave number of the incident field was $k_x = 1$, while $\epsilon_1 = .25$ (inside), and $\epsilon_2 = 1$ (outside).

Table 1 presents the maximum errors and estimated convergence rates for the second order method. The grid spacing for case N was $.1/N$.

grid	N	E_x	E_y	E_z	$\nabla \cdot \mathbf{E}/\nabla \mathbf{E}$
solidSphereInABox1	1	3.4×10^{-1}	9.8×10^{-1}	1.4×10^{-1}	3.2×10^{-1}
solidSphereInABox2	2	1.1×10^{-1}	1.8×10^{-1}	4.7×10^{-2}	7.1×10^{-2}
solidSphereInABox4	4	2.2×10^{-2}	3.1×10^{-2}	9.0×10^{-3}	1.7×10^{-2}
rate		1.99	2.49	1.98	2.10

Table 1: Cgmx, solidSphereInABoxNewe, order=2, $t = .5$, $k_x = 1$, $\epsilon_1 = 0.25$, $\epsilon_2 = 1$, cfl=0.8, diss=.5, Thu May 21 6:55:16 2009

grid	N	E_x	E_y	E_z	$\nabla \cdot \mathbf{E}/\nabla \mathbf{E}$
solidSphereInABox1	1	1.5×10^{-1}	6.1×10^{-1}	9.1×10^{-2}	2.2×10^{-1}
solidSphereInABox2	2	4.5×10^{-2}	1.8×10^{-1}	2.9×10^{-2}	8.5×10^{-2}
solidSphereInABox4	4	1.2×10^{-2}	4.8×10^{-2}	8.3×10^{-3}	2.4×10^{-2}
rate		1.81	1.83	1.72	1.61

Table 2: OLD: Maximum errors for scattering of a plane wave by a dielectric sphere, order=2, $t = 0.5$, diss=0.5

Table 3 shows results using the fourth-order accurate method.

grid	N	E_x	E_y	E_z	$\nabla \cdot \mathbf{E}/\nabla \mathbf{E}$
solidSphereInABox2	2	9.3×10^{-3}	4.2×10^{-2}	7.2×10^{-3}	1.8×10^{-2}
solidSphereInABox4	4	8.2×10^{-4}	2.8×10^{-3}	1.0×10^{-3}	1.1×10^{-2}
rate		3.50	3.92	2.80	0.68

Table 3: Cgmx, solidSphereInABoxFixedi, max-norm, order=4, $t = .5$, $k_x = 1$, $\epsilon_1 = 0.25$, $\epsilon_2 = 1$, cfl=0.8, diss=.5, Wed May 20 7:31:29 2009

grid	N	E_x	E_y	E_z	$\nabla \cdot \mathbf{E}/\nabla \mathbf{E}$
solidSphereInABoxe2	2	3.6×10^{-2}	1.2×10^{-1}	1.4×10^{-2}	7.3×10^{-2}
solidSphereInABoxe4	4	2.6×10^{-3}	3.0×10^{-3}	1.9×10^{-3}	1.9×10^{-2}
rate		3.79	5.29	2.87	1.91

Table 4: Cgmx, solidSphereInABoxe, method=NFDTD, max norm, order=4, $t = .5$, $k_x = 1$, $\epsilon_1 = 0.25$, $\epsilon_2 = 1$, cfl=.9, diss=.5, Mon May 25 19:18:45 2009

grid	N	E_x	E_y	E_z	$\nabla \cdot \mathbf{E}/\nabla \mathbf{E}$
solidSphereInABoxe2	2	1.2×10^{-1}	3.8×10^{-1}	4.9×10^{-2}	2.3×10^{-1}
solidSphereInABoxe4	4	1.0×10^{-2}	1.2×10^{-2}	3.2×10^{-3}	8.8×10^{-3}
solidSphereInABoxe8	4	1.1×10^{-3}	1.0×10^{-3}	1.7×10^{-3}	1.2×10^{-2}
rate		5.21	6.77	4.41	4.49

Table 5: Cgmx, solidSphereInABoxe, method=NFDTD, max norm, order=4, $t = .5$, $k_x = 1$, $\epsilon_1 = 0.25$, $\epsilon_2 = 1$, cfl=0.8, diss=2., Tue Jun 2 13:03:53 2009

grid	N	E_x	E_y	E_z	$\nabla \cdot \mathbf{E}/\nabla \mathbf{E}$
solidSphereInABoxi2	2	4.0×10^{-2}	6.7×10^{-2}	1.3×10^{-2}	3.7×10^{-2}
solidSphereInABoxi4	4	1.9×10^{-3}	2.1×10^{-3}	2.0×10^{-3}	1.7×10^{-2}
rate		4.38	5.02	2.72	1.11

Table 6: Cgmx, solidSphereInABoxi, method=NFDTD, max norm, order=4, $t = .5$, $k_x = 1$, $\epsilon_1 = 0.25$, $\epsilon_2 = 1$, cfl=.9, diss=.5, Mon May 25 20:45:15 2009

23.1.1 Scattering from a dielectric sphere - results for the FDTD (Yee) scheme

For comparison, tables 7 and 8 show max-norm and L_1 norm errors from the Yee (FDTD) scheme. The grid spacing for case N was $.1/N$. The Yee scheme does not converge when measuring maximum norm errors.

grid	N	E_x	E_y	E_z	H_x	H_y	H_z	$\nabla \cdot \mathbf{E}/\nabla \mathbf{E}$
bigBox1	1	7.9×10^{-1}	9.5×10^{-1}	4.3×10^{-1}	1.3×10^{-1}	7.3×10^{-2}	1.3×10^{-1}	2.2×10^0
bigBox2	2	9.2×10^{-1}	1.1×10^0	6.2×10^{-1}	9.1×10^{-2}	1.1×10^{-1}	1.2×10^{-1}	2.0×10^0
bigBox4	4	1.1×10^0	1.2×10^0	7.7×10^{-1}	7.8×10^{-2}	9.8×10^{-2}	8.2×10^{-2}	1.8×10^0
rate		-0.21	-0.18	-0.42	0.37	-0.21	0.35	0.16

Table 7: Cgmx, bigBox, method=Yee, max norm, order=2, $t = .5$, $k_x = 1$, $\epsilon_1 = 0.25$, $\epsilon_2 = 1$, cfl=.95, diss=0.5, Tue Jun 2 7:44:51 2009

grid	N	E_x	E_y	E_z	H_x	H_y	H_z	$\nabla \cdot \mathbf{E}/\nabla \mathbf{E}$
bigBox1	1	6.0×10^{-3}	2.6×10^{-2}	4.5×10^{-3}	6.0×10^{-3}	1.8×10^{-3}	2.5×10^{-2}	2.2×10^0
bigBox2	2	2.9×10^{-3}	8.1×10^{-3}	2.5×10^{-3}	2.0×10^{-3}	8.1×10^{-4}	6.6×10^{-3}	2.0×10^0
bigBox4	4	1.6×10^{-3}	3.0×10^{-3}	1.4×10^{-3}	8.1×10^{-4}	4.6×10^{-4}	1.9×10^{-3}	1.8×10^0
rate		0.94	1.54	0.83	1.45	0.97	1.83	0.16

Table 8: Cgmx, bigBox, method=Yee, L1 norm, order=2, $t = .5$, $k_x = 1$, $\epsilon_1 = 0.25$, $\epsilon_2 = 1$, cfl=.95, diss=0.5, Tue Jun 2 7:36:05 2009

23.2 Timings

Method	Grid points	sec/step/pt
order 4	5.1M	5.49e-07
order 2	5.1M	1.66e-07
Yee	4.5M	4.74e-07

Table 9: Timings for scattering from a dielectric sphere

23.3 Scattering by a PEC sphere

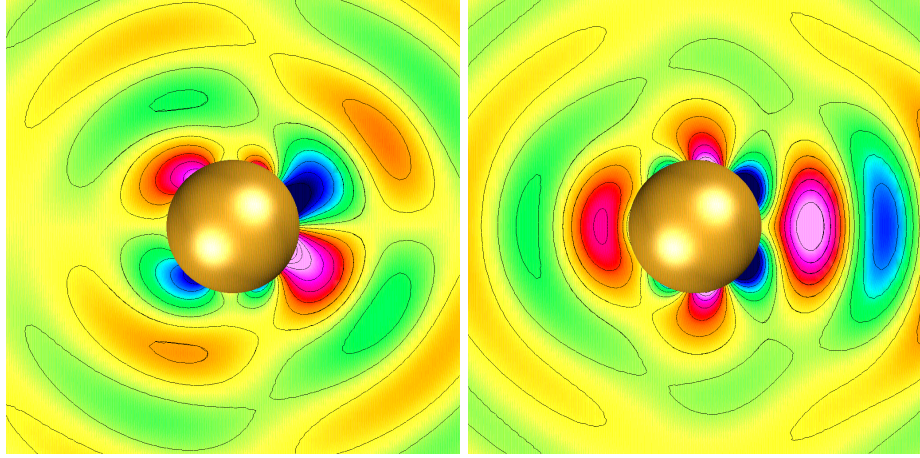


Figure 4: Scattering of a plane wave by a perfectly conducting sphere. The scattered fields for E_x and E_y are shown.

The three-dimensional computation of the scattering of a plane wave by a sphere of radius a is considered in this section. For an incident plane wave traveling in the x -direction, $\mathbf{E}^I = (e^{i(kx-\omega t)}, 0, 0)$, the total field in spherical polar coordinates (r, θ, ϕ) is given by the series expansion [?]

$$E_r = \frac{i \cos(\phi)}{(kr)^2} \sum_{n=1}^{\infty} (-i)^n (2n+1) [\psi_n(kr) - b_n \zeta_n^{(1)}(kr)] P_n^1(\cos(\theta)) e^{-i\omega t}, \quad (195)$$

$$E_\theta = \frac{\cos(\phi)}{kr} \sum_{n=1}^{\infty} (-i)^n \frac{2n+1}{n(n+1)} [A_n \frac{P_n^1(\cos(\theta))}{\sin(\theta)} + i B_n \partial_\theta P_n^1(\cos(\theta))] e^{-i\omega t}, \quad (196)$$

$$E_\phi = -\frac{\sin(\phi)}{kr} \sum_{n=1}^{\infty} (-i)^n \frac{2n+1}{n(n+1)} [A_n \partial_\theta P_n^1(\cos(\theta)) + i B_n \frac{P_n^1(\cos(\theta))}{\sin(\theta)}] e^{-i\omega t}, \quad (197)$$

where P_n^1 are the Legendre polynomials and

$$\begin{aligned} A_n &= \psi_n(kr) - a_n \zeta_n^{(1)}(kr), \quad B_n = \psi'_n(kr) - b_n \zeta_n^{(1)'}(kr), \\ j_n(z) &= \sqrt{\frac{\pi}{2z}} J_{n+1/2}(z), \quad h_n^{(1)}(z) = \sqrt{\frac{\pi}{2z}} H_{n+1/2}(z), \\ \psi(z) &= z j_n(z), \quad \zeta_n^{(1)}(z) = z h_n^{(1)}(z), \quad a_n = \frac{\psi_n(ka)}{\zeta_n^{(1)}(ka)}, \quad b_n = \frac{\psi'_n(ka)}{\zeta_n^{(1)'}(ka)}. \end{aligned}$$

The computed solution corresponds to the real part of equations (195-197).

As for the case of scattering of a plane wave by a cylinder, the known incident field can be subtracted out, leaving the solution to the scattered field, \mathbf{E}^S to be determined. A PEC boundary condition is imposed on the surface of the sphere, taking into account the incident field that has been removed. The initial conditions are taken as the exact solution for the scattered field at times $t = -\Delta t$ and $t = 0$. The exact solution is imposed on the outer boundaries of the domain. The solution is integrated to time $t = 3$. The grids, \mathcal{G}_1 , \mathcal{G}_2 and \mathcal{G}_4 used for the sphere in a box are the same as those described in section ???. Table 10 presents the maximum errors and estimated convergence rates. The computed values of \mathbf{E} are converging at rates close to 4. Figure 4 shows the scattered field for an incident wave with $ka = \pi$.

grid	$\ \mathbf{e}^{E_x}\ _\infty$	$\ \mathbf{e}^{E_y}\ _\infty$	$\ \mathbf{e}^{E_z}\ _\infty$	$\delta_{\mathbf{E}}$
\mathcal{G}_1	$1.3e-2$	$8.1e-3$	$6.7e-3$	$3.9e-3$
\mathcal{G}_2	$9.3e-4$	$5.8e-4$	$4.8e-4$	$4.2e-4$
\mathcal{G}_4	$6.2e-5$	$3.9e-5$	$3.2e-5$	$5.4e-5$
rate σ	3.86	3.86	3.85	3.09

Table 10: The maximum errors at $t = 3$ for the computation of a plane wave scattering from a perfectly conducting sphere.

24 Numerical results

We consider the test problem where the true solution is a travelling wave:

$$\begin{aligned} E_x^{\text{true}}(\mathbf{x}, t) &= \sin(2\pi(k_x x + k_y y - \tilde{c} t))(-k_y/(\epsilon \tilde{c})) \\ E_y^{\text{true}}(\mathbf{x}, t) &= \sin(2\pi(k_x x + k_y y - \tilde{c} t))(k_x/(\epsilon \tilde{c})) \\ H_z^{\text{true}}(\mathbf{x}, t) &= \sin(2\pi(k_x x + k_y y - \tilde{c} t)) \\ \tilde{c} &= c\sqrt{k_x k_x + k_y k_y} \end{aligned}$$

In all cases presented here we chose $k_x = k_y = 1$.

The schemes we have implemented are

Yee : for rectangular grids.

DSI : for structured grids

DSI : for unstructured grids (gives the identical answer to the structured version on a structured grid).

NFDTD : Non-orthogonal FDTD method, i.e. a centered finite difference scheme on curvilinear grids using the symmetric approximation to the Laplacian.

grid	Yee	DSI(quad)	NFDTD	DSI (tri)
square 21	$5.6e - 3, 8.1e - 3$	$1.8e - 2, 8.1e - 3$	$6.0e - 3, 8.5e - 3$	$7.0e - 2, 7.8e - 2$
square 41	$1.4e - 3, 2.0e - 3$	$4.6e - 3, 2.0e - 3$	$1.5e - 3, 2.1e - 3$	$1.8e - 2, 2.0e - 2$
square 81	$3.3e - 4, 4.7e - 4$	$1.1e - 3, 4.7e - 4$	$3.5e - 4, 5.0e - 4$	$4.6e - 3, 5.0e - 3$
rate				

Table 11: Two dimensional Maxwell equations. Errors in E_x, H_z . Convergence results for a square, $t = 1..$
The DSI scheme (tri) was stable to time $t = 500$. for “square 41”.

grid	DSI (quads)	NFDTD	DSI (with AD)
chevron 21	$1.83e + 1$	$1.93e - 1$	$5.18e - 1$
chevron 41	$1.14e + 18$	$5.94e - 2$	$1.35e - 1$
chevron 81	$5.74e + 103$	$1.87e - 2$	$3.45e - 2$
rate			

Table 12: Two dimensional Maxwell equations. Errors in E_x . Convergence results for the chevron grid, $t = 30$. The NFDTD scheme is stable and preserves a discrete energy. The DSI scheme is unstable. The DSI scheme can be stabilized with a 2nd order spatial dissipation, $ad2 = .8$.

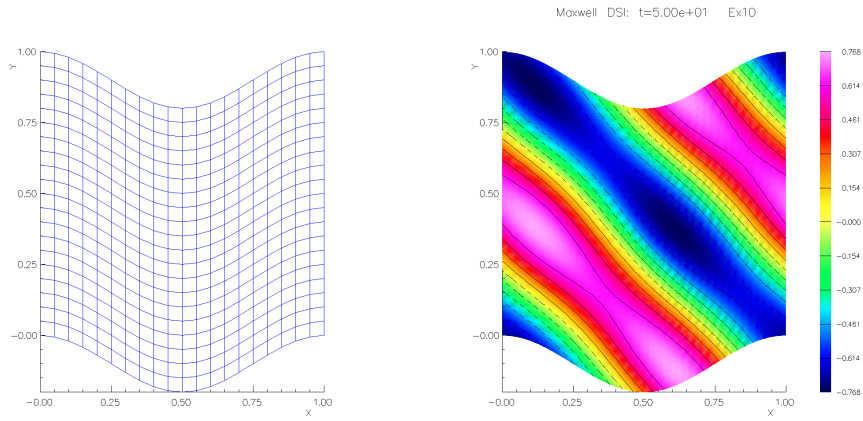


Figure 5: Left: the Sine grid. Right: DSI solution at $t = 50$ on a 41×41 grid.

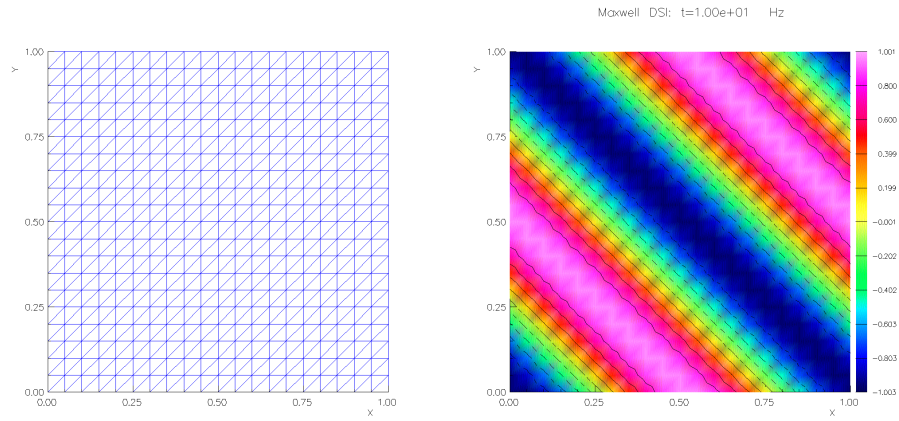


Figure 6: Left: Unstructured grid of triangles. Right: DSI solution at $t = 10$. on a 21×21 grid.

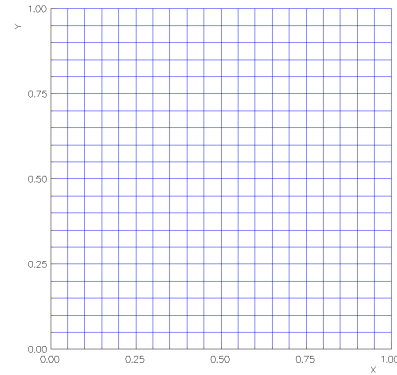


Figure 7: Left: Unstructured grid of quadrilaterals. Right: DSI solution at $t = 1$ on a 41×41 grid.

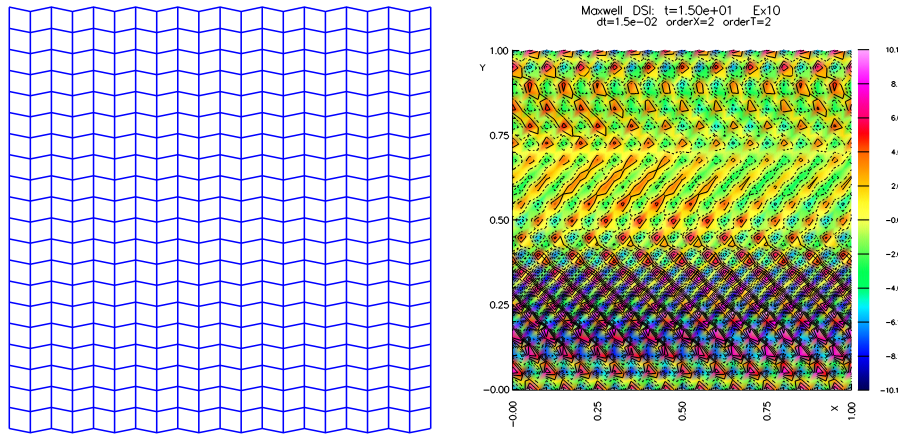
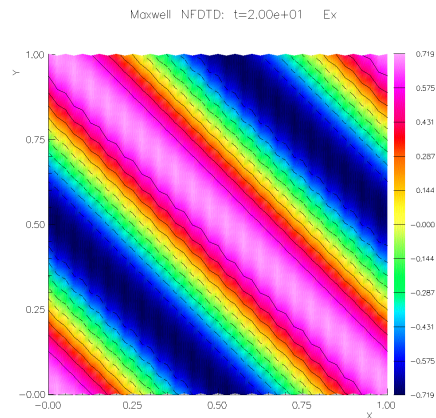


Figure 8: Left: the Chevron grid. Right: Unstable solution from the DSI scheme.



time	\mathcal{E}_h
0	$3.9594833e + 01$
5	$3.9594833e + 01$
10	$3.9594833e + 01$
15	$3.9594833e + 01$
20	$3.9594833e + 01$

Figure 9: Top: Solution on the 41×41 Chevron grid with the NFDTD scheme. Bottom: The discrete energy is conserved.

grid	DSI (quad)	NFDTD	DSI (tri)
sine 21	$1.08e + 0$	$1.42e + 0$	$1.5e + 0$
sine 41	$3.13e - 1$	$4.48e - 1$	$1.4e + 0$
sine 81	$8.01e - 2$	$1.16e - 1$	$4.9e - 1$
sine 161		$2.90e - 2$	$1.2e - 1$
rate			

Table 13: Two dimensional Maxwell equations. Errors in E_x . Convergence results for the sine grid, $t = 50$. The NFDTD scheme preserves a discrete energy. The DSI (quad) scheme was stable to time $t = 1000$. The DSI (tri) scheme went unstable at $t \approx 60$ for *sine41*

25 Convergence results

25.1 The method of analytic solutions

The *method of analytic solutions* is an extremely useful technique for constructing exact solutions that can be used to check the accuracy of a code.

The *method of analytic solutions* is used to choose f and g so that the exact solution to (??-??) is known. For example, any sufficiently smooth function $w(\mathbf{x})$ will be a solution provided $f = \Delta w$ and $g = \alpha_1 \frac{\partial w}{\partial n} + \alpha_0 w$. With this approach the error in the discrete solution can be easily determined. Two common choices for exact solutions are a low degree polynomial or a trigonometric function such as $w(\mathbf{x}) = \cos(f_x \pi x) \cos(f_y \pi y) \cos(f_z \pi z)$. The trigonometric function will be used in the examples given in this section.

Table (29) shows convergence results for solutions computed on overlapping grids for the region exterior to a sphere and interior to a larger box. The finest grid in this case had about 6.4 million grid points.

grid	N	E_x	E_y	E_z	$\nabla \cdot \mathbf{u}$
sib1.order4	40	$8.3e - 4$	$4.5e - 4$	$7.5e - 4$	$2.8e - 3$
sib1x2.order4	80	$5.4e - 5$	$2.5e - 5$	$5.3e - 5$	$2.1e - 4$
sib1x4.order4	160	$3.4e - 6$	$1.7e - 6$	$3.3e - 6$	$2.4e - 5$
rate		3.97	4.02	3.91	3.41

Table 14: Sphere in a box domain, order=4, $t = .25$, sib, trig TZ, bc=pec, cfl=.95, ad=.1

Table (15) shows convergence results for a grid covering the interior of a sphere.

grid	N	E_x	E_y	E_z	$\nabla \cdot \mathbf{u}$
bis1a.order4	10	1.8×10^{-3}	7.2×10^{-4}	4.5×10^{-4}	6.2×10^{-2}
bis2a.order4	20	5.6×10^{-5}	3.0×10^{-5}	6.5×10^{-5}	5.1×10^{-3}
bis3a.order4	40	6.2×10^{-6}	3.4×10^{-6}	7.2×10^{-6}	3.4×10^{-4}
bis4a.order4	80	3.8×10^{-7}	2.6×10^{-7}	4.4×10^{-7}	2.3×10^{-5}
rate		3.99	3.75	3.32	3.80

Table 15: Spherical domain, nfstd, order=4, $t = 0.025$, bis, trig TZ, bc=pec, cfl=.8

grid	N	E_x	E_y	E_z	$\nabla \cdot \mathbf{u}$
tube1.order4	10	8.1×10^{-4}	7.5×10^{-4}	1.3×10^{-3}	7.6×10^{-3}
tube2.order4	20	4.5×10^{-5}	5.1×10^{-5}	8.1×10^{-5}	6.9×10^{-4}
tube3.order4	40	2.6×10^{-6}	2.7×10^{-6}	3.2×10^{-6}	8.8×10^{-5}
tube4.order4	80	1.8×10^{-7}	1.8×10^{-7}	1.4×10^{-7}	3.0×10^{-5}
rate		4.04	4.04	4.43	2.69

Table 16: Cylinder, nfstd, order=4, $t = .25$, tube, trig TZ, bc=pec, cfl=.85

25.2 Eigenfunctions on a disk

The eigenfunctions for a unit disk, $x^2 + y^2 < 1$ are

$$\begin{aligned} u_{p,n}(x, y, t) &= \frac{1}{\omega_{p,n}} \left\{ \omega_{p,n} J'_n(\omega_{p,n} r) \sin(\theta) \cos(n\theta) - \frac{n}{r} J_n(\omega_{p,n} r) \cos(\theta) \sin(n\theta) \right\} \sin(\omega_{p,n} t) \\ v_{p,n}(x, y, t) &= -\frac{1}{\omega_{p,n}} \left\{ \omega_{p,n} J'_n(\omega_{p,n} r) \cos(\theta) \cos(n\theta) + \frac{n}{r} J_n(\omega_{p,n} r) \sin(\theta) \sin(n\theta) \right\} \sin(\omega_{p,n} t) \\ w_{p,n}(x, y, t) &= J_n(\omega_{p,n} r) \cos(n\theta) \cos(\omega_{p,n} t) \quad n = 0, 1, 2, \dots, p = 1, 2, \dots \end{aligned}$$

where for a fixed n , $\omega_{p,n}$ is the p -th zero of the derivative of the Bessel function

$$J'_n(\omega_{p,n}) = 0$$

For $n = 0$ we do not include the root $\omega_{1,n} = 0$

The eigenfunctions for a circular disk define some exact solutions to the Maxwell equations. These solutions can be used to test the accuracy of the method. The computation is initialized with the exact values of the eigen-function for $t = 0$ and $t = -\Delta t$. The equations are integrated to time $t = 1$ and the errors are computed.

The tables show results for different eigen modes.

grid	N	E_x	E_y	H_z	$\nabla \cdot \mathbf{u}$
sic2.order4	17	3.8×10^{-4}	3.8×10^{-4}	7.5×10^{-4}	4.1×10^{-5}
sic3.order4	30	3.9×10^{-5}	3.9×10^{-5}	6.6×10^{-5}	4.8×10^{-6}
sic4.order4	56	3.2×10^{-6}	3.2×10^{-6}	5.4×10^{-6}	4.1×10^{-7}
sic5e.order4	103	1.8×10^{-7}	1.8×10^{-7}	3.1×10^{-7}	1.6×10^{-8}
sic6.order4	226	1.1×10^{-8}	1.1×10^{-8}	1.9×10^{-8}	1.0×10^{-9}
rate		4.09	4.09	4.15	4.21

Table 17: nfdtd, order=4, $t = 1$, sic, eigen-mode 0,0,0

grid	N	E_x	E_y	H_z	$\nabla \cdot \mathbf{u}$
sic2.order4	17	3.4×10^{-3}	8.5×10^{-3}	8.2×10^{-3}	3.8×10^{-3}
sic3.order4	30	4.6×10^{-4}	1.1×10^{-3}	1.3×10^{-3}	2.8×10^{-4}
sic4.order4	56	3.5×10^{-5}	8.2×10^{-5}	9.1×10^{-5}	4.9×10^{-6}
sic5e.order4	103	2.0×10^{-6}	4.7×10^{-6}	5.3×10^{-6}	4.1×10^{-7}
sic6.order4	226	1.2×10^{-7}	2.9×10^{-7}	3.3×10^{-7}	5.4×10^{-8}
rate		4.05	4.07	4.02	4.48

Table 18: nfdtd, order=4, $t = 1$, sic, eigen-mode 1,2,0

grid	N	E_x	E_y	H_z	$\nabla \cdot \mathbf{u}$
sic2.order4	17	1.4×10^{-2}	1.4×10^{-2}	8.6×10^{-2}	1.2×10^{-2}
sic3.order4	30	2.4×10^{-3}	2.4×10^{-3}	1.3×10^{-2}	2.0×10^{-3}
sic4.order4	56	2.3×10^{-4}	2.3×10^{-4}	1.0×10^{-3}	1.3×10^{-4}
sic5e.order4	103	1.5×10^{-5}	1.5×10^{-5}	5.9×10^{-5}	4.9×10^{-6}
sic6.order4	226	10.0×10^{-7}	10.0×10^{-7}	3.6×10^{-6}	2.5×10^{-7}
rate		3.79	3.79	4.00	4.32

Table 19: nfdtd, order=4, $t = 1$, sic, eigen-mode 4,3,0

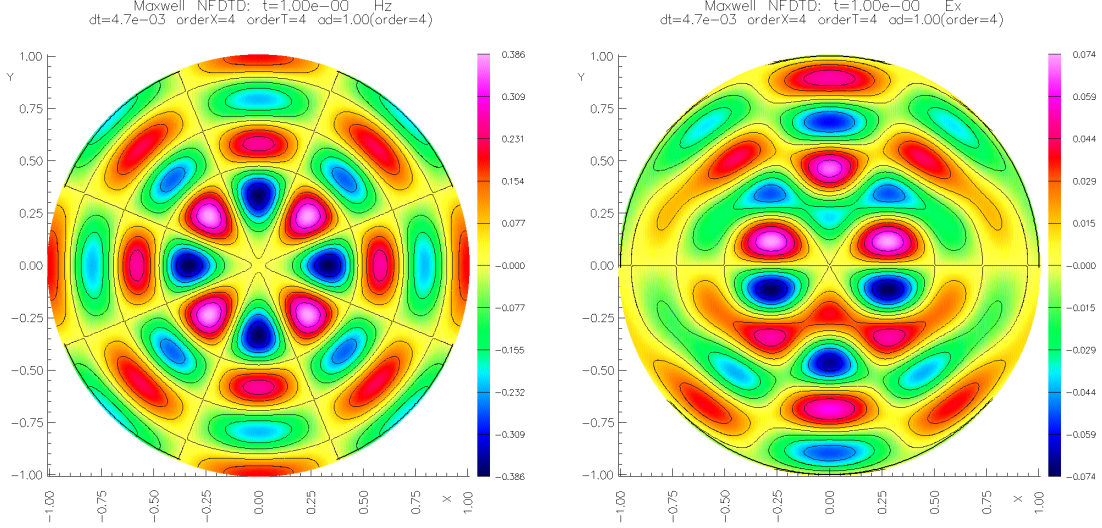


Figure 10: Eigenmode (4, 3) of the circular disk.

25.3 Eigenfunctions of a cylinder

Consider a cylinder of length d , denoted by $C(d)$. The eigenfunctions of the domain $C(d)$ are

$$\begin{aligned}
 u_{p,n,k}(r, \theta, z, t) &= -\frac{(k\pi/d)}{\lambda^2} \left\{ \lambda J'_n(\lambda r) \cos(\theta) \cos(n\theta) + \frac{n}{r} J_n(\lambda r) \sin(\theta) \sin(n\theta) \right\} \sin(k\pi z/d) \cos(\omega t) \\
 v_{p,n,k}(r, \theta, z, t) &= -\frac{(k\pi/d)}{\lambda^2} \left\{ \lambda J'_n(\lambda r) \sin(\theta) \cos(n\theta) - \frac{n}{r} J_n(\lambda r) \cos(\theta) \sin(n\theta) \right\} \sin(k\pi z/d) \cos(\omega t) \\
 w_{p,n,k}(r, \theta, z, t) &= J_n(\lambda r) \cos(n\theta) \cos(k\pi z/d) \cos(\omega t) \\
 \lambda &= \lambda_{p,n}, \quad \text{with } J_n(\lambda_{p,n}) = 0, \\
 \omega &= \omega_{p,n,k} = \sqrt{(k\pi/d)^2 + \lambda_{p,n}^2} \\
 n &= 0, 1, 2, 3, \dots, \quad p = 1, 2, 3, \dots, \quad k = 1, 2, 3, \dots
 \end{aligned}$$

Tables (20-??) presents some convergence results.

25.4 Scattering by a cylinder

The scattering of a plane wave by a two-dimensional cylinder of radius a is considered. For an incident field

$$\mathbf{E}^i = -\hat{y} Z e^{-ikx}, \quad H_z^i = \hat{z} e^{-ikx}, \quad Z = \sqrt{\mu/\epsilon},$$

grid	N	E_x	E_y	E_z	$\nabla \cdot \mathbf{u}$
tube1.order4	10	2.2×10^{-5}	2.2×10^{-5}	1.5×10^{-5}	6.7×10^{-4}
tube2.order4	20	1.1×10^{-6}	1.1×10^{-6}	1.1×10^{-6}	3.8×10^{-5}
tube3.order4	40	1.1×10^{-7}	1.1×10^{-7}	7.0×10^{-8}	1.3×10^{-6}
rate		3.83	3.82	3.85	4.51

Table 20: nfdtd, order=4, $t = 0.1$, tube, eigen-mode 0,0,1, cfl=0.75

grid	N	E_x	E_y	E_z	$\nabla \cdot \mathbf{u}$
tube1.order4	10	7.6×10^{-3}	3.4×10^{-3}	9.9×10^{-3}	6.5×10^{-3}
tube2.order4	20	5.7×10^{-4}	2.5×10^{-4}	7.3×10^{-4}	1.5×10^{-3}
tube3.order4	40	3.7×10^{-5}	1.6×10^{-5}	4.7×10^{-5}	3.3×10^{-5}
tube4.order4	80	2.3×10^{-6}	1.0×10^{-6}	3.0×10^{-6}	3.0×10^{-6}
rate		3.90	3.90	3.90	3.87

Table 21: nfdtd, order=4, $t = .25$, tube, eigen-mode 1,1,2, cfl=.9

the scattered field is given by

$$H_z^s = - \sum_{n=0}^{\infty} \epsilon_n (-i)^n \frac{J'_n(ka)}{H_n^{(1)'}(ka)} H_n^{(1)}(k\rho) \cos(n\phi)$$

where J_n and Y_n are the Bessel functions and $H_n^{(1)}(z) = J_n + iY_n$ is the Hankel function of the first kind and $\epsilon_0 = 1$, $\epsilon_n = 2$, $n = 1, 2, \dots$

In real space the solution will be given by $H_z^s(\mathbf{x}, t) = \text{Re}(H_z^s(\mathbf{x}, \omega))e^{-i\omega t}$. **check**

The solution is computed on a large domain and the error is computed within the region $r < 2$.

25.5 Scattering by a sphere

The scattering of a plane wave by a sphere is considered.

For an incident wave

$$\mathbf{E}^i = \hat{x}e^{-ikz}$$

grid	N	E_x	E_y	E_z	$\nabla \cdot \mathbf{u}$
tube1a.order4	10	$1.4e-3$	$1.2e-3$	$5.2e-3$	$3.8e-2$
tube2a.order4	20	$1.1e-4$	$2.9e-5$	$3.4e-4$	$3.4e-3$
tube3a.order4	40	$5.0e-6$	$2.4e-6$	$1.2e-5$	$7.0e-5$
tube4a.order4	80	$2.7e-7$	$1.8e-7$	$4.6e-7$	$6.2e-6$
rate		4.16	4.17	4.53	4.34

Table 22: Maximum errors in computing eigen-mode (1, 1, 2) of a cylinder, order=4, $t = 1.0$, tube, cfl=.9, ad=.5(?)

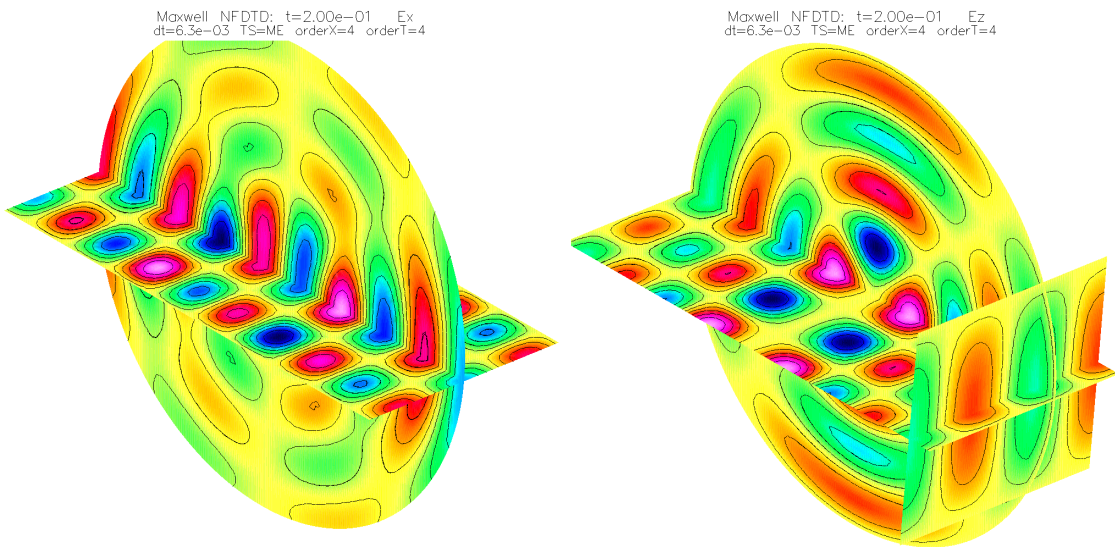


Figure 11: Eigenmode (2, 3, 3) of a cylinder, grid=tube3.order4.

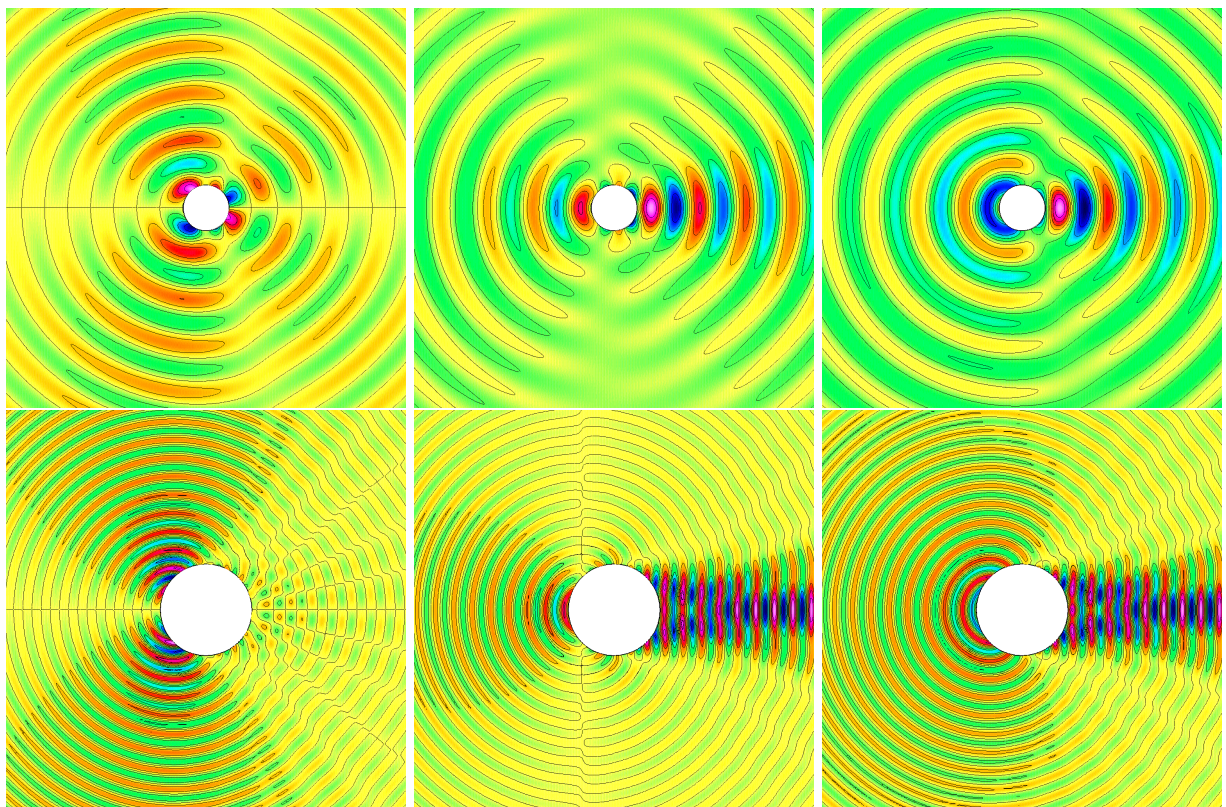


Figure 12: Scattering of a plane wave by a cylinder. Top: scattered field E_x , E_y and H_z for $ka = 1/2$. Bottom: scattered field E_x , E_y and H_z for $ka = 5/2$

grid	N	E_x	E_y	E_z	$\nabla \cdot \mathbf{u}$
tube1a.order4	10	$1.8e - 3$	$8.9e - 4$	$1.8e - 3$	$3.0e - 2$
tube2a.order4	20	$6.7e - 5$	$2.7e - 5$	$8.0e - 5$	$1.2e - 3$
tube3a.order4	40	$2.8e - 6$	$1.4e - 6$	$5.3e - 6$	$8.8e - 5$
tube4a.order4	80	$1.9e - 7$	$9.1e - 8$	$3.1e - 7$	$7.7e - 6$
rate		4.43	4.40	4.13	3.96

Table 23: nfdtd, order=4, $t = 1.0$, tube, eigen-mode 1,1,2, cfl=.95, ad=.1

grid	N	E_x	E_y	E_z	$\nabla \cdot \mathbf{u}$
tube1a.order4	10	$3.8e - 2$	$3.8e - 2$	$1.8e - 1$	$1.2e - 1$
tube2a.order4	20	$2.5e - 3$	$2.5e - 3$	$1.4e - 2$	$3.6e - 3$
tube3a.order4	40	$2.0e - 4$	$2.0e - 4$	$9.5e - 4$	$4.9e - 4$
tube4a.order4	80	$1.4e - 5$	$1.4e - 5$	$6.2e - 5$	$3.6e - 5$
rate		3.79	3.79	3.85	3.80

Table 24: Maximum errors in computing eigen-mode (2, 3, 3), nfdtd, order=4, $t = 1.0$, tube, cfl=.95, ad=.25

the total field is given by the series expansion

$$\begin{aligned}
E_r &= \frac{i \cos(\phi)}{(kr)^2} \sum_{n=1}^{\infty} (-i)^n (2n+1) [\psi_n(kr) - b_n \zeta_n^{(1)}(kr)] P_n^1(\cos(\theta)) \\
E_\theta &= \frac{\cos(\phi)}{kr} \sum_{n=1}^{\infty} (-i)^n \frac{2n+1}{n(n+1)} [A_n \frac{P_n^1(\cos(\theta))}{\sin(\theta)} + i B_n \partial_\theta P_n^1(\cos(\theta))] \\
E_\phi &= -\frac{\sin(\phi)}{kr} \sum_{n=1}^{\infty} (-i)^n \frac{2n+1}{n(n+1)} [A_n \partial_\theta P_n^1(\cos(\theta)) + i B_n \frac{P_n^1(\cos(\theta))}{\sin(\theta)}]
\end{aligned}$$

where

$$\begin{aligned}
A_n &= \psi_n(kr) - a_n \zeta_n^{(1)}(kr) \\
B_n &= \psi'_n(kr) - b_n \zeta_n^{(1)'}(kr) \\
j_n(z) &= \sqrt{\frac{\pi}{2z}} J_{n+1/2}(z), \quad h_n^{(1)}(z) = \sqrt{\frac{\pi}{2z}} H_{n+1/2}(z) \\
\psi(z) &= z j_n(z), \quad \zeta_n^{(1)}(z) = z h_n^{(1)}(z), \quad a_n = \frac{\psi_n(ka)}{\zeta_n^{(1)}(ka)}, \quad b_n = \frac{\psi'_n(ka)}{\zeta_n^{(1)'}(ka)}
\end{aligned}$$

The solution is computed on a large domain...

grid	N	E_x	E_y	E_z	$\nabla \cdot \mathbf{u}$
tube1a.order4	10	$2.5e - 2$	$2.5e - 2$	$1.2e - 1$	$1.1e - 1$
tube2a.order4	20	$1.4e - 3$	$1.4e - 3$	$7.5e - 3$	$4.2e - 3$
tube3a.order4	40	$1.1e - 4$	$1.1e - 4$	$5.1e - 4$	$4.9e - 4$
tube4a.order4	80	$7.4e - 6$	$7.4e - 6$	$3.3e - 5$	$3.5e - 5$
rate		3.89	3.89	3.94	3.78

Table 25: nfdtd, order=4, $t = 1.0$, tube, eigen-mode 2,3,3, cfl=.95, ad=.125

grid	h_0/h	E_x	E_y	H_z	$\nabla \cdot \mathbf{u}$
cibc.order4	1	$3.5436e - 04$	$4.8524e - 04$	$6.7498e - 05$	$4.44e - 03$
cibc2.order4	2	$2.4547e - 05$	$3.2046e - 05$	$4.6754e - 06$	$3.58e - 04$

Table 26: Errors in the scattering of a plane wave by a cylinder, order=4, **check $\text{div}(\mathbf{E})$ values

grid	N	E_x	E_y	H_z	$\ \nabla \cdot \mathbf{E}\ /\ \nabla \mathbf{E}\ $
cic.order4	121	$4.1e - 4$	$6.0e - 4$	$1.3e - 4$	$8.6e - 4$
cic2.order4	241	$2.8e - 5$	$4.1e - 5$	$8.3e - 6$	$7.0e - 5$
cic3.order4	481	$1.8e - 6$	$2.7e - 6$	$5.2e - 7$	$5.0e - 6$
rate		3.93	3.92	4.00	3.74

Table 27: Errors in the scattering of a plane wave by a cylinder, order=4, $t = 3.$, cic, scattering, cfl=.95, (exact solution used as far field BC)

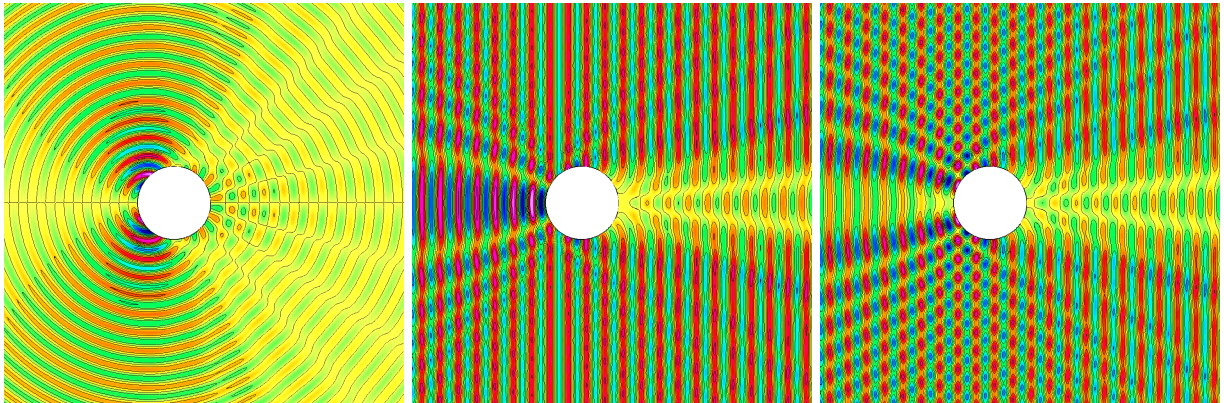


Figure 13: Scattering of a plane wave by a cylinder. Total field E_x , E_y and H_z for $ka = 2$.

grid	h_0/h	E_x	E_y	E_z	$\nabla \cdot \mathbf{u}$
sib1.order4	1	$1.11e - 2$	$7.84e - 3$	$5.60e - 3$	$3.71e - 2$
sib1x2.order4	2	$8.00e - 4$	$5.54e - 4$	$4.03e - 4$	$3.99e - 3$
sib1x4.order4	4	$5.33e - 5$	$3.66e - 5$	$2.66e - 5$	$4.71e - 4$
rate					

Table 28: Errors in the scattering of a plane wave by a sphere, order=4, $t = 3$. Initial conditions and far field boundary conditions set to the exact solution

grid	N	E_x	E_y	E_z	$\nabla \cdot \mathbf{u}$
sib1.order4	40	$1.3e - 2$	$8.1e - 3$	$6.7e - 3$	$3.9e - 3$
sib1x2.order4	80	$9.3e - 4$	$5.8e - 4$	$4.8e - 4$	$4.2e - 4$
sib1x4.order4	160	$6.2e - 5$	$3.9e - 5$	$3.2e - 5$	$5.4e - 5$
rate		3.86	3.86	3.85	3.09

Table 29: Errors in the scattering of a plane wave by a sphere, order=4, $t = 2.$, sib, scattering, cfl=.95, Initial conditions and far field boundary conditions set to the exact solution

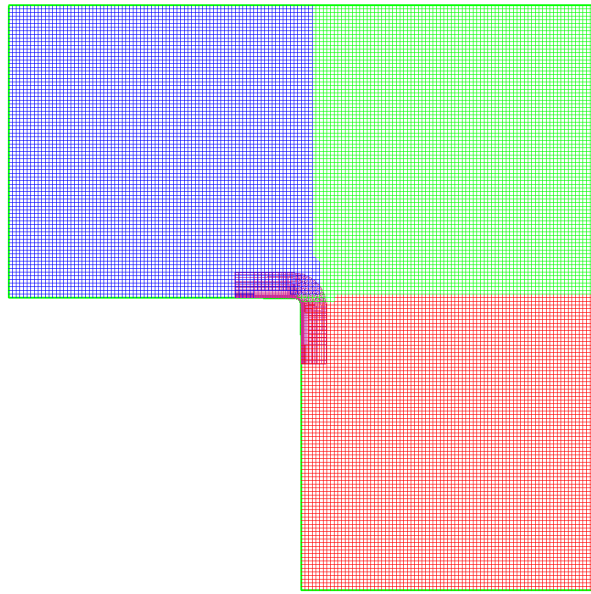


Figure 14: Grid for the L-shaped region.

25.6 Computing eigenvalues of an L-shaped domain with time series

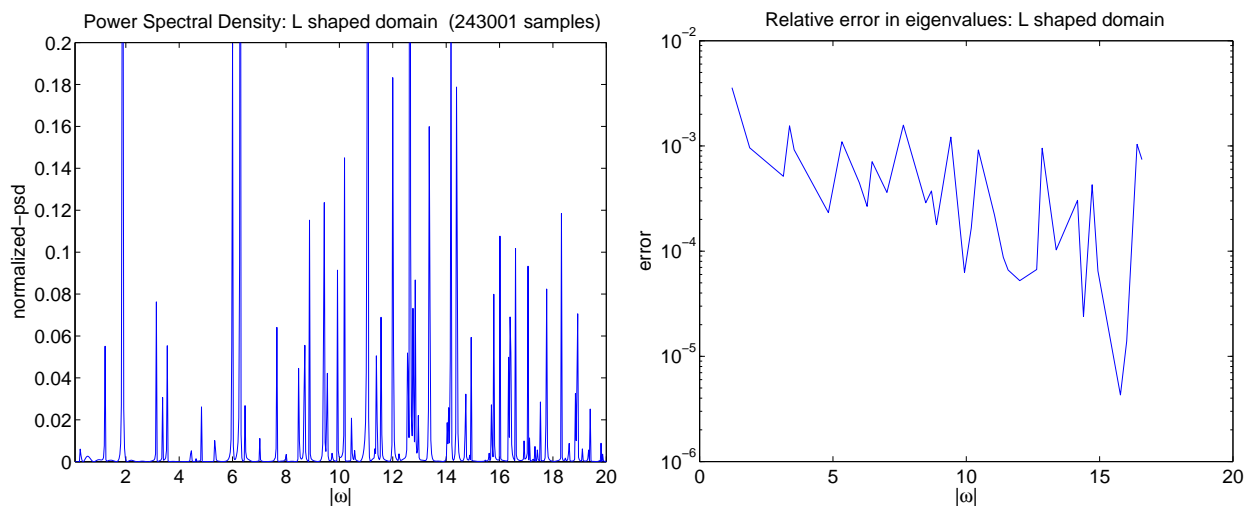


Figure 15: Left: Power-Spectral-Density for the L-shaped region, lgrid2e.order4. Right: relative errors in the eigenvalues.

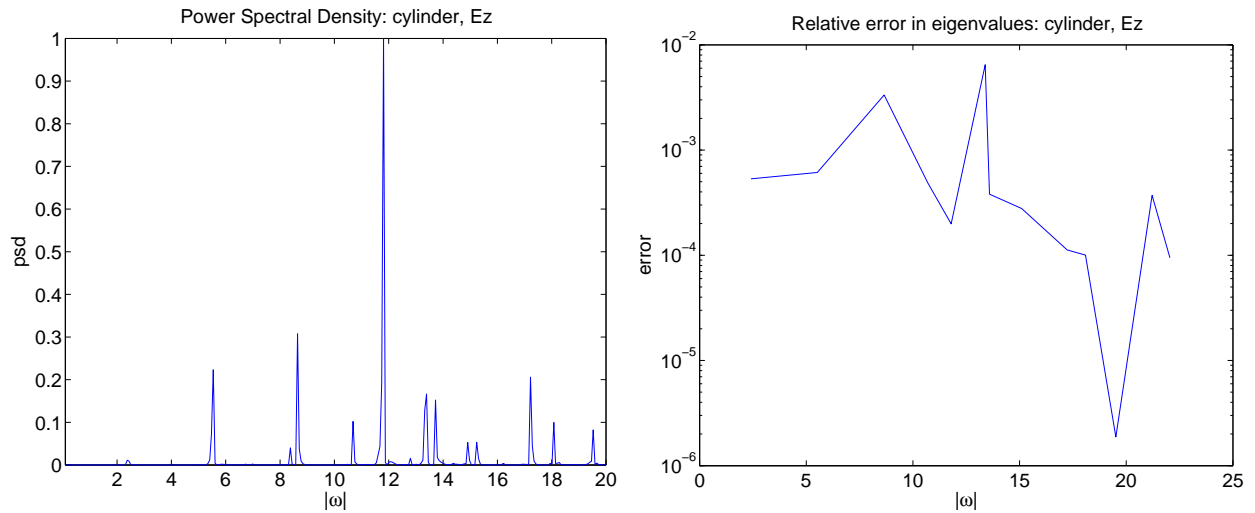


Figure 16: Left: Power-Spectral-Density for a cylinder. Right: relative errors in the eigenvalues.

25.7 Computing eigenvalues of a cylinder with time series

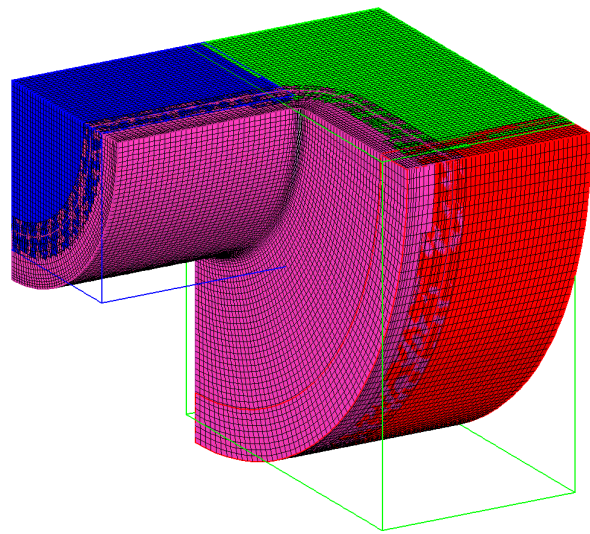


Figure 17: Grid for a pill-box.

25.8 Computing eigenvalues of a pill-box with time series

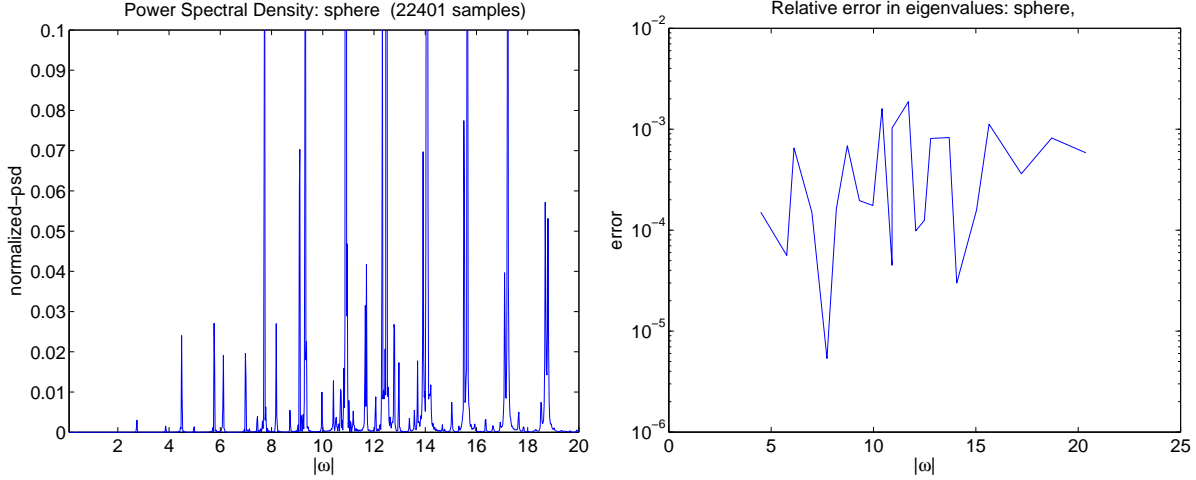


Figure 18: Left: Power-Spectral-Density for a sphere, bis2e.order4. Right: relative errors in the eigenvalues.

25.9 Computing eigenvalues of a sphere with time series

The first set of eigenvalues for modes inside a sphere are given by the positive roots of

$$J_{n+\frac{1}{2}}(\sqrt{\lambda_{np}} a) = 0, \quad n = 1, 2, 3, \dots \quad p = 1, 2, 3, \dots$$

A few values are $\sqrt{\lambda_{11}} a \approx 4.49$, $\sqrt{\lambda_{2,1}} a \approx 5.76$, $\sqrt{\lambda_{3,1}} a \approx 6.99$, $\sqrt{\lambda_{1,2}} a \approx 7.73$

The second set of eigenvalues are given by the positive roots of

$$J_{n+1+\frac{1}{2}}(z_{np}) + \frac{n+1}{z_{np}} J_{n+\frac{1}{2}}(z_{np}) = 0, \quad n = 1, 2, 3, \dots \quad p = 1, 2, 3, \dots$$

for $z_{np} = \sqrt{\lambda_{np}} a$. A few values are $\sqrt{\lambda_{11}} a \approx 2.743$, $\sqrt{\lambda_{2,1}} a \approx 3.87$, $\sqrt{\lambda_{1,2}} a \approx 6.11$ and $\sqrt{\lambda_{2,2}} a \approx 7.44$. Table (18) shows the PSD for a sphere and the relative errors in some of the eigenvalues.

25.10 Scattering of a plane wave by a dielectric cylinder

Table 30 shows convergence results for the scattering of a plane wave by a dielectric cylinder with different material properties.

grid	N	E_x	E_y	H_z	$\ \nabla \cdot \mathbf{E}\ /\ \nabla \mathbf{E}\ $
innerOuter2.order4.hdf	1	$6.0e - 3$	$1.2e - 2$	$1.4e - 2$	$4.1e - 3$
innerOuter4.order4.hdf	2	$4.0e - 4$	$7.9e - 4$	$8.9e - 4$	$2.7e - 4$
innerOuter8.order4.hdf	4	$2.6e - 5$	$5.0e - 5$	$5.6e - 5$	$1.8e - 5$
rate		3.93	3.97	3.97	3.93

Table 30: nfdtd, order=4, $t = 1.$, innerOuter, material interface, $k_x = 2$, inner $\epsilon = 1/4$, outer $\epsilon = 1$, cfl=.8, ad=.5

25.11 Serial performance and memory usage

Timings:	seconds	sec/step	sec/step/pt	%
total time.....	1.85e+03	1.73e+00	4.55e-07	100.000
setup and initialize.....	1.34e+00	1.25e-03	3.29e-10	0.072
initial conditions.....	5.57e+01	5.20e-02	1.37e-08	3.004
advance.....	1.79e+03	1.67e+00	4.39e-07	96.502
advance rectangular grids	1.32e+03	1.24e+00	3.25e-07	71.420
advance curvilinear grids	2.59e+02	2.42e-01	6.35e-08	13.950
(advOpt).....	1.37e+03	1.28e+00	3.36e-07	73.894
add dissipation.....	3.09e+01	2.89e-02	7.59e-09	1.668
boundary conditions.....	1.97e+02	1.84e-01	4.84e-08	10.632
interpolation.....	8.51e+00	7.94e-03	2.09e-09	0.459
get errors.....	6.34e+00	5.92e-03	1.56e-09	0.342
compute dt.....	9.65e-03	9.01e-06	2.37e-12	0.001
plotting.....	2.82e+00	2.63e-03	6.91e-10	0.152

Table 31: grid=cic5.order4.hdf, 3805020 grid points, 9400 interp points, 1071 steps taken, 1 processors.

Timings:	seconds	sec/step	sec/step/pt	%
total time.....	3.65e+02	4.80e+00	1.94e-06	100.000
setup and initialize.....	9.06e+00	1.19e-01	4.83e-08	2.484
initial conditions.....	9.09e+00	1.20e-01	4.84e-08	2.492
advance.....	3.53e+02	4.65e+00	1.88e-06	96.899
advance rectangular grids	6.86e+01	9.03e-01	3.66e-07	18.821
advance curvilinear grids	2.05e+02	2.70e+00	1.09e-06	56.236
boundary conditions.....	3.96e+01	5.21e-01	2.11e-07	10.864
interpolation.....	3.69e+01	4.86e-01	1.97e-07	10.128
compute dt.....	5.80e-02	7.63e-04	3.09e-10	0.016
plotting.....	2.22e+00	2.92e-02	1.18e-08	0.608

Table 32: grid=bis3e.order4.hdf, 2468750 grid points, 236176 interp points, 76 steps taken, 1 processors.

Memory usage	Mbytes	real/point	real/var	percent
CompositeGrid	71.70	3.81	1.27	31.9
finite difference operators	0.01	0.00	0.00	0.0
Interpolant	5.42	0.29	0.10	2.4
Grid functions	147.34	7.82	2.61	65.6
total (of above items)	224.48	11.92	3.97	100.0

Table 33: Sphere, bis3e.order4.hdf, 2468750 grid points, 236176 interp points, 1 processors. Memory usage. (Memory from top=231M)

25.12 Parallel performance

Here are some results from running the code in parallel.

NP	sec/step	ratio	NP	sec/step	ratio
1	2.14	1.	1	.	1.
2	1.01	2.1	2	5.10	
3	.59	3.6	3	2.69	

Table 34: Square. Left: square2048.order4, 4.2M grid points. Right: square4096.order4, 16.8M grid points. Dell workstations 2.2GHz pentium.

NP	sec/step	ratio	NP	sec/step	ratio
1	11.8	1.	1	61.3	1.
2	5.67		2	29.0	
4	3.00		4	14.2	

Table 35: Cylinder. Left tube4.order4, 2.6e6 grid points. Right: tube5.order4, 17.3e6 grid points. Compaq gps320, 1 GHz alpha Processor.